Sensor and Simulation Notes
Note

November 1972

FIELD DISTRIBUTION FOR PARALLEL PLATE TRANSMISSION LINE OF FINITE WIDTH IN PROXIMITY TO A CONDUCTING PLANE

Soon K. Cho and Chiao-Min Chu
The University of Michigan Radiation Laboratory
Department of Electrical and Computer Engineering
Ann Arbor, Michigan 48105

Abstract

A parametric study of a parallel plate transmission line of finite width near a perfectly conducting plane ground is carried out by a numerical method for various ground proximities and the plate widths. In particular, the impedance factor f_g of the transmission line system and relative electric field in some region surrounding the transmission line system are computed.

11323-1-T = RL-2219

THE UNIVERSITY OF MICHIGAN

COLLEGE OF ENGINEERING

DEPARTMENT OF ELECTRICAL AND COMPUTER ENGINEERING

Radiation Laboratory

Field Distribution for Parallel Plate Transmission Line of Finite Width

By

Soon K. Cho
Chiao-Min Chu

November 1972

Technical Report No. 011323-1-T
Contract No. F29601-72-C-0087
Purchase Order No. DC-SC-72-09

Prepared for:

The Dikewood Corporation
1009 Bradbury Drive, S. E.
Albuquerque, New Mexico 87106

Ann Arbor, Michigan 48105

ABSTRACT

A parametric study of a parallel plate transmission line of finite width near a perfectly conducting plane ground is carried out by a numerical method for various ground proximities and the plate widths. In particular, the impedance factor f_g of the transmission line system and relative electric field in some region surrounding the transmission line system are computed.

Table of Contents

List of Graphs

Graphs of Relative Fields

Remarks: I in $\frac{y}{b}$ represents $\frac{y}{b} = 0, 0.2, 0.4, 0.6, 0.8, 1.2, 1.4$;

II in $\frac{y}{b}$ represents $\frac{y}{b} = 1_-$ and 1_+.

List No.	Range of $\frac{y}{b}$	Parameters $\frac{a}{b}$	Parameters $\frac{d}{b}$	Field Components	Figure No.	Page No.
10	I	0.1	0.1	E_{yrel}	3-1-a	27
11	II	0.1	0.1	E_{yrel}	3-1-b	28
12	II	0.1	0.1	E_{xrel}	3-1-c	29
13	II	0.1	0.1	E_{xrel}	3-1-d	30
14	I	0.1	0.2	E_{yrel}	3-2-a	31
15	II	0.1	0.2	E_{yrel}	3-2-b	32
16	I	0.1	0.2	E_{xrel}	3-2-c	33
17	II	0.1	0.2	E_{xrel}	3-2-d	34
18	I	0.1	0.5	E_{yrel}	3-3-a	35
19	II	0.1	0.5	E_{yrel}	3-3-b	36
20	I	0.1	0.5	E_{xrel}	3-3-c	37
21	II	0.1	0.5	E_{xrel}	3-3-d	38
22	I	0.1	1.0	E_{yrel}	3-4-a	39
23	II	0.1	1.0	E_{yrel}	3-4-b	40
24	I	0.1	1.0	E_{xrel}	3-4-c	41
25	II	0.1	1.0	E_{xrel}	3-4-d	42

Graphs for Comparison of Relative Fields

List No.	Range of $\frac{y}{b}$	Parameters $\frac{d}{b}, \frac{a}{b}$	Field Components	Figure No.	Page No.
82	1.4	0.5	E_{yrel}	3-17-9	99
83	1.5	0.5	E_{yrel}	3-17-10	100
84	0.2	0.5	E_{xrel}	3-18-1	101
85	0.4	0.5	E_{xrel}	3-18-2	102
86	0.6	0.5	E_{xrel}	3-18-3	103
87	0.8	0.5	E_{xrel}	3-18-4	104
88	1_-, 1_+	0.5	E_{xrel}	3-18-5	105
89	1.2	0.5	E_{xrel}	3-18-6	106
90	1.4	0.5	E_{xrel}	3-18-7	107
91	1.5	0.5	E_{xrel}	3-18-8	108

I

INTRODUCTION

The ultimate goal we hope to achieve is the computation of propagation constant and field distribution for a parallel plate transmission line of finite width which is placed near a finitely conducting plane ground. See Figure 1-1 for the geometry of the transmission line system.

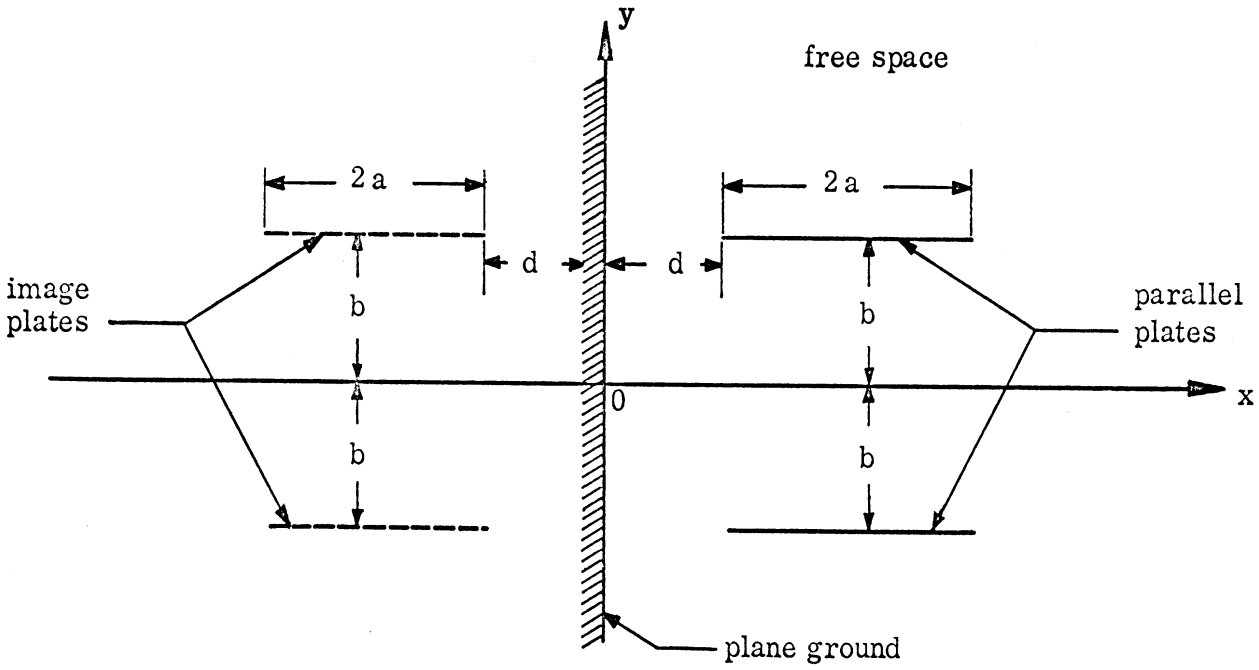

FIG. 1-1: Geometry of a parallel plate transmission line of finite width near a plane ground in (x, y) coordinate system.

Such a problem poses a series of mathematical difficulties and requires an extensive analytical investigation. As a step leading to that problem, one can consider a simpler case where the plane ground is perfectly conducting. In that

case, the transmission line system supports dominantly an unattenuated TEM mode propagation and hence enables a formulation of electrostatic problems.

In this report, we are concerned essentially with the field distribution in an immediate neighborhood of a parallel plate transmission line of finite width when a perfectly conducting plane ground is present to a varying degree of proximity. The cases of the ground proximity considered in terms of normalized form, d/b, are: 0.1, 0.2, 0.5 and 1.0; the cases of variation of the line width, a/b, are: 0.1, 0.2, 0.5 and 1.0; the range of the field points where the relative electric field intensities are computed are taken to be: $0 \leq \frac{|x|}{b} \leq \frac{3|a|+d}{b}$*, $0 \leq \frac{y}{b} \leq 1.5$.

In Section II, the mathematical formulation of the problem is presented; a more detailed version will be found in Appendix A. Starting with an integral equation for the electric potential for the transmission line system of the geometry as shown in Fig. 2-1, the electric charge density function is found by means of numerical method following the Kammler's[3] procedure. Based on the charge density function computed, then the impedance factor, $f_g^{(1)}$, and electric field intensity are derived. The latter is derived through the complex potential function.

In Section III, we present in plot the numerical results of relative electric field intensity for some representative cases of ground proximity and transmission line width, in a different cartesian coordinate system (cf Fig. 3-0-c) employed in our previous work[4]. In this coordinate system, the edges of the parallel plates facing the ground are on the y-axis for all different ground proximities. It is to be noted that this coordinate system is introduced solely for the graphical presentation of relative field strengths and is not to be confused with the coordinate system shown in Fig. 1-1.

---

*See Section 3.1 to see the meaning of absolute signs for $|x|$ and $|a|$.

Based on the study of the numerical results shown in Section III, conclusion is drawn in Section IV on the effect of the presence of a perfectly conducting plane ground upon the field intensity.

II

MATHEMATICAL FORMULATION

For a parallel plate transmission line of finite width in the proximity of a perfectly conducting plane ground (cf Fig. 1-1), the complex potential at any point (x, y) in the rectangular coordinate system may be expressed in the integral form

$$V(x,y) + i\,\psi(x,y) = \frac{1}{2\pi\epsilon_0}\int_a^{2a+d} dx'\,\sigma(x')\,\mathrm{Ln}\left[\frac{(x+iy-x'+ib)(x+iy+x'-ib)}{(x+iy-x'-ib)(x+iy+x'+ib)}\right] \quad (1)$$

where $\sigma(x')$ represents the electric charge density function of the upper plate. $\sigma(x')$ is an unknown function and we will find it by a numerical method with a known constant potential of the upper plate, V_0. For that purpose, it is convenient to introduce the following change of variables:

$$s = \frac{x' - a - d}{a}, \quad (2)$$

$$\xi = \frac{x - a - d}{a}, \quad (3)$$

$$\eta = \frac{y - b}{a}, \quad (4)$$

and

$$D = 2\,\frac{a + d}{a}, \quad (5)$$

$$B = 2\,\frac{b}{a}. \quad (6)$$

In the (ξ, η) coordinate system, the geometry of the transmission line system shown in Fig. 1-1 takes a form as shown in Fig. 2-1.

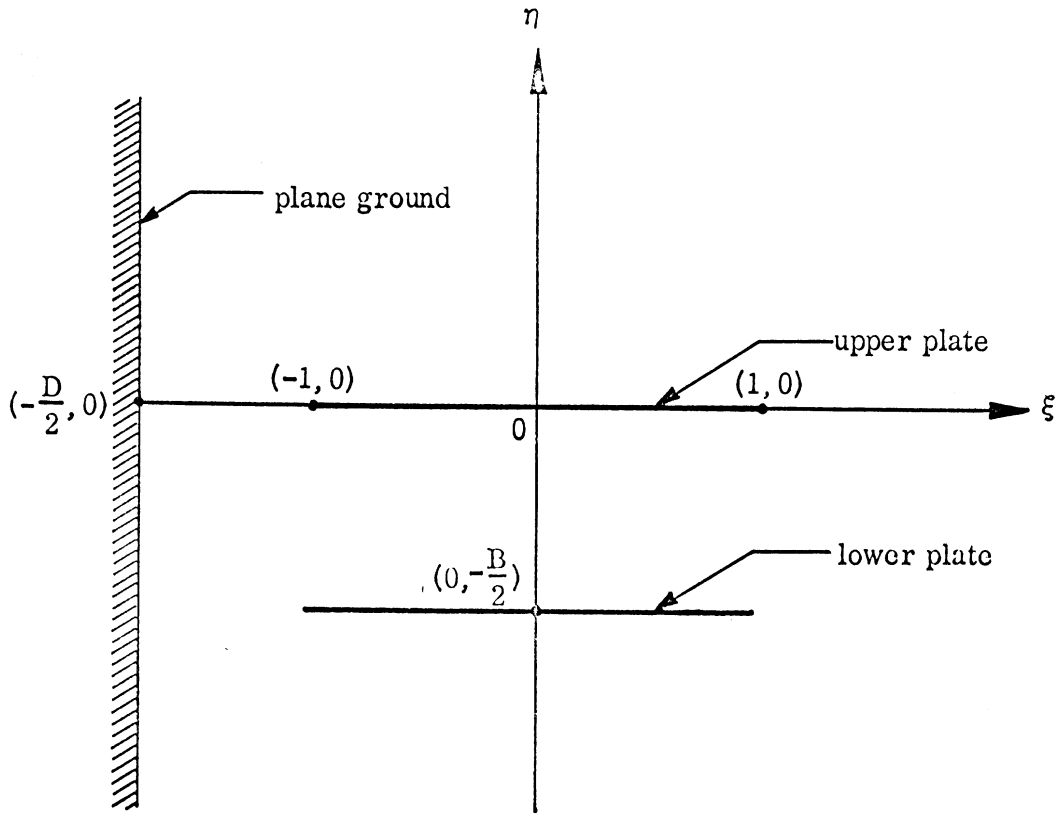

FIG. 2-1: Geometry of parallel plate transmission line near a plane ground in (ξ, η) coordinate system.

The geometric parameters involved in the problem is then represented by D and B. For practical purposes, however, it is convenient to compute electric field intensity in a coordinate system normalized with respect to b, $(\frac{x}{b}, \frac{y}{b})$, conforming to our previous work[4].

In this normalization

$$\frac{a}{b} = \frac{2}{B} \tag{7}$$

and

$$\frac{d}{b} = \frac{D-2}{B} \quad . \tag{8}$$

Conversion of $\frac{d}{b}$ and $\frac{a}{b}$ to D and B is presented in Table 1 for the set of values of our interest for $\frac{d}{b}$ and $\frac{a}{b}$.

TABLE 1

D and B Chart

$$D = 2\frac{a+d}{a}, \quad B = 2\frac{b}{a}$$

a/b d/b	0.1	0.2	0.5	1.0
0.1	4	3	2.4	2.2
0.2	6	4	2.8	2.4
0.5	12	7	4	3
1.0	22	12	6	4

In the (ξ, η) coordinate system, Eq. (1) becomes

$$V(\xi, \eta) + i\psi(\xi, \eta) = \frac{a}{2\pi\epsilon_o} \int_{-1}^{1} ds\, \sigma(s)\, Ln \frac{(\xi+i\eta-s+iB)(\xi+i\eta+s+D)}{(\xi+i\eta-s)(\xi+i\eta+s+D+iB)} \quad . \tag{9}$$

If we introduce, mainly for notational convenience,

$$z = \xi + i\eta \quad , \tag{10}$$

then

$$V(z)+i\psi(z) = \frac{a}{2\pi\epsilon_o} \int_{-1}^{1} ds\, \sigma(s)\, \mathrm{Ln} \frac{(z-s+iB)(z+s+D)}{(z-s)(z+s+D+iB)} \quad , \tag{9-a}$$

where $V(z)$ and $\psi(z)$ are real functions of ξ, η.

Now, a point on the upper plate in (ξ, η) coordinate system is $(\xi, 0)$, $-1 \leq \xi \leq 1$, as seen in Fig. 2-1. Thus, by letting $\eta = 0$ in Eq. (9) and denoting $V(\xi, 0)$ by V_0, we obtain

$$V_0 = \frac{a}{2\pi\epsilon_o} \int_{-1}^{1} ds\, \sigma(s)\, G(\xi, s) \; ; \; -1 \leq \xi \leq 1, \tag{11}$$

where

$$G(\xi, s) = \mathrm{Ln} \left[\frac{|\xi+s+d| \sqrt{(\xi-s)^2 + B^2}}{|\xi-s| \sqrt{(\xi+s+d)^2 + B^2}} \right] . \tag{12}$$

Solution of the integral equation of the type described by Eq. (11) has been investigated by Kammler[3]. In spite of singularities of $\sigma(s)$ at $s = \pm 1$ due to edge effect, reasonably accurate results may be obtained by representing $\sigma(s)$ in terms of a series of piece-wise linear equations in s.

Thus, let us divide the interval $-1 \leq s \leq 1$ into 2M segments by a set of 2M+1 points: $\{s_j\}$, $j = 1, 2, 3, \ldots, 2M+1$. In each of the segments, (s_j, s_{j+1}), $j = 1, 2, \ldots, 2M$, we approximate the charge variation by a linear equation, i.e.,

$$\sigma(s) = \tau_j + \frac{\tau_{j+1} - \tau_j}{s_{j+1} - s_j} (s - s_j) \; ; \quad s_j \leq s \leq s_{j+1} \quad , \tag{13}$$

where τ_j's are unknown constants yet to be determined. Substituting Eq. (13) into Eq. (11), one obtains

$$\frac{2\pi\epsilon_0}{a} V_0 = \sum_{j=1}^{2M} \int_{s_j}^{s_{j+1}} ds \left[\tau_j + \frac{\tau_{j+1} - \tau_j}{s_{j+1} - s_j} (s - s_j) \right] G(\xi, s) . \qquad (14)$$

Next, let us evaluate the integral on the right-hand side of Eq. (14) at a set of (2N+1) discrete points of s: $\{\xi_k\} = 1, 2, \ldots, 2N+1$, where $N \neq M$. Formally, then, we obtain a set of 2M+1 linear equations for τ_j:

$$\frac{2\pi\epsilon_0}{a} V_0 = \sum_{j=1}^{2M+1} A_{j,k} \tau_j \qquad (15)$$

where

$$A_{j,k} = \frac{(1-\delta_{j,\,2M+1})}{s_{j+1} - s_j} \left[s_{j+1} (f_{j+1,k} - f_{j,k}) - (g_{j+1,k} - g_{j,k}) \right]$$

$$+ \frac{(1 - \delta_{j,1})}{s_j - s_{j-1}} \left[(g_{j,k} - g_{j-1,k}) - s_{j-1} (f_{j,k} - f_{j-1,k}) \right] , \qquad (16)$$

$$f_{j,k} = (\xi_k - s_j) \, \mathrm{Ln} \frac{\left| \xi_k - s_j \right|}{\sqrt{(\xi_k - s_j)^2 + B^2}}$$

$$+ (\xi_k + s_j + D) \, \mathrm{Ln} \frac{\left| \xi_k + s_j + D \right|}{\sqrt{(\xi_k + s_j + D)^2 + B^2}}$$

$$+ B \left[\tan^{-1}\left(\frac{B}{\xi_k - s_j} \right) + \tan^{-1}\left(\frac{B}{\xi_k + s_j + D} \right) \right] \qquad (17)$$

and

$$g_{j,k} = \frac{\xi_k - s_j^2}{2} \operatorname{Ln} \frac{|\xi_k - s_j|}{\sqrt{(\xi_k - s_j)^2 + B^2}} - \frac{(\xi_k + D)^2 - s_j^2}{2} \operatorname{Ln} \frac{|\xi_k + s_j + D|}{\sqrt{(\xi_k + s_j + D)^2 + B^2}}$$

$$+ \frac{B^2}{2} \operatorname{Ln} \frac{\sqrt{(\xi_k - s_j)^2 + B^2}}{\sqrt{(\xi_k + s_j + D)^2 + B^2}} + B\,\xi_k \tan^{-1}\left(\frac{B}{\xi_k - s_j}\right) - B(\xi_k + D)\tan^{-1}\left(\frac{B}{\xi_k + s_j + D}\right). \tag{18}$$

For further details for derivation of $f_{j,k}$ and $g_{j,k}$ see Appendix A.

To determine $\{\tau_j\}$ in Eq. (15), we use the least square method with $M \neq N$. Thus, we set

$$\sum_{k=1}^{2N+1} \left(\frac{2\pi\epsilon_0}{a} V_0 - \sum_{j=1}^{2M+1} A_{j,k}\,\tau_j \right)^2 = \text{Minimum.} \tag{19}$$

Whence, one obtains for each $\ell = 1, 2, 3, \ldots, 2M+1$,

$$\sum_{j=1}^{2M+1} \left(\sum_{k=1}^{2N+1} A_{j,k}\, A_{k,\ell} \right) \tau_j = \frac{2\pi\epsilon_0}{a} V_0 \sum_{k=1}^{2N+1} A_{\ell,k} \quad . \tag{20}$$

Note that, for $\ell = 1, 2, \ldots, 2M+1$, Eq. (20) can be written in the matrix form

$$[A]\,[A^T]\,[\tau] = \frac{2\pi\epsilon_0}{a}\,[A]\,[I_C]\,, \tag{21}$$

where

$$[A] = [A_{j,k}]; \quad j = 1,2,\ldots,2M+1, \quad k = 1.2,..,2N+1\,,$$

$[A^T]$ = Transpose of $[A]$,

$$\left[\tau\right] = \left[\tau_j\right] = \text{Column matrix of } 1 \times (2M+1) \ .$$

and

$$\left[I_C\right] = 1 \times (2N+1) \text{ Column matrix of element 1.}$$

$\left[A\right]\left[A^T\right]$ is a $(2M+1) \times (2M+1)$ square matrix and Eq. (21) is our $(2M+1)$ linear equation for $\left\{\tau_j\right\}$, $j = 1, 2, \ldots, 2M+1$. Without loss of generality, we may set $\frac{2\pi\epsilon_0}{a} V_0 = 1$ in Eq. (21) for computational convenience.

It is pointed out by Kammler[3] that accurate results may be obtained if the interval $-1 \leq s \leq 1$ is sinusoidally divided into segments by

$$s_j = \sin\left[(j-M-1)\frac{\pi}{2M}\right] \ ; \ j = 1, 2, \ldots, 2M+1 \tag{22}$$

and

$$\xi_k = \sin\left[(k - N - 1)\frac{\pi}{2N}\right] ; \ k = 1, 2, \ldots, 2N+1 \ . \tag{23}$$

We let $N = 2M$.

In principle, the greater the value of M one chooses, the higher the degree of accuracy one attains for charge density function represented by τ in Eq. (21), but the greater the cost incurred in computation. Therefore, one would desire to find an optimum upper limit of M for a given degree of accuracy one is to maintain for charge density function. In our present work, we used the impedance factor, f_g, as a criterion in obtaining such an optimum upper limit of M: the numerical value of f_g for the case where the ground is not present (i.e., the ground is removed infinitely far away from the transmission line) for a given value of a/b is compared with the value of f_g, for the same a/b and a sufficiently large d/b, by taking a series of monotonically increasing values for M. It turned out that, for $a/b = 1$ and $d/b = 1,000$, the impedance factor, f_g, is 0.47244 for $M = 10$, which compares favorably with

$f_g = 0.46264$[2] without the ground presence.* In Table 2 we present the computed numerical values of f_g for different d/b and M; in Fig. 2-2, the corresponding plots, including f_g for the case where there is no ground present. M = 10 is chosen in our present work. Figures 2-3-a through 2-3-c show electric charge density for different M.

TABLE 2

Variation of f_g for different d/b as a function of M with a/b = 1.0

$$f_{g\ d/b=\infty} = 0.47264 \text{ for } a/b = 1.0.$$

M \ d/b	0.1	0.2	1.0
1	0.30548	0.3332	0.41811
2	0.29669	0.33442	0.42642
3	0.29753	0.33631	0.42852
4	0.298455	0.337284	0.42936
5	0.299042	0.337811	0.429770
6	0.299414	0.338122	0.430022
8	0.299830	0.338454	0.430239
10	0.30041	0.338617	0.430352

The concept of the impedance factor, denoted by f_g, was introduced by Baum[1], which is defined as the normalized impedance of the trans-

*An extensive tabulation is compiled in Ref. (2) for f_g for various b/a for the case where the ground is not present.

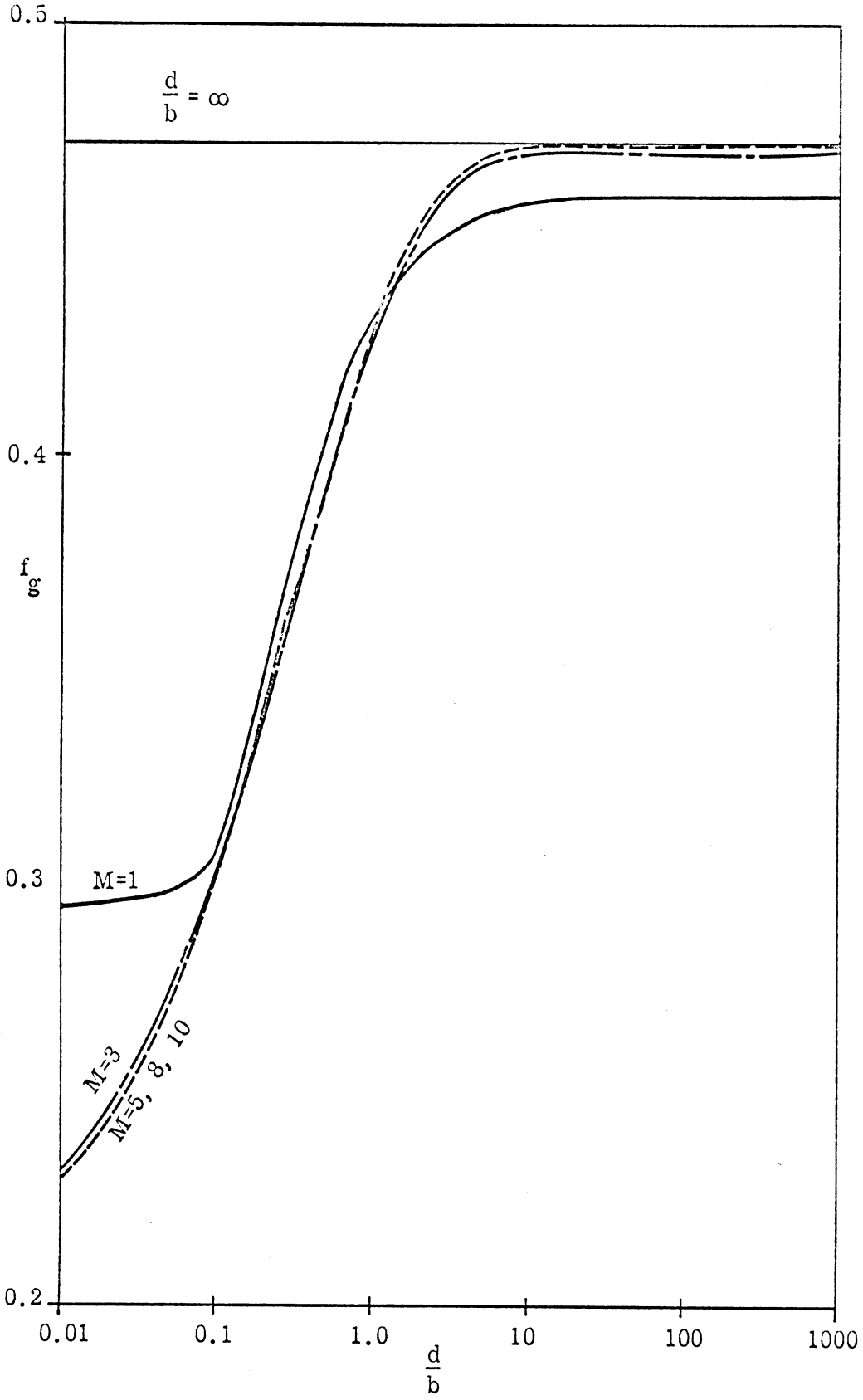

FIG. 2-2: Variation of the impedance factor f_g as a function of $\frac{d}{b}$ for different M. $\frac{a}{b} = 1.0$.

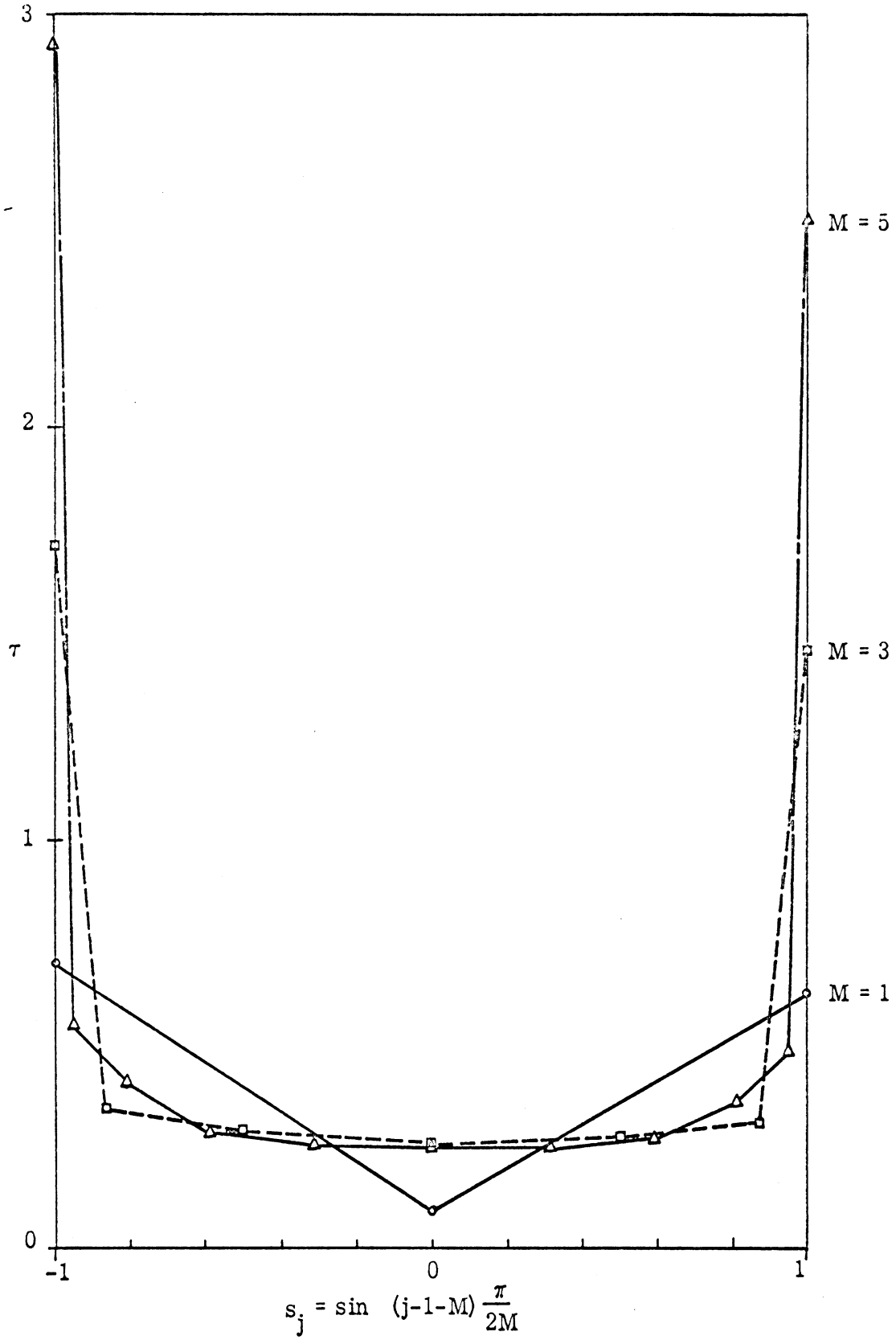

FIG. 2-3a: Charge density function for $\frac{d}{b} = 0.5$, $\frac{a}{b} = 1.0$ with various M.

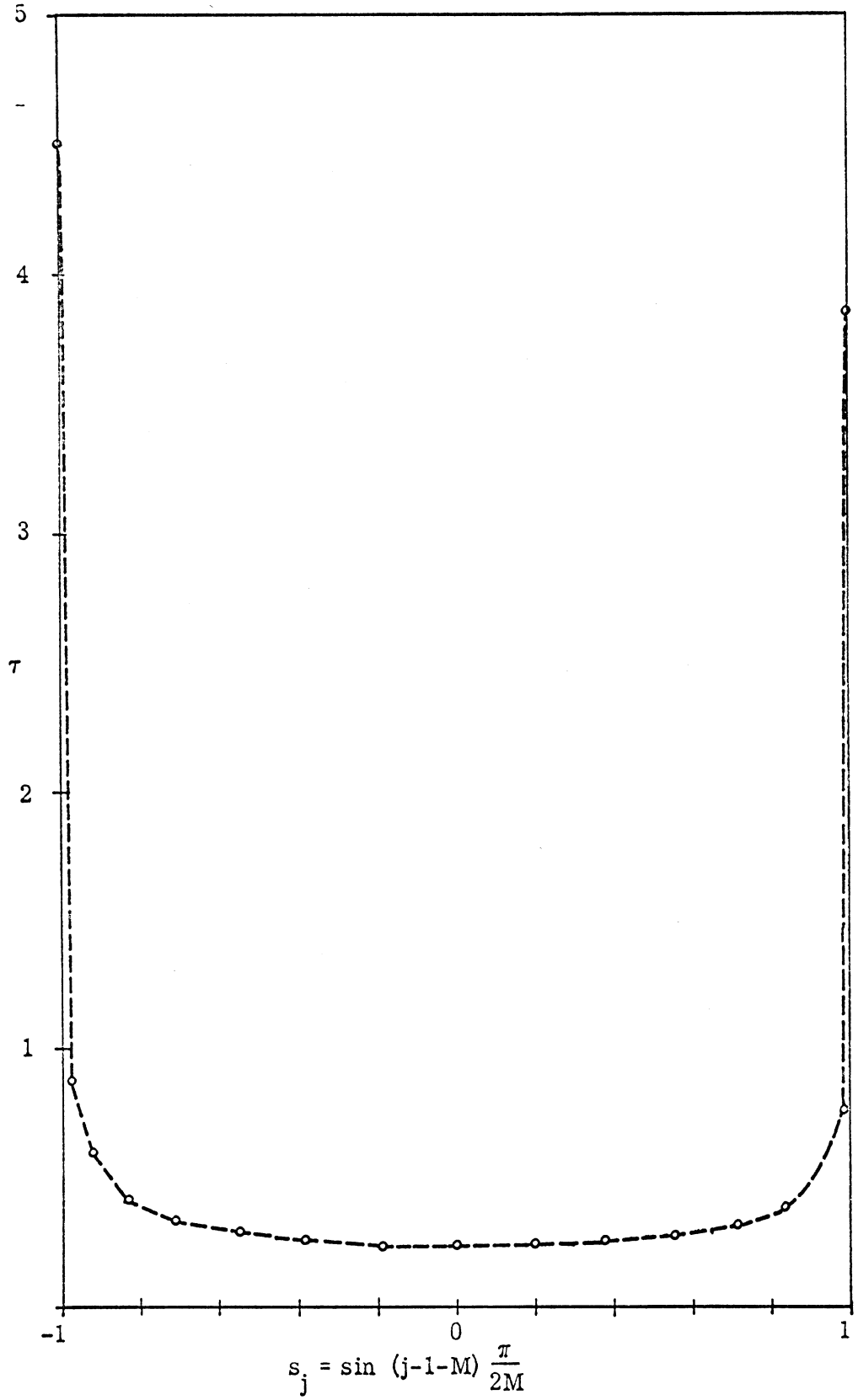

FIG. 2-3b: Charge density function for $\frac{d}{b} = 0.5$, $\frac{a}{b} = 1.0$ with $M = 8$.

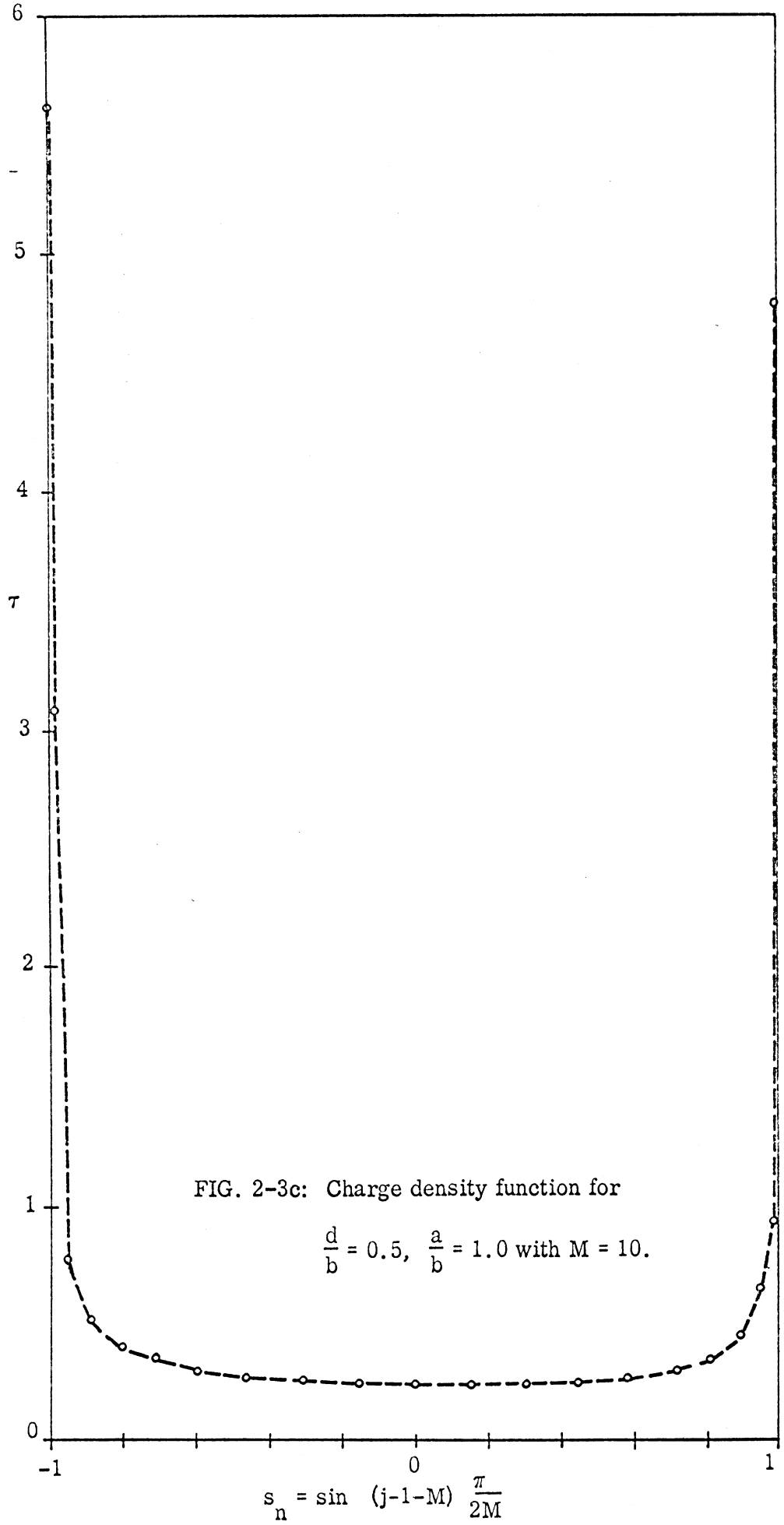

FIG. 2-3c: Charge density function for

$\frac{d}{b} = 0.5, \ \frac{a}{b} = 1.0$ with M = 10.

mission line with respect to the wave impedance. In our present case, then, if L and C denote the inductance and the capacitance per unit length of the line, and μ_0 and ϵ_0 the free space permeability and permitivity, $Z = \sqrt{\frac{L}{C}}$, $Z_0 = \sqrt{\frac{\mu_0}{\epsilon_0}}$ representing the impedances of the line and the free-space respectively, we have

$$f_g = \frac{Z}{Z_0} = \frac{\epsilon_o}{C} \quad . \tag{24}$$

Since $C = \frac{q}{\Delta V}$, where q and ΔV denote the total charge on the upper plate and the potential difference between the upper and the lower plates, respectively, and

$$q = \int_d^{2a+d} \sigma(x)\, dx = a \int_{-1}^{1} \sigma(s)\, ds$$

$$= a \sum_{j=1}^{2M} \int_{s_j}^{s_{j+1}} ds \left[\tau_j + \frac{\tau_{j+1} - \tau_j}{s_{j+1} - s_j} (s - s_j) \right]$$

$$= \frac{a}{2} \sum_{j=1}^{2M} (\tau_{j+1} + \tau_j)(s_{j+1} - s_j) \quad ,$$

$\Delta V = \frac{a}{\pi \epsilon 0}$, we obtain for the geometric factor

$$f_g = \frac{2}{\pi} \cdot \frac{1}{\sum_{j=1}^{2M} (\tau_{j+1} + \tau_j)(s_{j+1} - s_j)} \tag{25}$$

Equation (25) is used for numerical computation of f_g for various geometries of the transmission line.

We now derive the expression for the electric field intensity at a point in the z-plane. From Eqs. (9-a) and (13), after a little algebraic manipulation, we obtain the following:

$$V(z) + i\psi(z) = \frac{a}{2\pi\epsilon_0} \sum_{j=1}^{2M} \frac{1}{s_{j+1} - s_j} \left\{ (\tau_j s_{j+1} - \tau_{j+1} s_j) \right.$$

$$\left. \cdot \left[P(z, s_{j+1}) - P(z, s_j) \right] - (\tau_j - t_{j+1}) \left[Q(z, s_{j+1}) - Q(z, s_j) \right] \right\}, \tag{26}$$

where

$$P(z, s_j) = (z + s_j + D) \operatorname{Ln} (z + s_j + D)$$

$$+ (z - s_j) \operatorname{Ln} (z - s_j)$$

$$- (z - s_j + i B) \operatorname{Ln} (z - s_j + i B)$$

$$- (z + s_j + D + i B) \operatorname{Ln} (z + s_j + D + i B) \tag{27}$$

and $$Q(z, s_j) = -\frac{(z+D)^2 - s_j^2}{2} \operatorname{Ln}(z + s_j + D)$$

$$-\frac{(z+iB)^2 - s_j^2}{2} \operatorname{Ln}(z - s_j + iB)$$

$$+\frac{z^2 - s_j^2}{2} \operatorname{Ln}(z - s_j)$$

$$+\frac{(s+D+iB)^2 - s_j^2}{2} \operatorname{Ln}(z + s_j + D + iB)$$

$$+ i\left(\frac{BD}{2} - s_j B\right). \tag{28}$$

Now the electric field components E_x and E_y are related to the complex potential functions $V(z)$ and $\psi(z)$ in $V(z) + i\psi(z)$ as

$$E_x = -\frac{\partial V(z)}{\partial x} = -\frac{\partial V(z)}{a\,\partial \xi}\,, \tag{29}$$

$$E_y = -\frac{\partial V(z)}{\partial y} = \frac{\partial \psi(z)}{\partial x} = \frac{\partial \psi(z)}{a\,\partial \xi}\,. \tag{30}$$

Hence, by Eqs. (26) through (30), we obtain the electric field intensity for $V_0 = \frac{a}{2\pi\epsilon_0}$:

$$-E_x(z) + i E_y(z) = \frac{1}{2\pi\epsilon_0} \sum_{j=1}^{2M+1} \tau_j R_j'(z)\,, \tag{31}$$

$E_x(z)$, $E_y(z)$ being real functions of x and y,

where

$$R'_j(z) = \frac{(1 - \delta_{j,2M+1})}{s_{j+1} - s_j} \left\{ s_{j+1} \left[P'_{j+1}(z) - P'_j(z) \right] - \left[Q_{j+1}(z) - Q'_j(z) \right] \right\}$$

$$+ \frac{(1-\delta_{j,2M})}{s_j - s_{j-1}} \left\{ \left[Q'_j(z) - Q'_{j-1}(z) \right] - s_{j-1} \left[P'_j(z) - P'_{j-1}(z) \right] \right\} , \tag{32}$$

$$\delta_{j,r} = \begin{cases} 1 & \text{if } j = r \\ 0 & \text{if } r \neq r \end{cases} , \tag{33}$$

$$P'_j(z) \equiv \frac{\partial}{\partial \xi} P(z, s_j) = \text{Ln} \frac{(z+s_j+D)(z - s_j)}{(z + s_j+D+iB)(z - s_j+ i B)} \tag{34}$$

and

$$Q'_j(z) \equiv \frac{\partial}{\partial \xi} Q(z, s_j)$$

$$= - (z + D) \text{ Ln} (z + s_j + D)$$

$$- (z + i B) \text{ Ln} (z - s_j + i B)$$

$$+ z \text{ Ln} (z - s_j)$$

$$+ (z + D + i B) \text{ Ln} (z + s_j + D + i B) . \tag{35}$$

For convenience and to conform to our previous work[4], we shall normalize the field intensity with respect to the constant field that exists between the upper and the lower plates of infinite extent of the line; i.e., $\frac{a}{2\pi\epsilon_0 b}$. Thus, from Eq. (31), the relative field intensity is given by

$$-E_{x\,rel} + i E_{y\,rel} = \frac{b}{a} \sum_{j=1}^{2M+1} \tau_j R'_j(z) = \frac{B}{2} \sum_{j=1}^{2M+1} \tau_j R'_j(z) \quad . \qquad (36)$$

Equation (36) is used for computation of relative field intensity at a set of the field points in a surrounding area of the transmission line for different ground proximity and line width.

III

IMPEDANCE FACTOR AND ELECTRIC FIELD INTENSITIES

For the geometry of the system shown in Fig. 1-1, impedance factor f_g is compared for various ground proximity $\frac{d}{b}$ and is presented in Fig. 3-0-a. In Fig. 3-0-b, the difference of f_g for the cases of $\frac{d}{b} = 10$ and ∞ is presented. For reference we also present in Table 3-1 the impedance factor f_g for $\frac{a}{b}$, $\frac{d}{b} = 0.01$, 0.02, 0.05, 0.1, 0.2, 0.5, 1.0, 2.0, 5.0 and 10.0 are presented.

As mentioned in the Introduction, for the graphical presentation of relative fields, we adopt a cartesian coordinate system different from that shown in Fig. 1-1 (see Fig. 3-0-c). The coordinate system shown in Fig. 3-0-c is the same as the one employed in our previous work[4] for graphical presentation of relative fields and the adaptation of the same coordinate system for our present case will enable us to compare field variations for finite and semi-infinite transmission lines. It should be noted that the coordinate system shown in Fig. 3-0-c is valid only in connection with the graphs of relative fields.

In this new coordinate system, then, the edge of the upper plate facing the ground falls on the y-axis regardless of the ground proximity and the positive end of the x-axis in the graphs Figs. 3-1-a through 3-18-8 corresponds to the position of the ground plane. The introduction of this coordinate system for field variations is advantageous in that one is easily able to locate the x-coordinate of both edges of the upper plate: the x-coordinate of the upper plate facing the ground is on the $\frac{x}{b} = 0$ line (i.e., $\frac{y}{b}$ - axis) and that of the other edge is on the $\frac{x}{b} = -\frac{2a}{b}$ line.

In section 3.1, variations of relative electric field intensity are presented graphically for 16 representative cases corresponding to permutation

of the cases $\frac{|a|}{b}$, $\frac{d}{b} = 0.1,\ 0.2,\ 0.5$ and 1.0. The region of the field points for all cases is limited to $0 \leq \frac{|x|}{b} \leq \frac{3|a|+d}{b}$, $0 \leq \frac{y}{b} \leq 1.5$. The mode of the presentation is the same as that in our previous work where the width of the parallel plates was infinite (c.f. section 3 in our previous work[4]). We mention that the numerical computation for relative electric field intensity was carried out for wider range of $\frac{|a|}{b}$, $\frac{d}{b}$ variations, but because of the time and also the fact that the examination of the data revealed no significant information which is not contained in the above cases, we chose to present in this report only 16 cases.

In section 3.2, we compare the field variations between the case of $\frac{|a|}{b} = 0.5$ and ∞ for the ground proximity $\frac{d}{b} = 0.5$

3.1 Relative Electric Field Intensities, E_{yrel}, E_{xrel}.

As previously noted, for the field points, the $\frac{|x|}{b}$ interval is taken as $0 \leq \frac{|x|}{b} \leq \frac{3|a|+d}{a}$ and the $\frac{y}{b}$ interval as $0 \leq \frac{y}{b} \leq 1.5$ by the steps of $\frac{y}{b} = 0.2$. The upper plate lies on the $\frac{y}{b} = 1$ line. The variation of relative fields on the inner and the outer surfaces of the upper plate, which we denote by $\frac{y}{b} = 1-$, $1+$, respectively, are also presented.

The dotted and solid lines in the graphs in Figs. 3-1-a through 3-16-d represent the positive and the negative values, respectively.

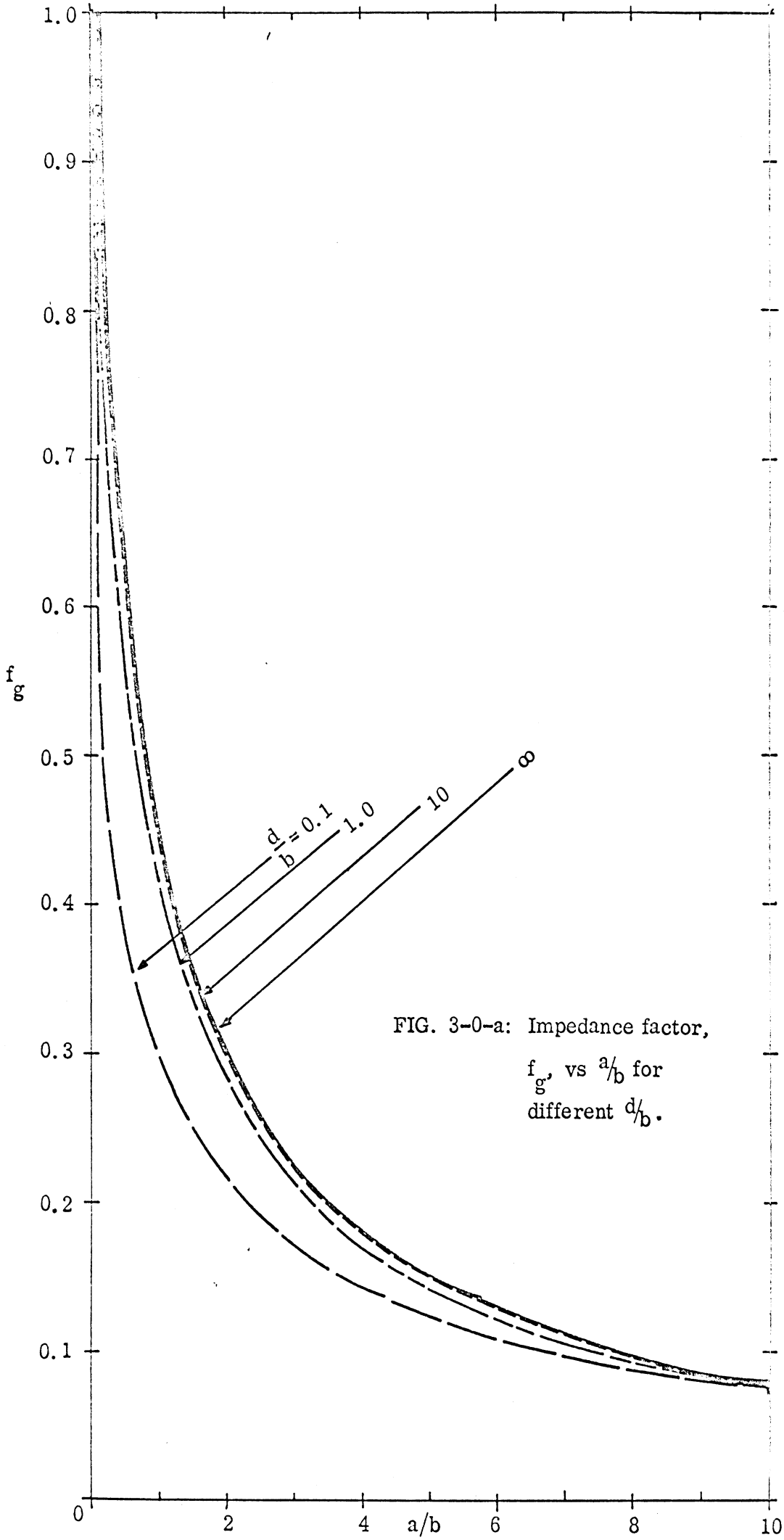

FIG. 3-0-a: Impedance factor, f_g, vs a/b for different d/b.

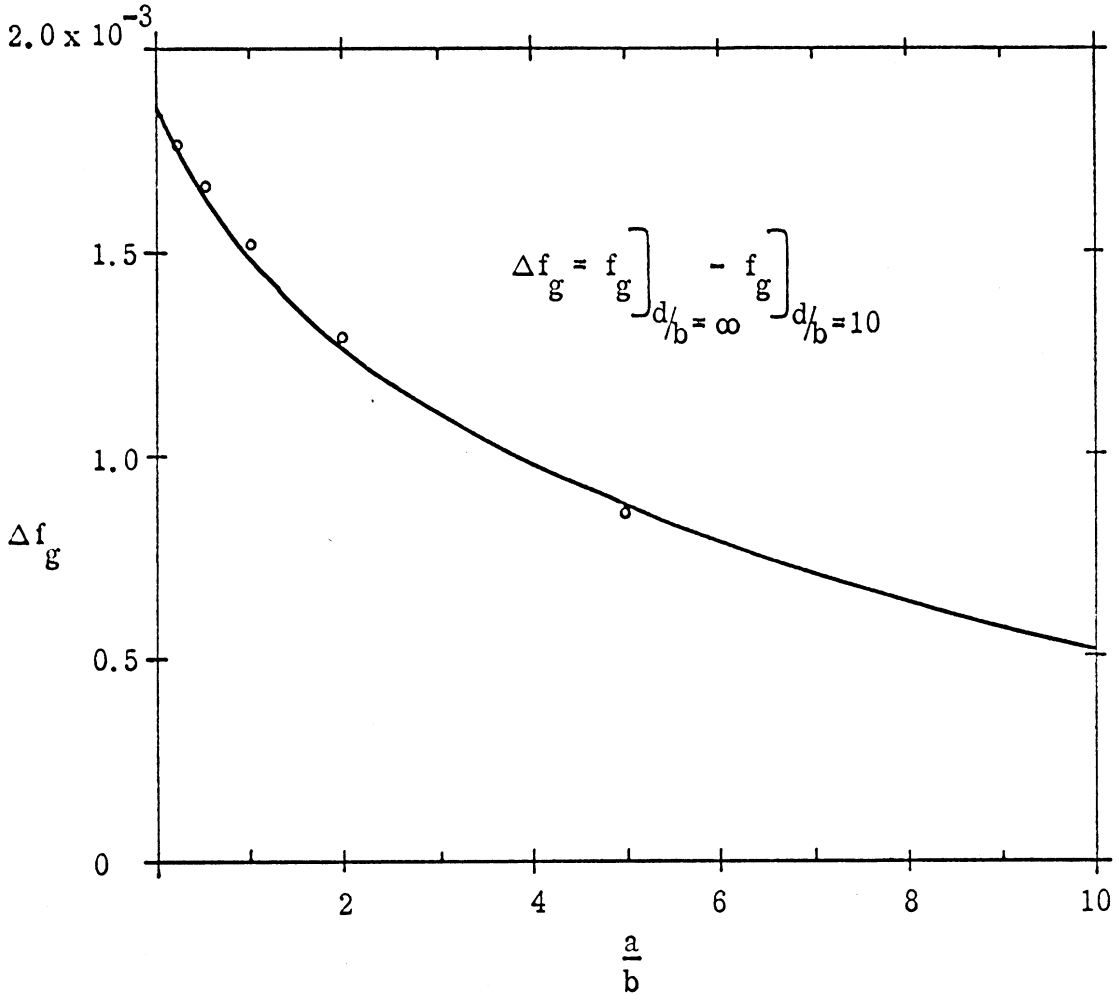

FIG. 3-0-b: The difference of f_g as a function of $\frac{a}{b}$ between $\frac{d}{b}=\infty$ and $\frac{d}{b}=10$.

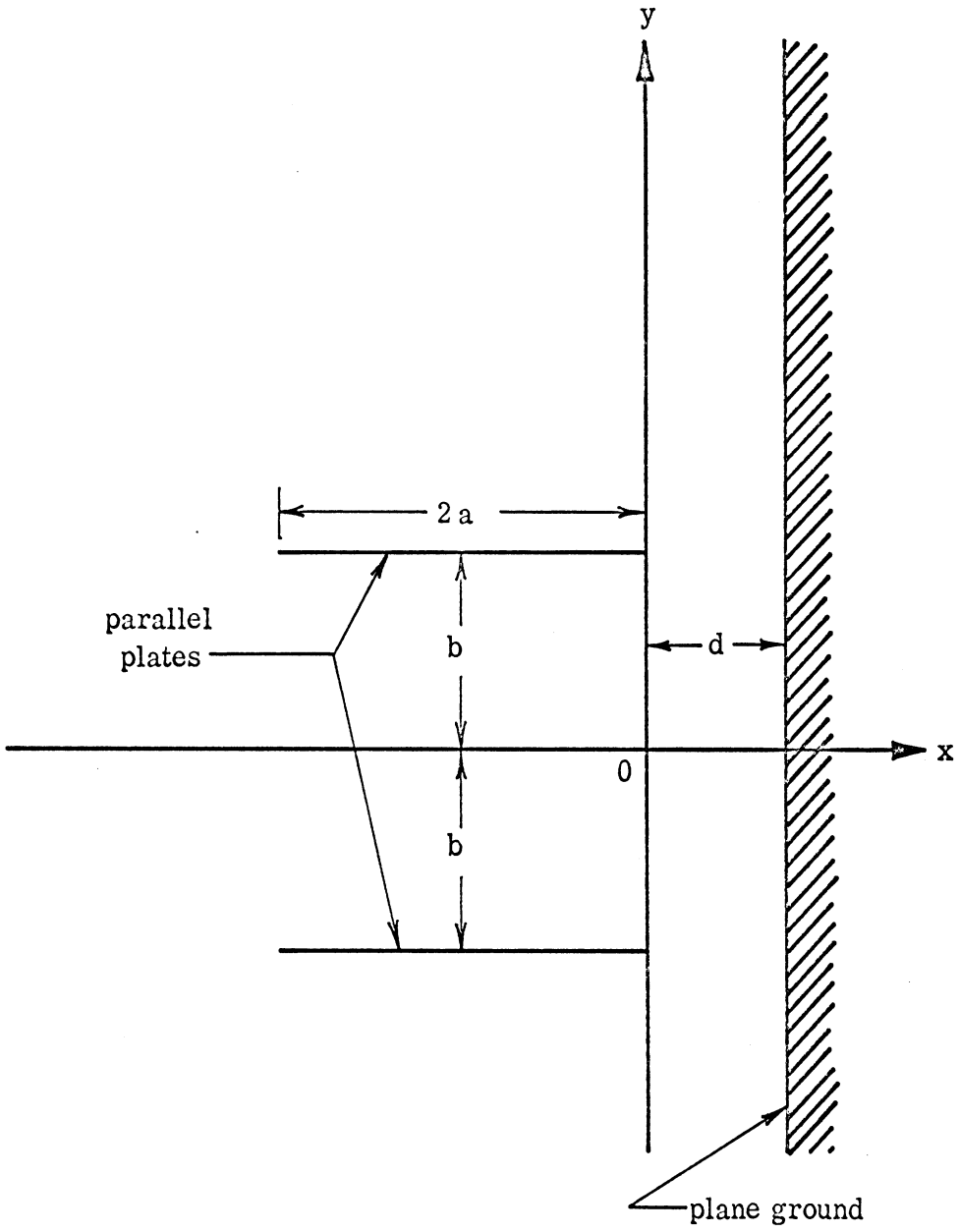

Fig. 3-0-c: Geometry of a parallel plate transmission line of finite width near a plane ground in (x, y) coordinate system for the relative fields.

Table 3-1: Impedance Factor f_g

d/b \ a/b	0.01	0.02	0.05	0.1	0.2	0.5	1.0	2.0	5.0	10.0
0.01	.6393	.5257	.4145	.3531	.3048	.2510	.1958	.1542	.1064	.0686
0.02	.78131	.6391	.4944	.4136	.3506	.2822	.2317	.1785	.1111	.07007
0.05	1.009	.8323	.6380	.5232	.4324	.3354	.2671	.1991	.1187	.0728
0.1	1.2017	1.0069	.7781	.6340	.5156	.3876	.3000	.2172	.1250	.0751
0.2	1.4031	1.1962	.9406	.7685	.6190	.4515	.3386	.2372	.1316	.0774
0.5	1.6557	1.4399	1.1618	.9610	.7726	.5463	.3940	.2645	.1399	.0803
1.0	1.7982	1.5791	1.2919	1.07811	.8698	.6085	.4304	.2822	.1451	.0821
2.0	1.8718	1.6514	1.3607	1.1418	.9249	.6467	.4543	.2946	.1490	.08340
5.0	1.9007	1.6801	1.3885	1.1683	.9491	.6657	.4680	.3029	.1521	.0846
10.0	1.9053	1.6847	1.3931	1.1728	.9534	.6695	.4711	.3051	.1532	.0851

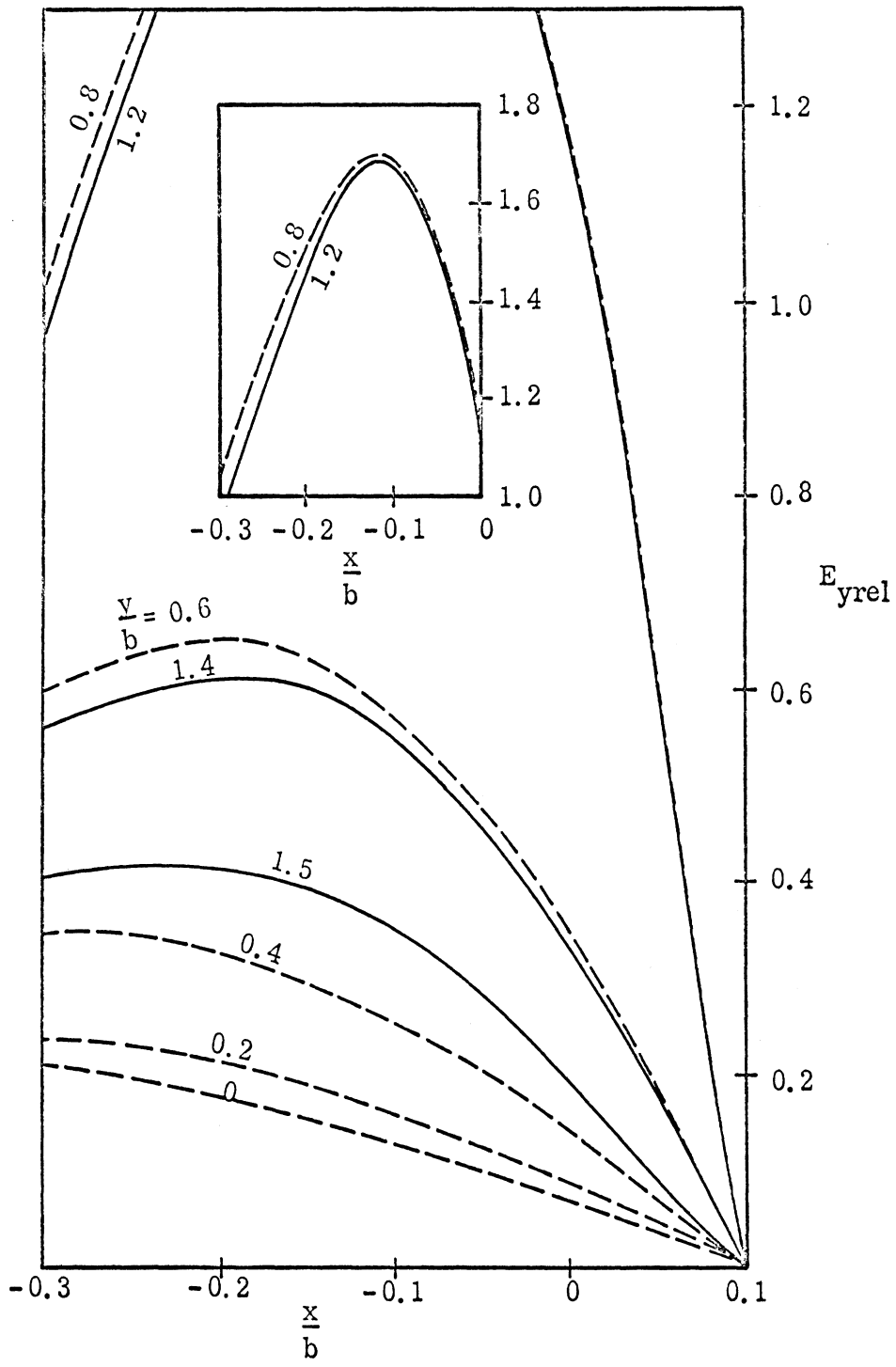

Fig. 3-1-a: E_{yrel} on $\frac{y}{b}$ = 0, 0.2, 0.4, 0.6, 0.8, 1.2, 1.4 and 1.5 lines for the case of $\frac{|a|}{b}$ = 0.1, $\frac{d}{b}$ = 0.1.

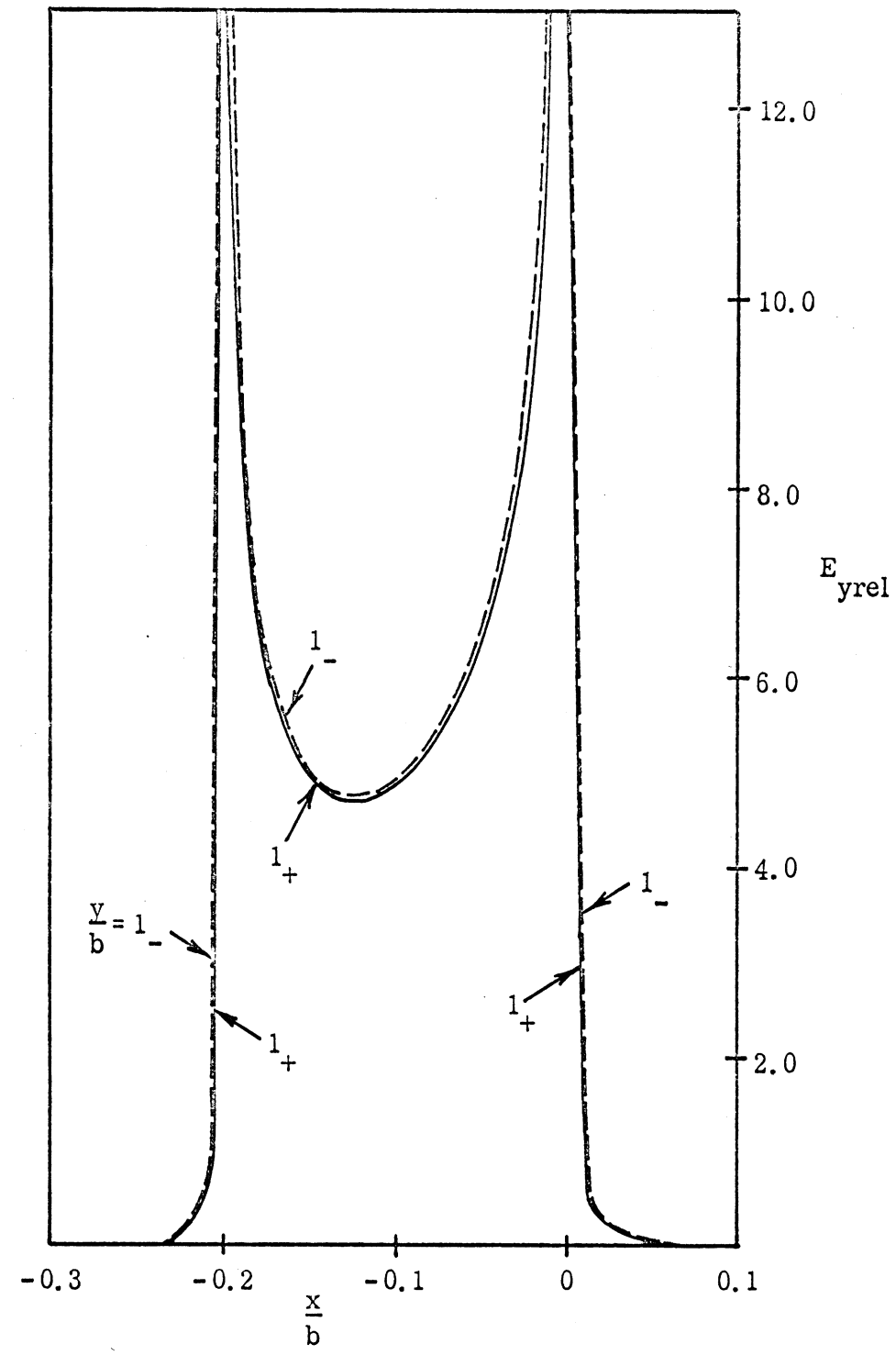

Fig. 3-1-b: E_{yrel} on $\frac{y}{b} = 1_-$ and 1_+ lines for the case of $\frac{|a|}{b} = 0.1$, $\frac{d}{b} = 0.1$.

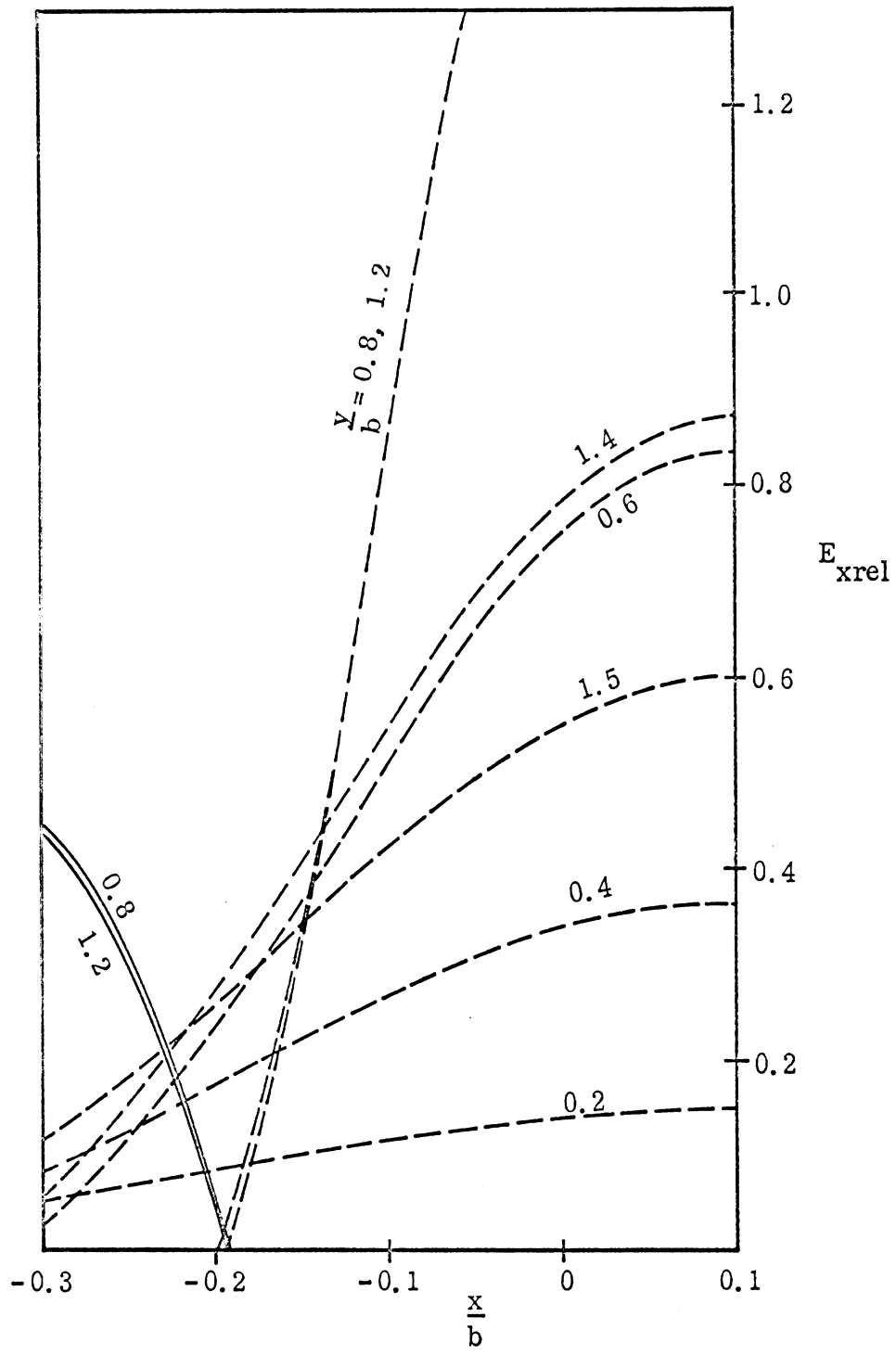

Fig. 3-1-c: E_{xrel} on $\frac{y}{b}$ = 0, 0.2, 0.4, 0.6, 0.8, 1.2, 1.4 and 1.5 lines for the case of $\frac{|a|}{b}$ = 0.1, $\frac{d}{b}$ = 0.1 (E_{xrel} on $\frac{y}{b}$ = 0 line is zero).

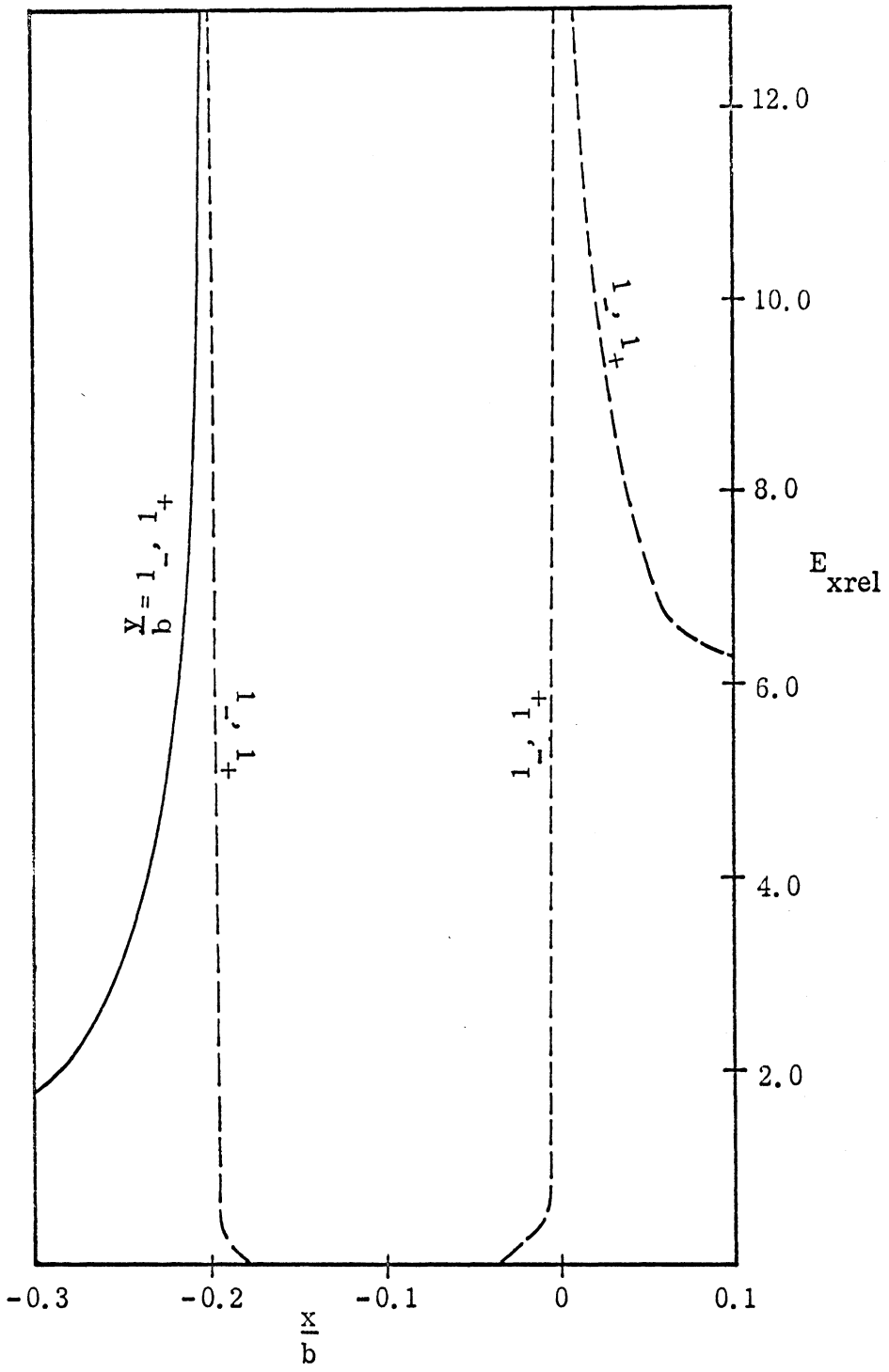

Fig. 3-1-d: E_{xrel} on $\frac{y}{b} = 1_-, 1_+$ lines for the case of $\frac{|a|}{b} = 0.1$, $\frac{d}{b} = 0.1$.

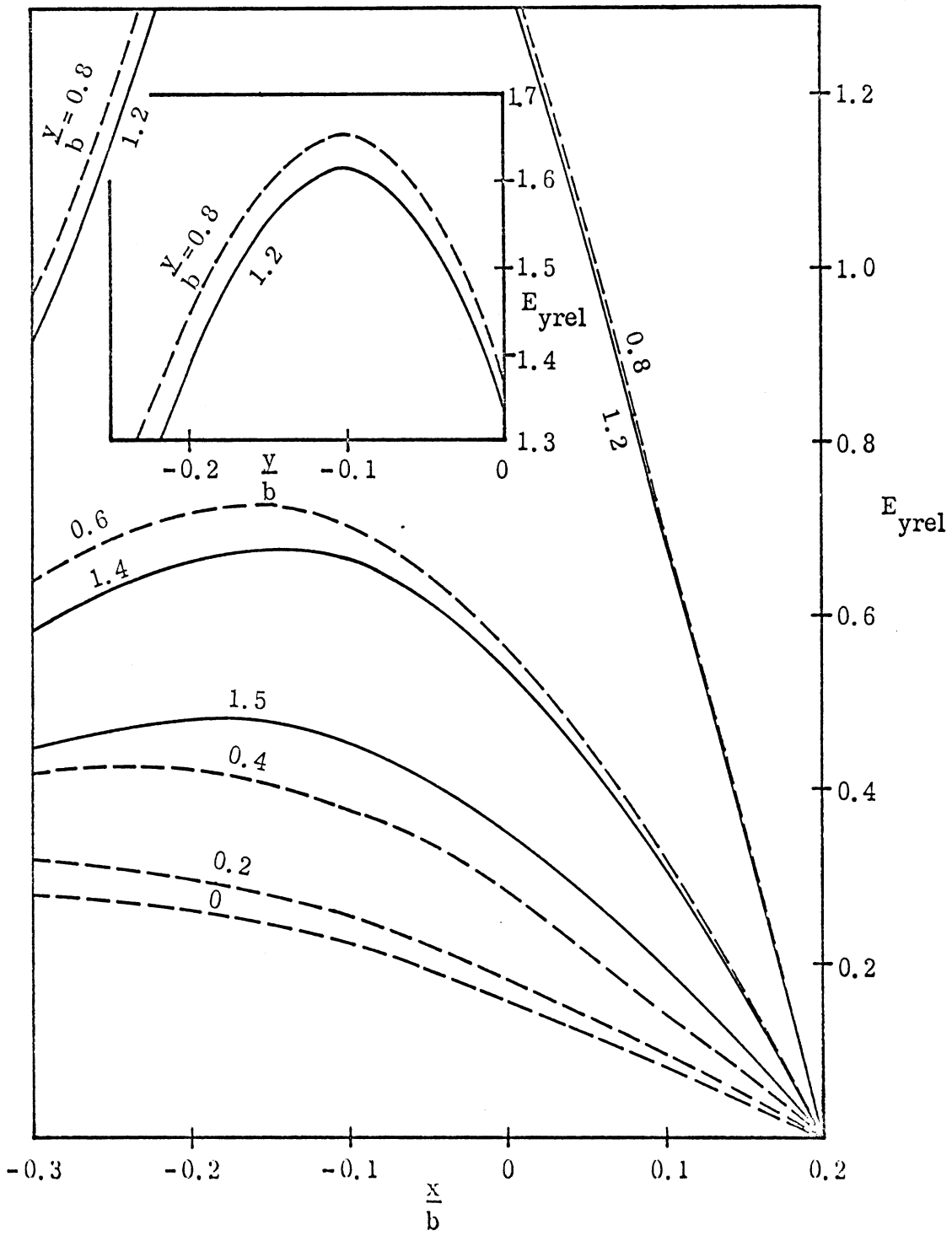

Fig. 3-2-a: E_{yrel} on $\frac{y}{b} = 0,\ 0.2,\ 0.4,\ 0.6,\ 0.8,\ 1.2,\ 1.4$ and 1.5 lines for the case of $\frac{a}{b} = 0.1,\ \frac{d}{b} = 0.2$.

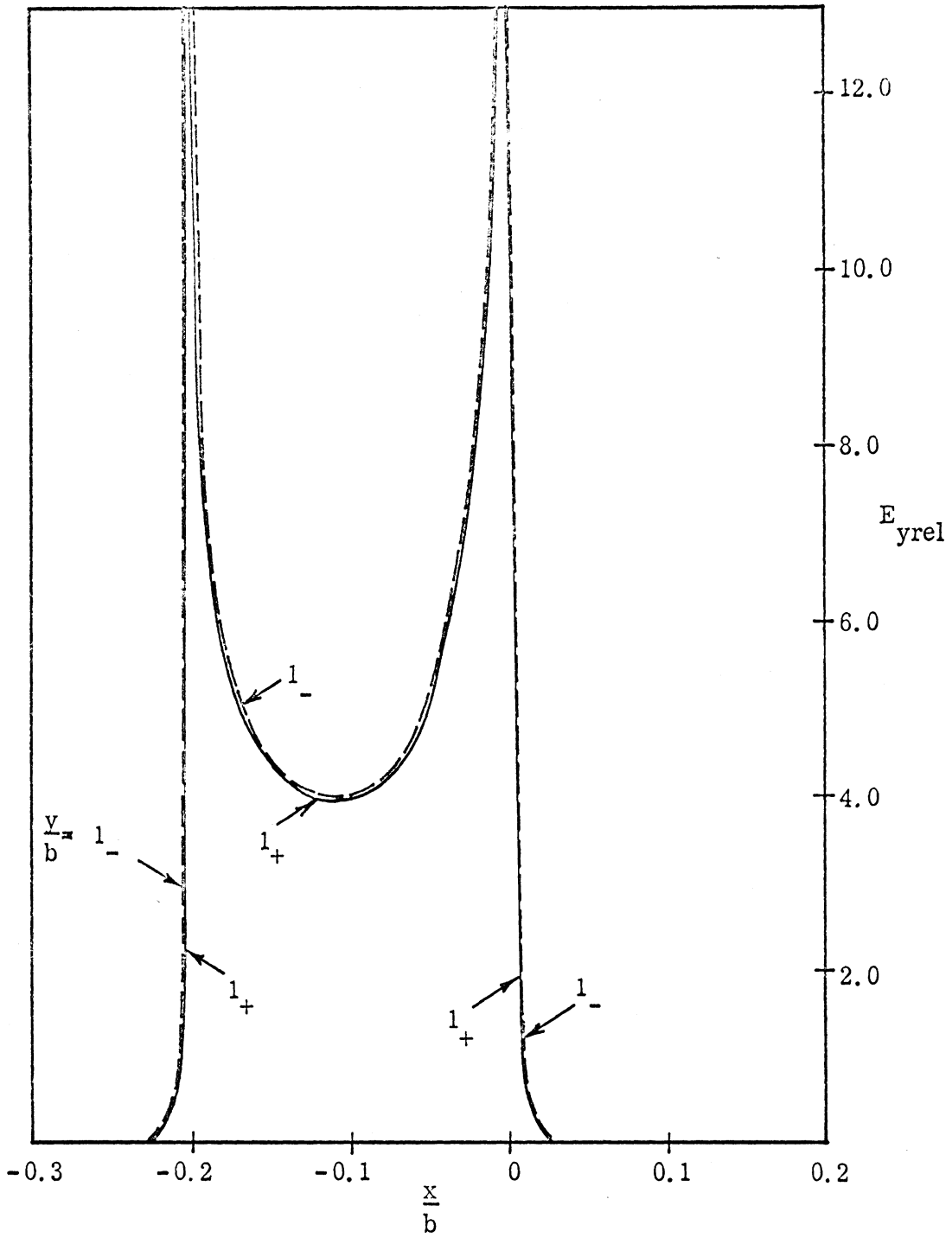

Fig. 3-2-b: E_{yrel} on $\frac{y}{b} = 1_-$ and 1_+ lines for the case of $\frac{|a|}{b} = 0.1$, $\frac{d}{b} = 0.2$.

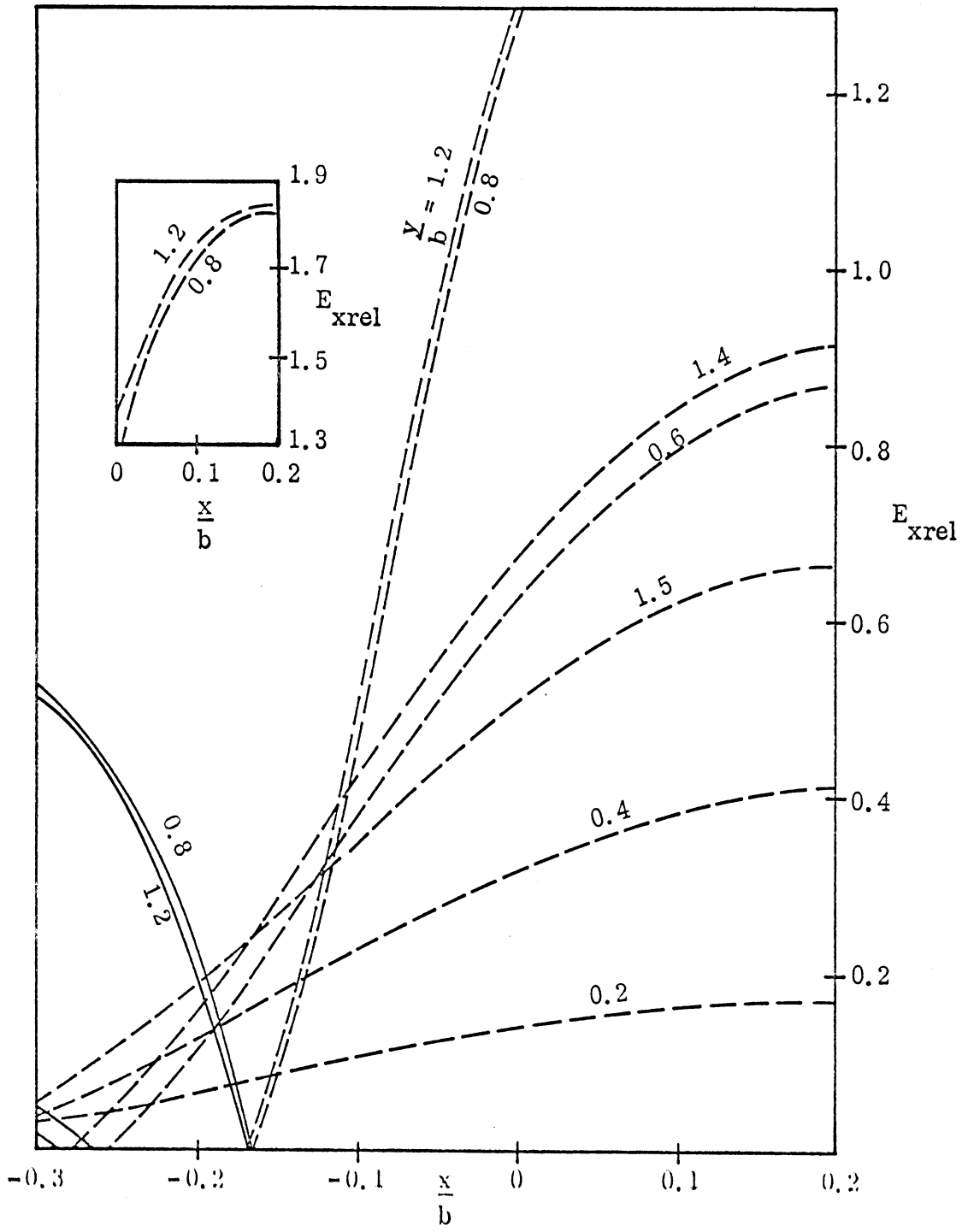

Fig. 3-2-c: E_{xrel} on $\frac{y}{b}$ = 0, 0.2, 0.4, 0.6, 0.8, 1.2, 1.4 and 1.5 lines for the case of $\frac{|a|}{b}$ = 0.1, $\frac{d}{b}$ = 0.2 (E_{xrel} on $\frac{y}{b}$ = 0 is zero).

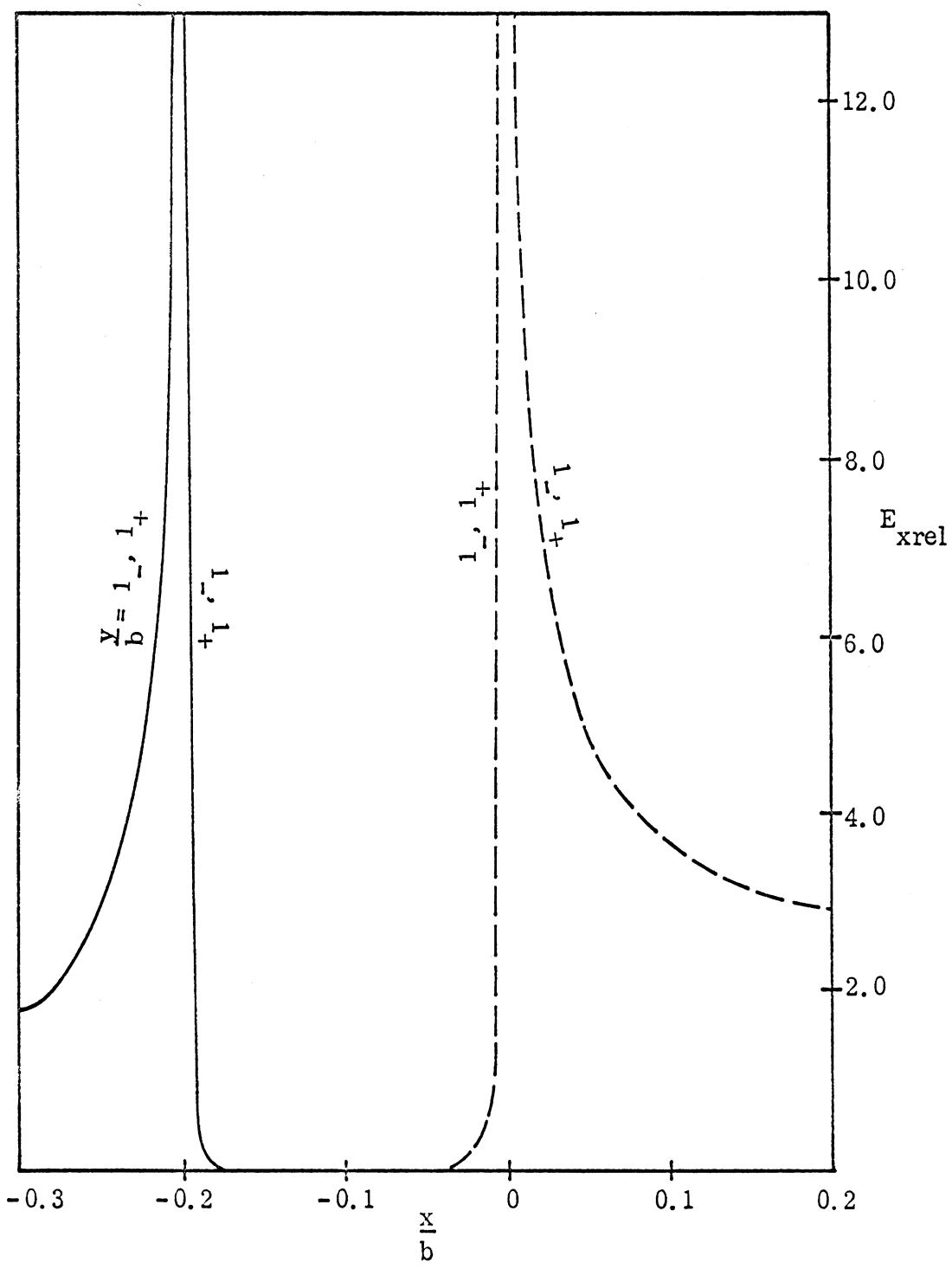

Fig. 3-2-d: E_{xrel} on $\frac{y}{b} = 1_-$ and 1_+ lines for the case of $\frac{|a|}{b} = 0.1$, $\frac{d}{b} = 0.2$.

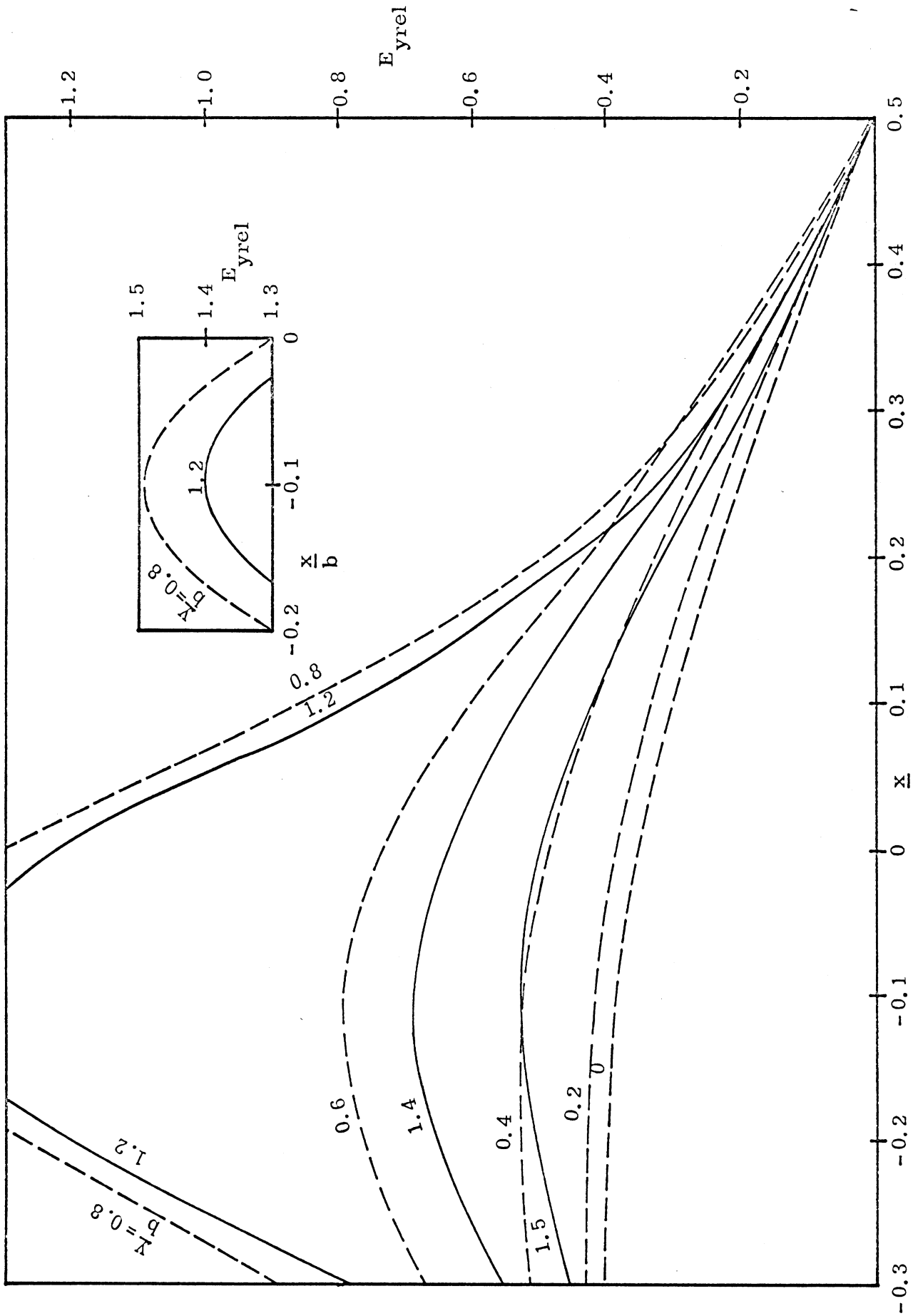

Fig. 3-3-a: E_{yrel} on $\frac{Y}{b}$ = 0, 0.2, 0.4, 0.6, 0.8, 1.2, 1.4 and 1.5 lines for the case of $\frac{|a|}{b}$ = 0.1, $\frac{d}{b}$ = 0.5.

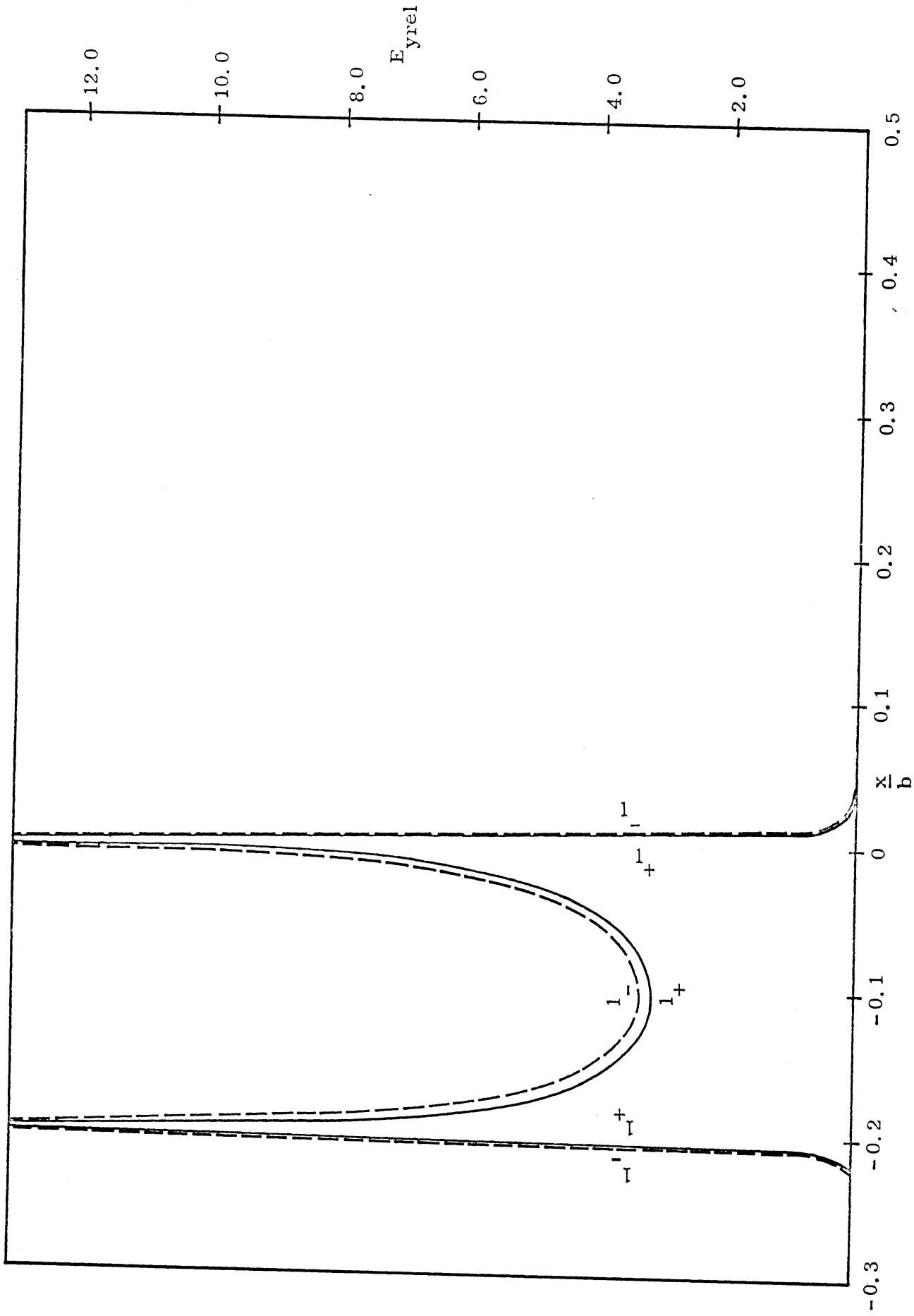

Fig. 3-3-b: E_{yrel} on $\frac{y}{b} = l_-$ and l_+ lines for the case of $\frac{|a|}{b} = 0.1$, $\frac{d}{b} = 0.5$.

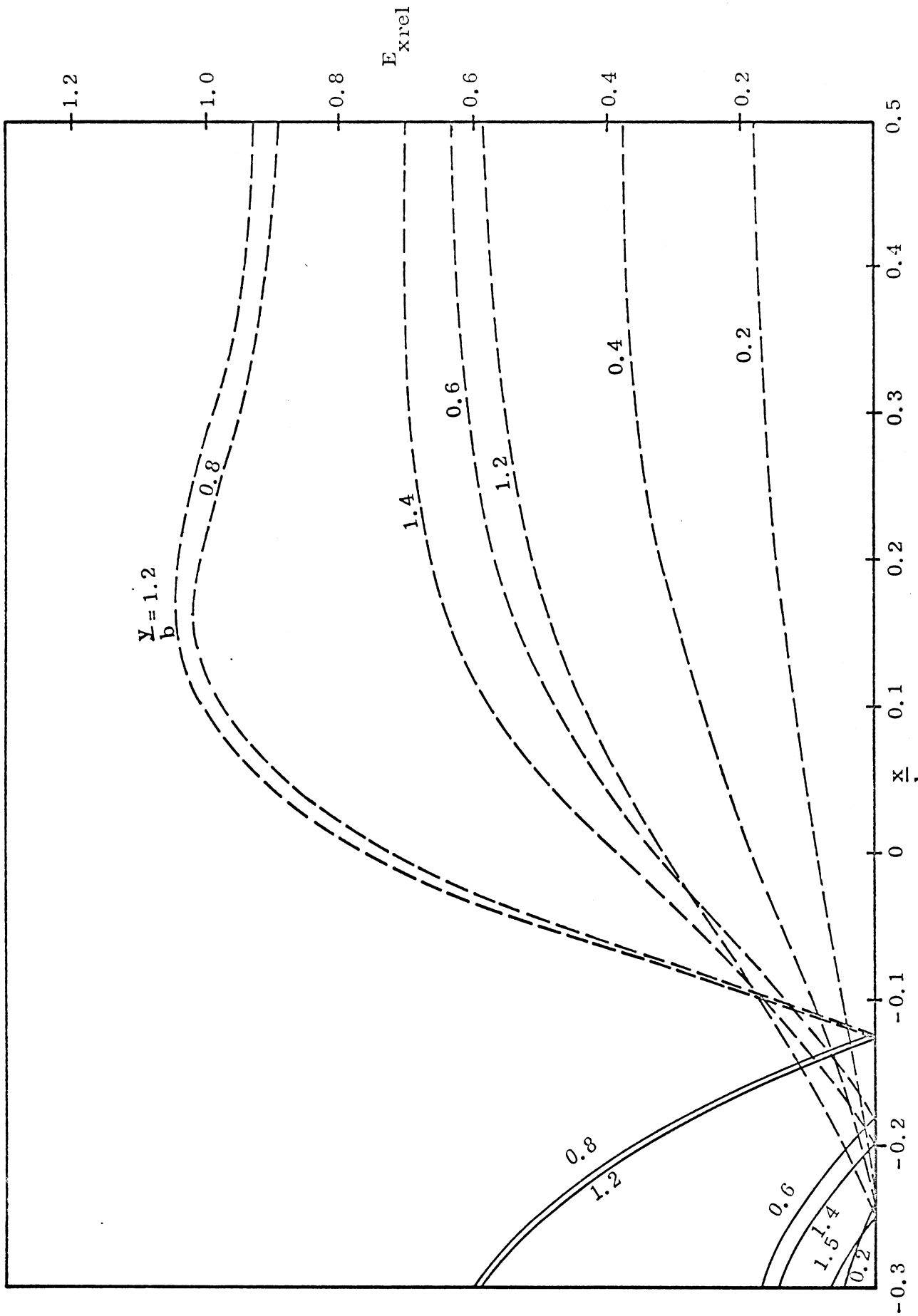

Fig. 3-3-c: E_{xrel} on $\frac{y}{b}$ = 0, 0.2, 0.4, 0.6, 0.8, 1.2, 1.4 and 1.5 lines for the case of $\frac{|a|}{b}$ = 0.1, $\frac{d}{b}$ = 0.5.
(E_{xrel} on $\frac{y}{b}$ = 0 line is zero).

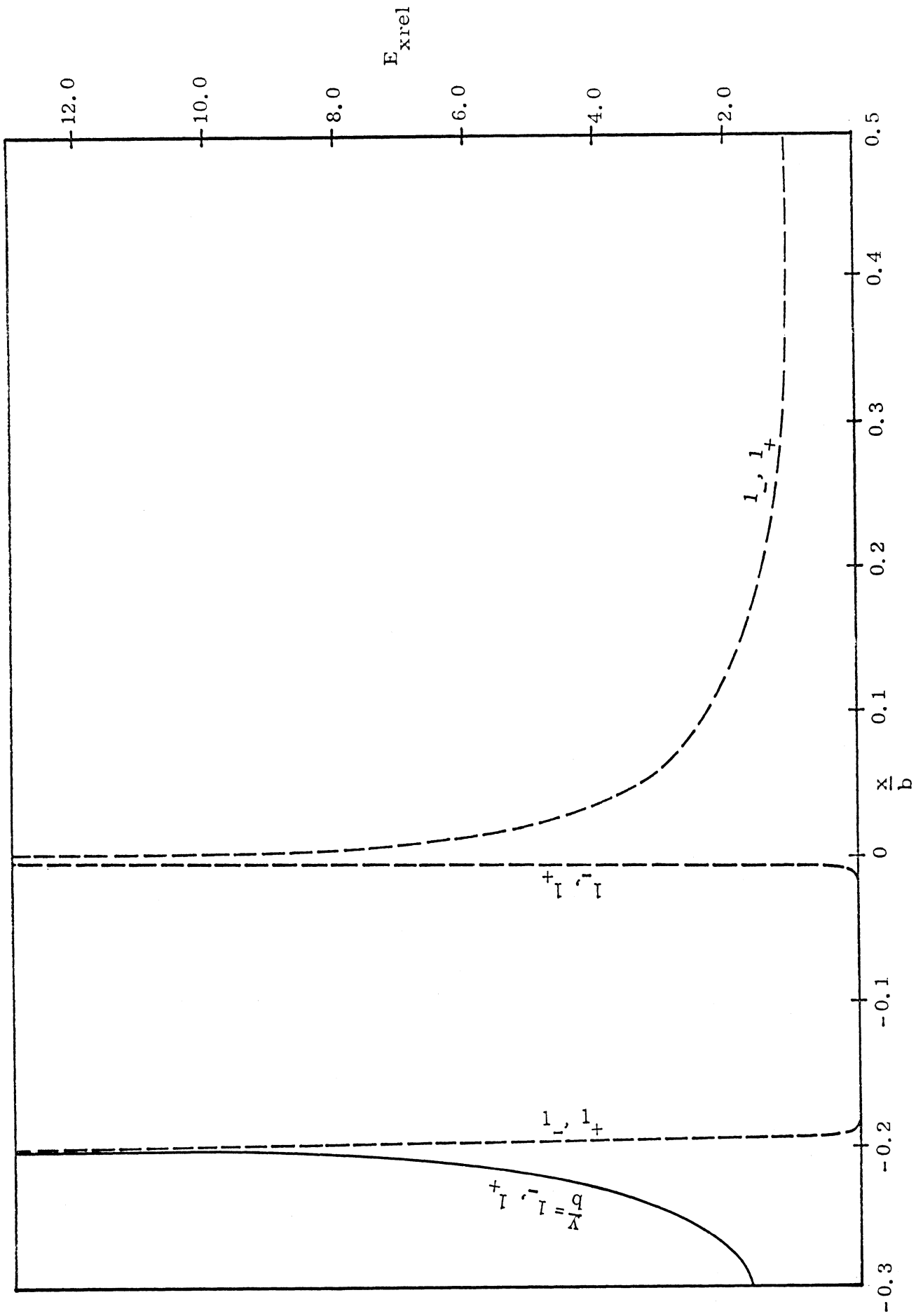

Fig. 3-3-d: E_{xrel} on $\frac{y}{b} = l_-$ and l_+ lines for the case of $\frac{|a|}{b} = 0.1$, $\frac{d}{b} = 0.5$.

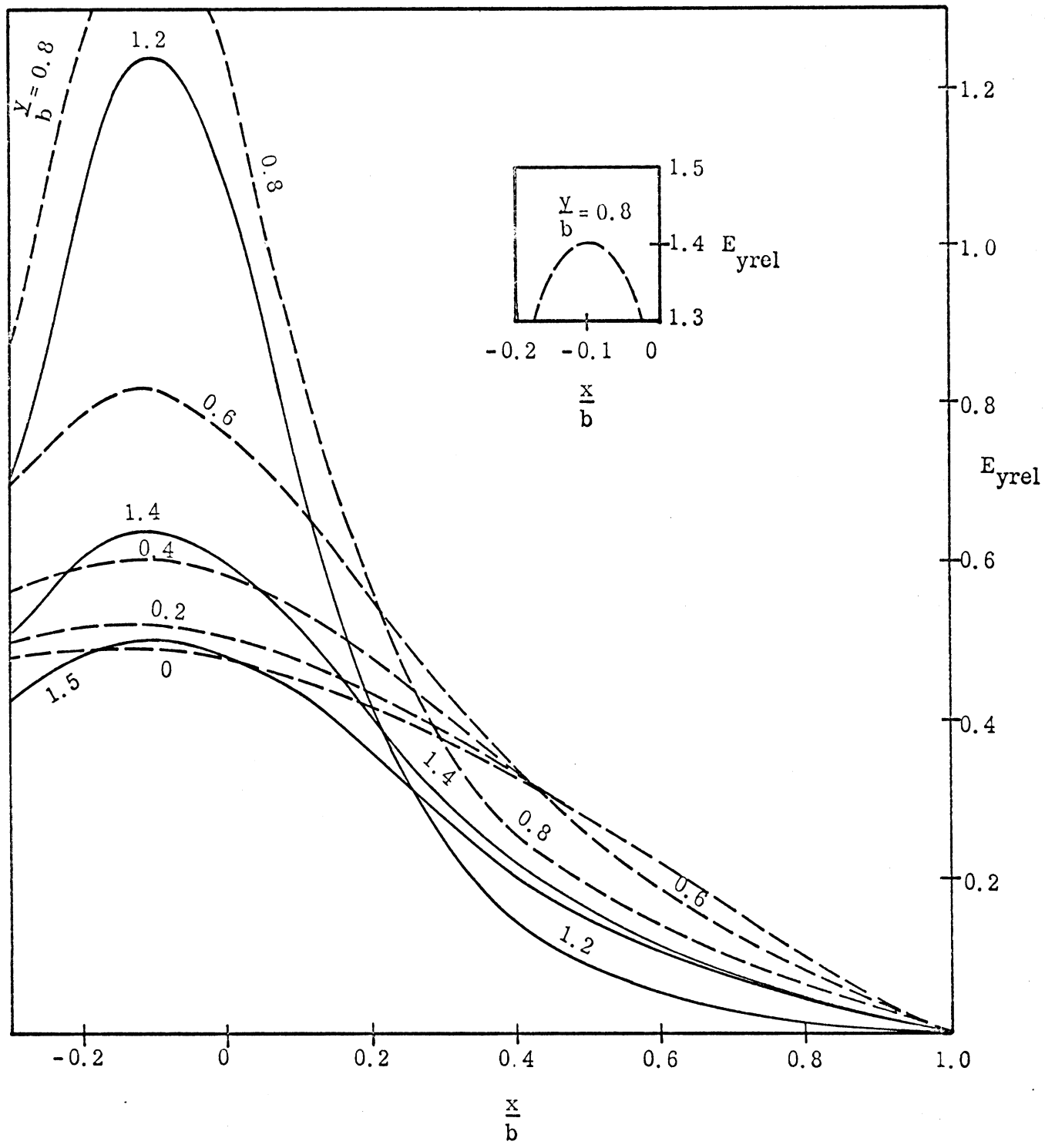

Fig. 3-4-a: E_{yrel} on $\frac{y}{b}$ = 0, 0.2, 0.4, 0.6, 0.8, 1.2, 1.4 and 1.5 lines for $\frac{|a|}{b}$ = 0.1, $\frac{d}{b}$ = 1.0.

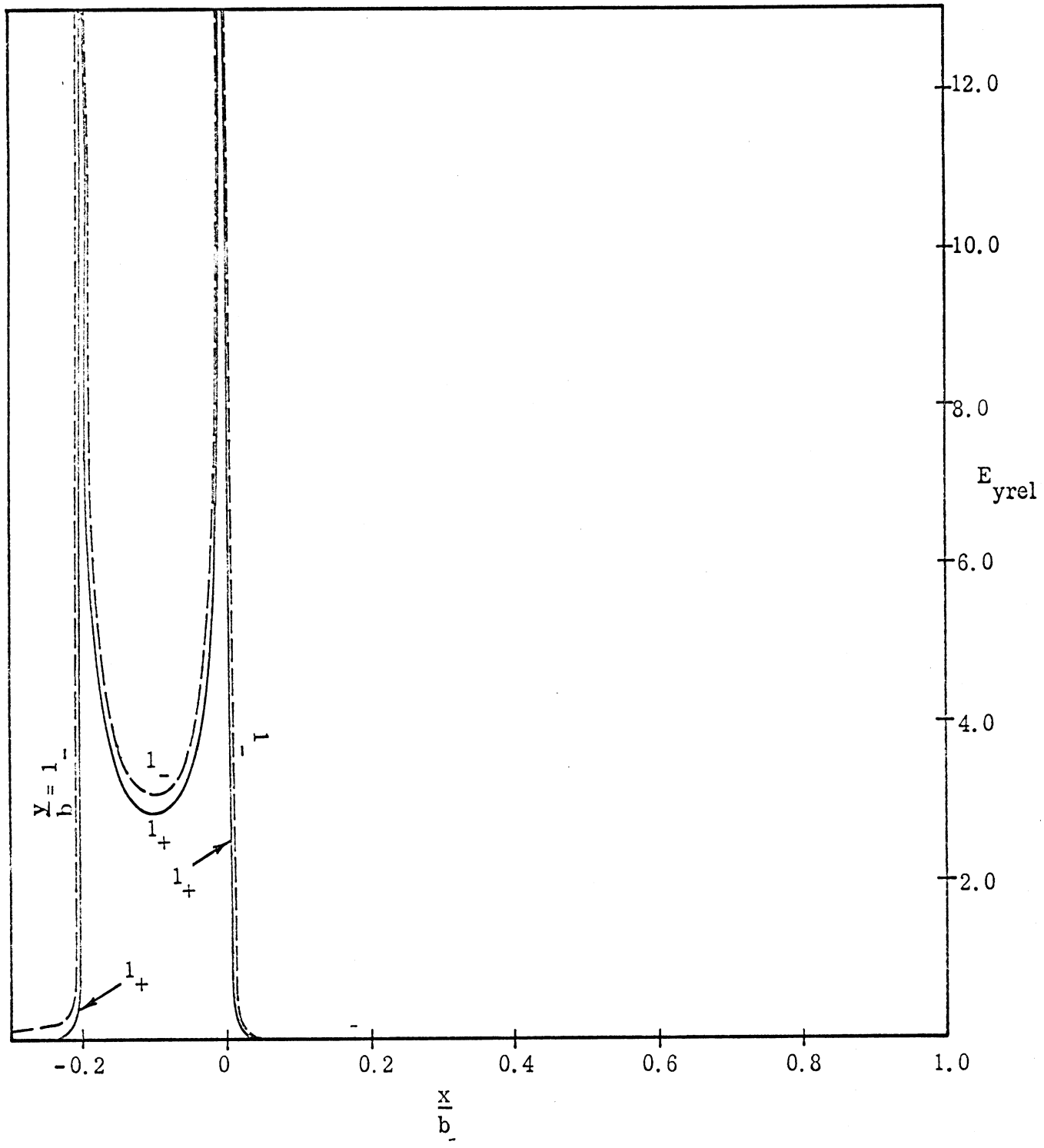

Fig. 3-4-b: E_{yrel} on $\frac{y}{b} = 1_-$ and 1_+ lines for the case of $\frac{|a|}{b} = 0.1$, $\frac{d}{b} = 1.0$.

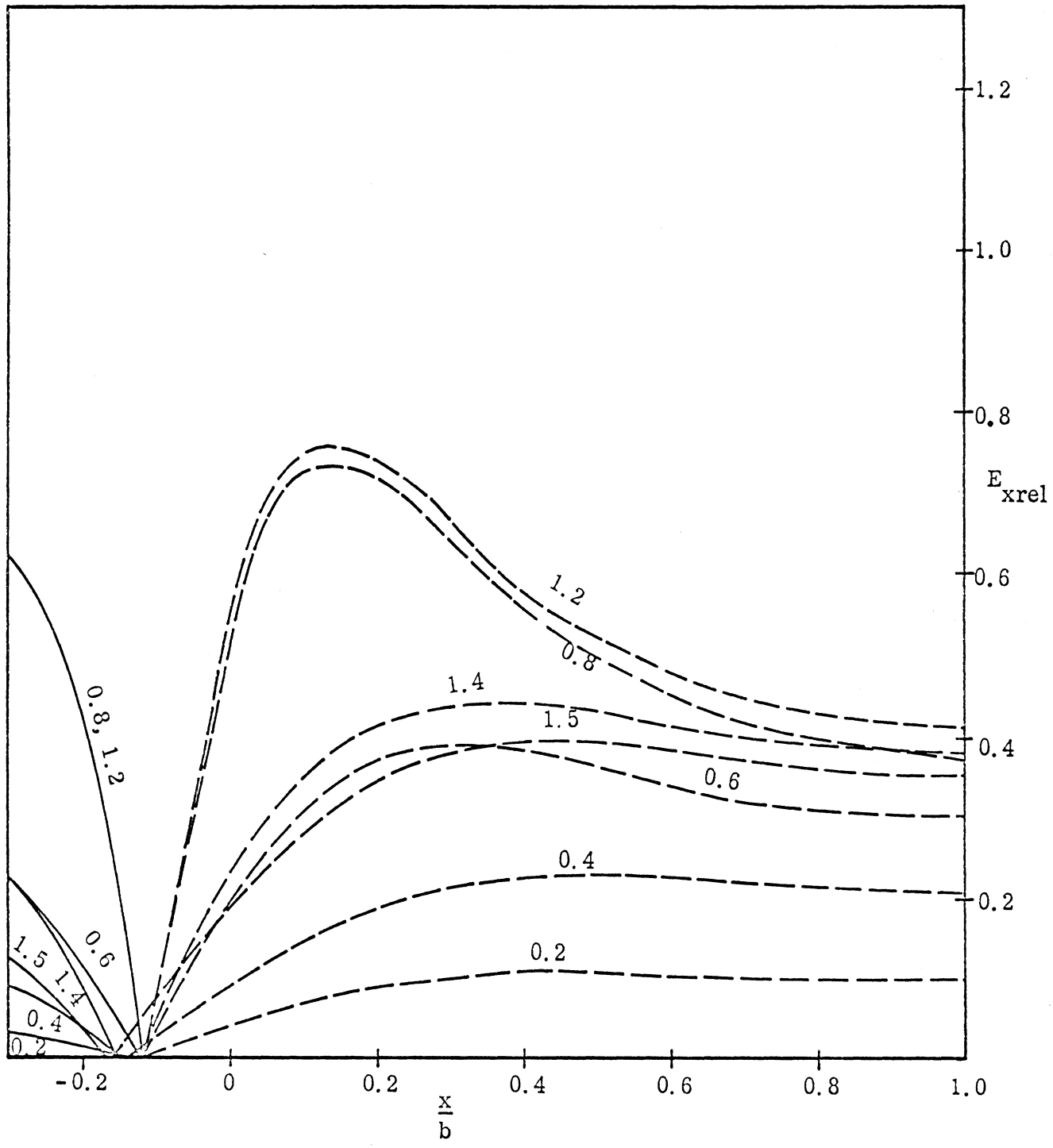

Fig. 3-4-c: E_{xrel} on $\frac{y}{b}$ = 0, 0.2, 0.4, 0.6, 0.8, 1.2, 1.4 and 1.5 lines for the case of $\frac{|a|}{b}$ = 0.1, $\frac{d}{b}$ = 1.0 (E'_{xrel} on $\frac{y}{b}$ = 0 line is zero).

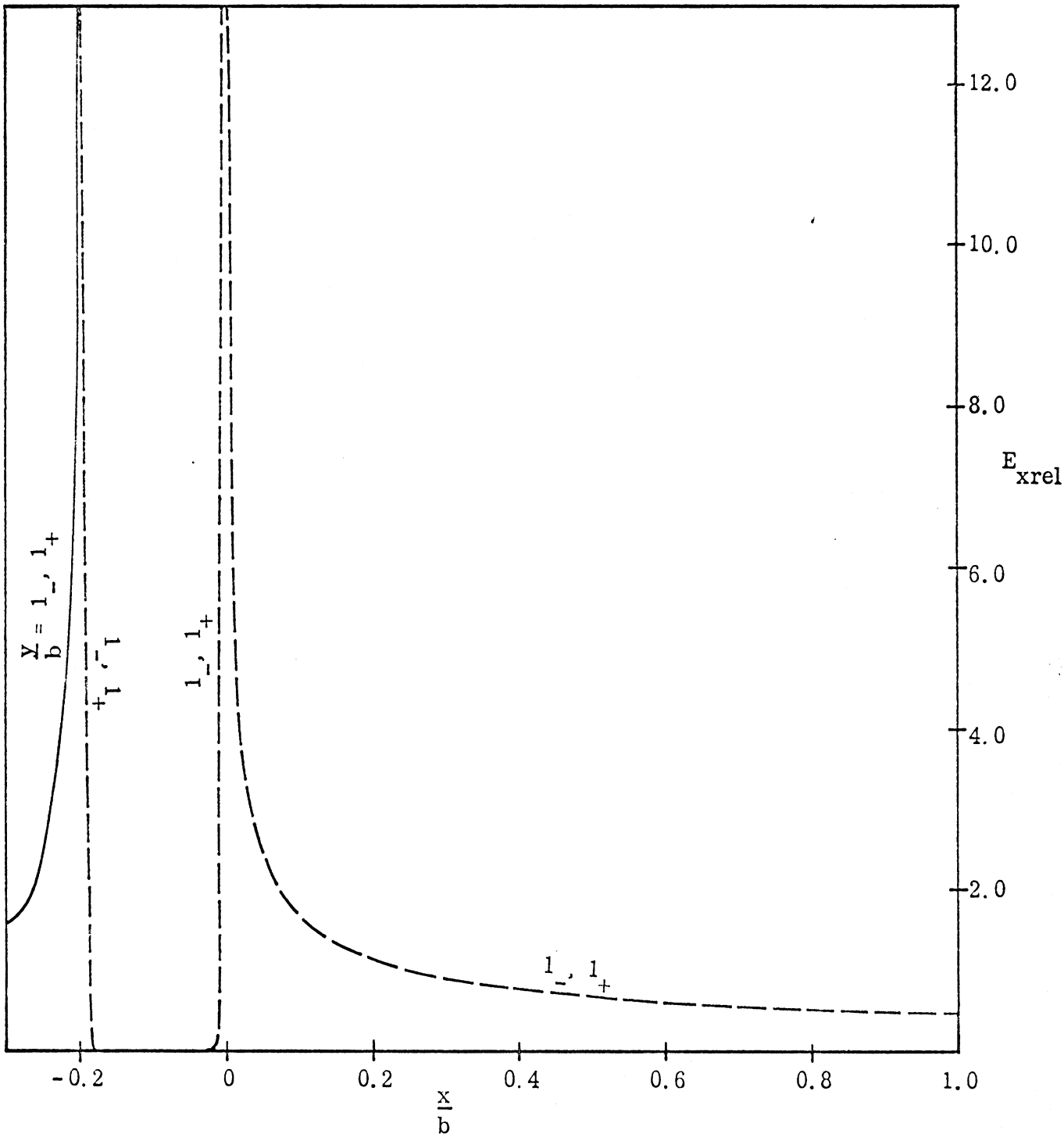

Fig. 3-4-d: E_{xrel} on $\frac{y}{b} = 1_-$ and 1_+ lines for the case of $\frac{|a|}{b} = 0.1$, $\frac{d}{b} = 1.0$.

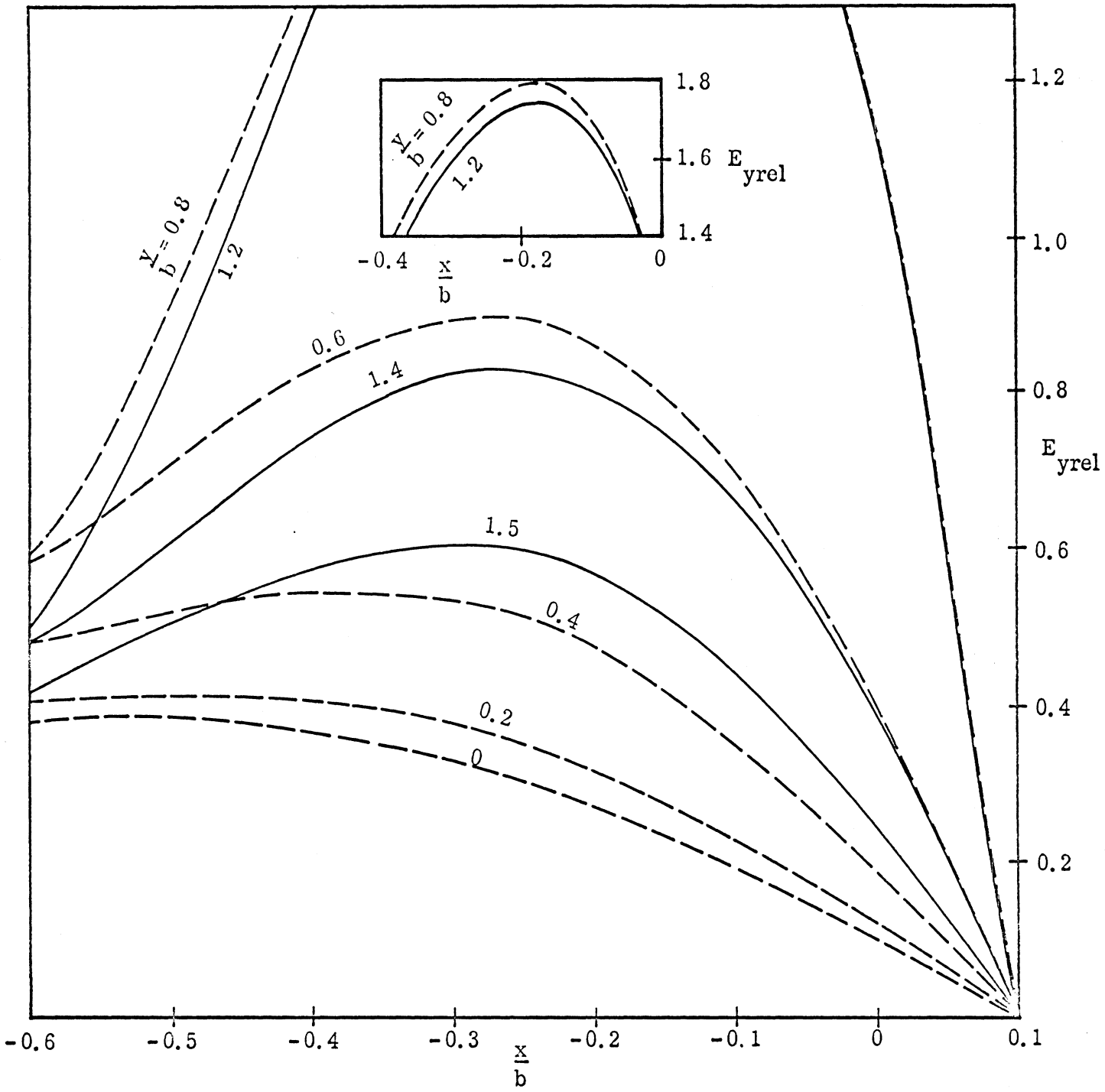

Fig. 3-5-a: E_{yrel} on $\frac{y}{b}$ = 0, 0.2, 0.4, 0.6, 0.8, 1.2, 1.4 and 1.5 lines for the case of $\frac{|a|}{b}$ = 0.2, $\frac{d}{b}$ = 0.1.

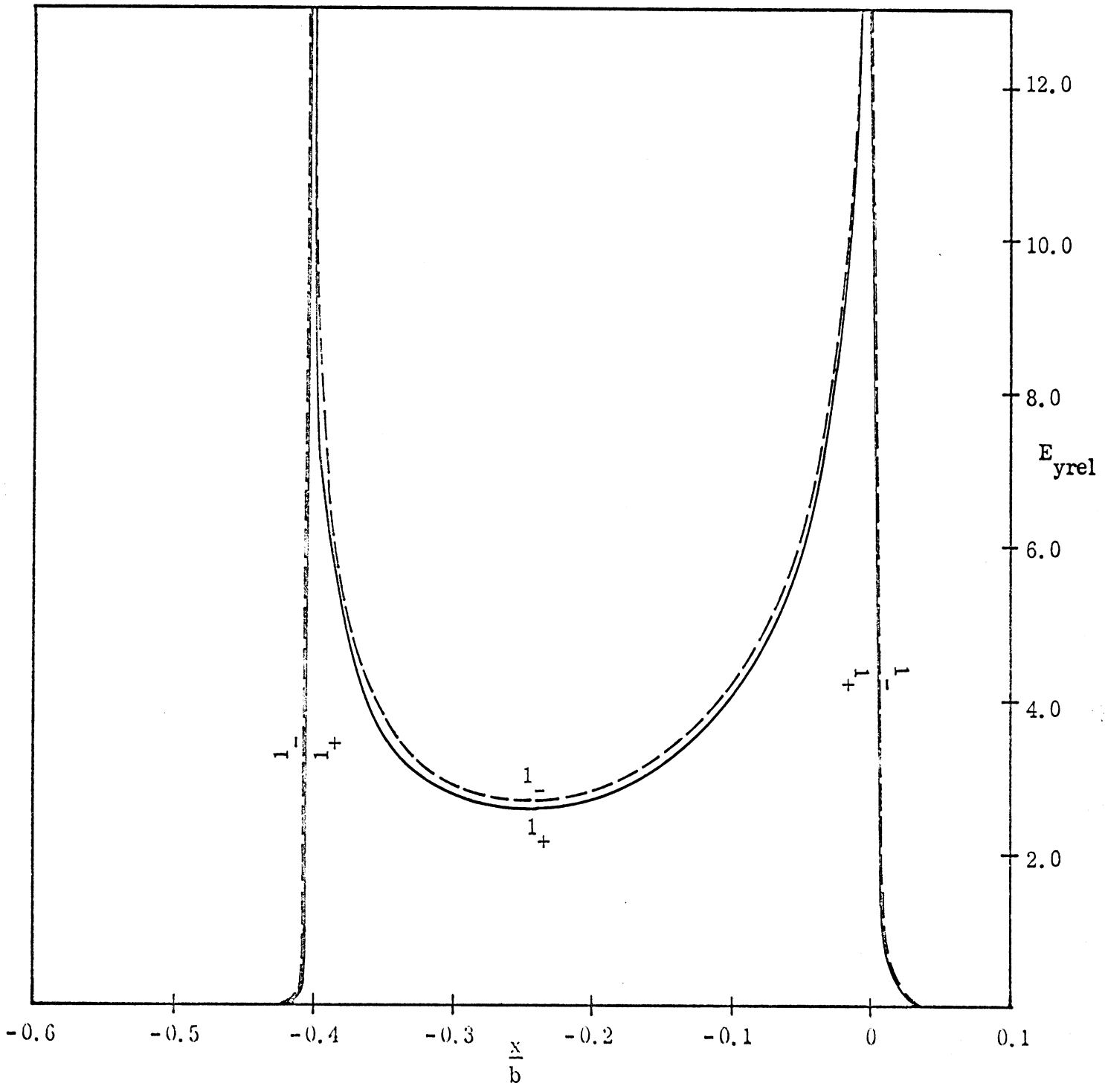

Fig. 3-5-b: E_{yrel} on $\frac{y}{b} = 1_-$ and 1_+ lines for the case of $\frac{|a|}{b} = 0.2$, $\frac{d}{b} = 0.1$.

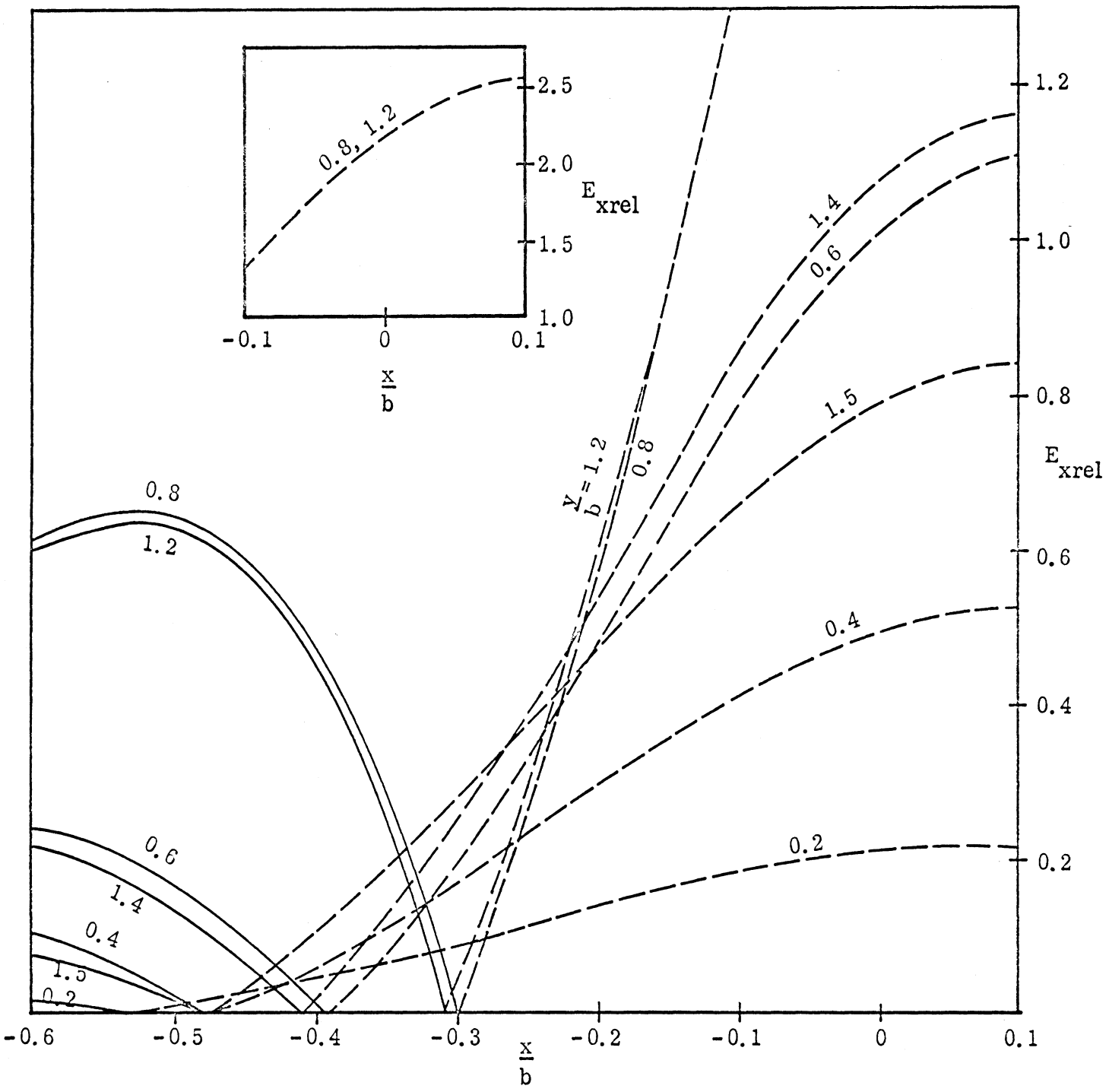

Fig. 3-5-c: E_{xrel} on $\frac{y}{b} = 0$, 0.2, 0.4, 0.6, 0.8, 1.2, 1.4 and 1.5 lines for the case of $\frac{|a|}{b} = 0.2$, $\frac{d}{b} = 0.1$ (E_{xrel} on $\frac{y}{b} = 0$ line is zero).

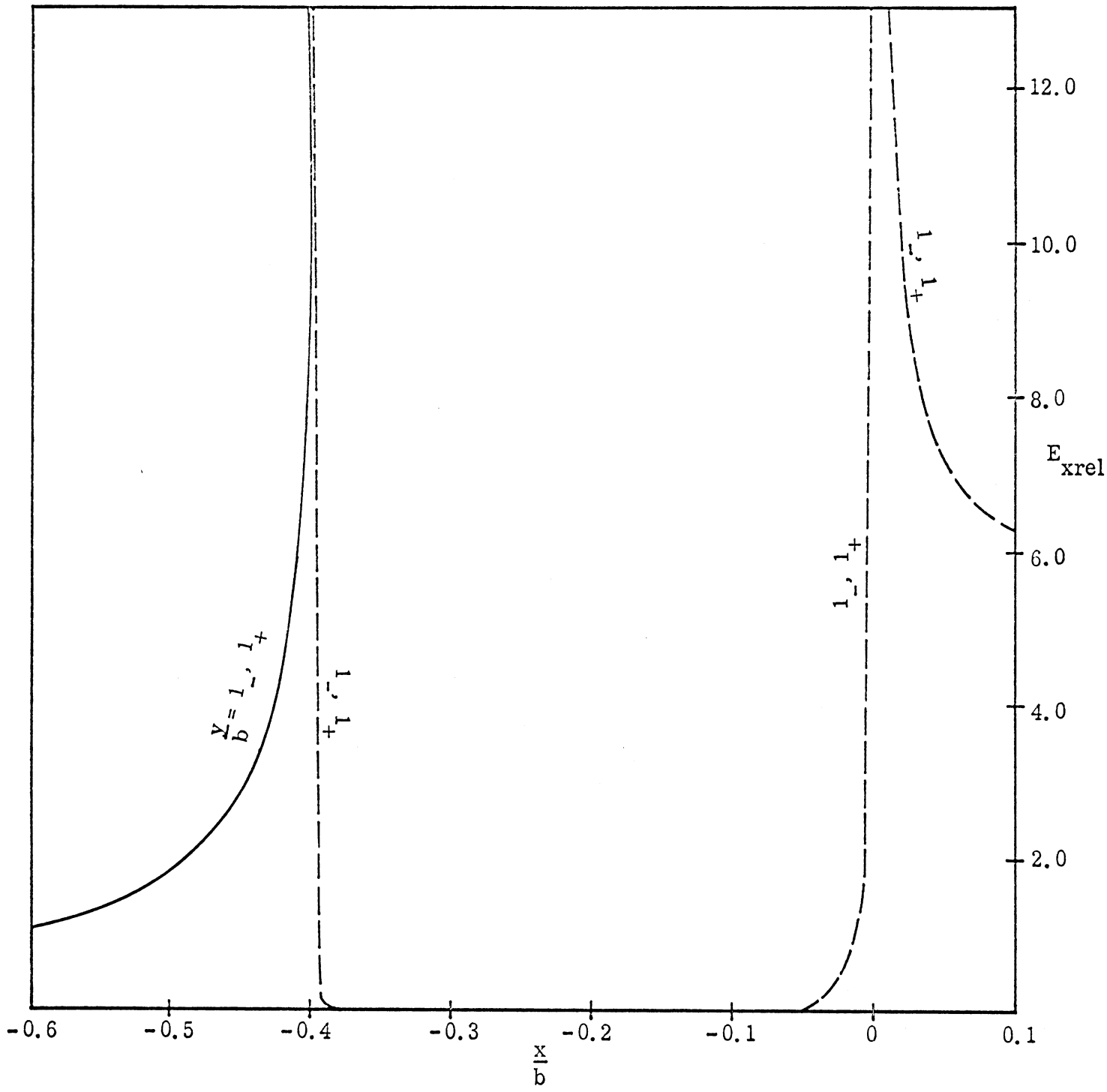

Fig. 3-5-d: E_{xrel} on $\frac{y}{b} = 1_-, 1_+$ lines for the case of $\frac{|a|}{b} = 0.2$, $\frac{d}{b} = 0.1$.

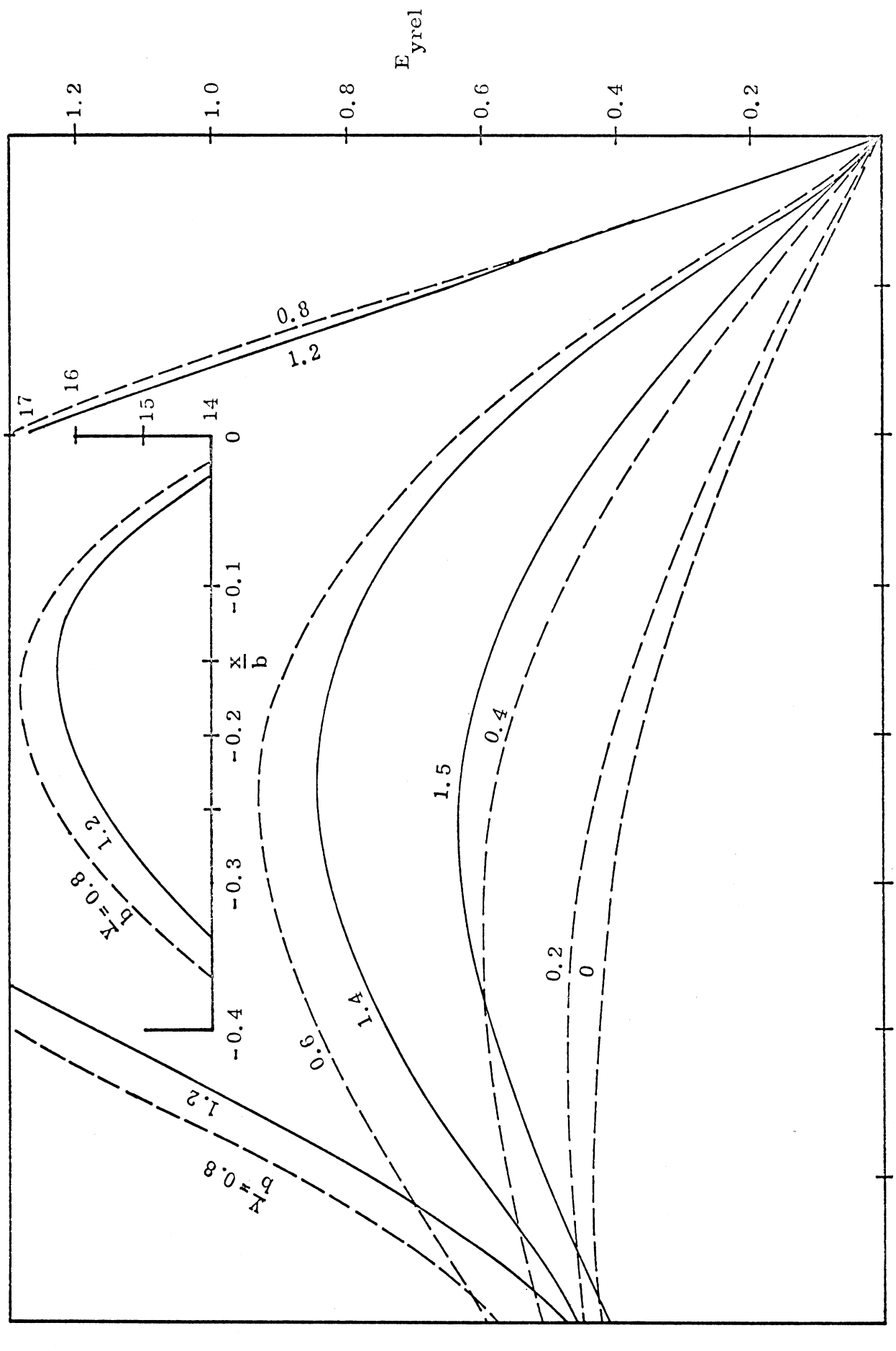

Fig. 3-6-a: E_{yrel} on $\frac{Y}{b}$ = 0, 0.2, 0.4, 0.6, 0.8, 1.2, 1.4 and 1.5 lines for the case of $\frac{|a|}{b}$ = 0.2, $\frac{d}{b}$ = 0.2.

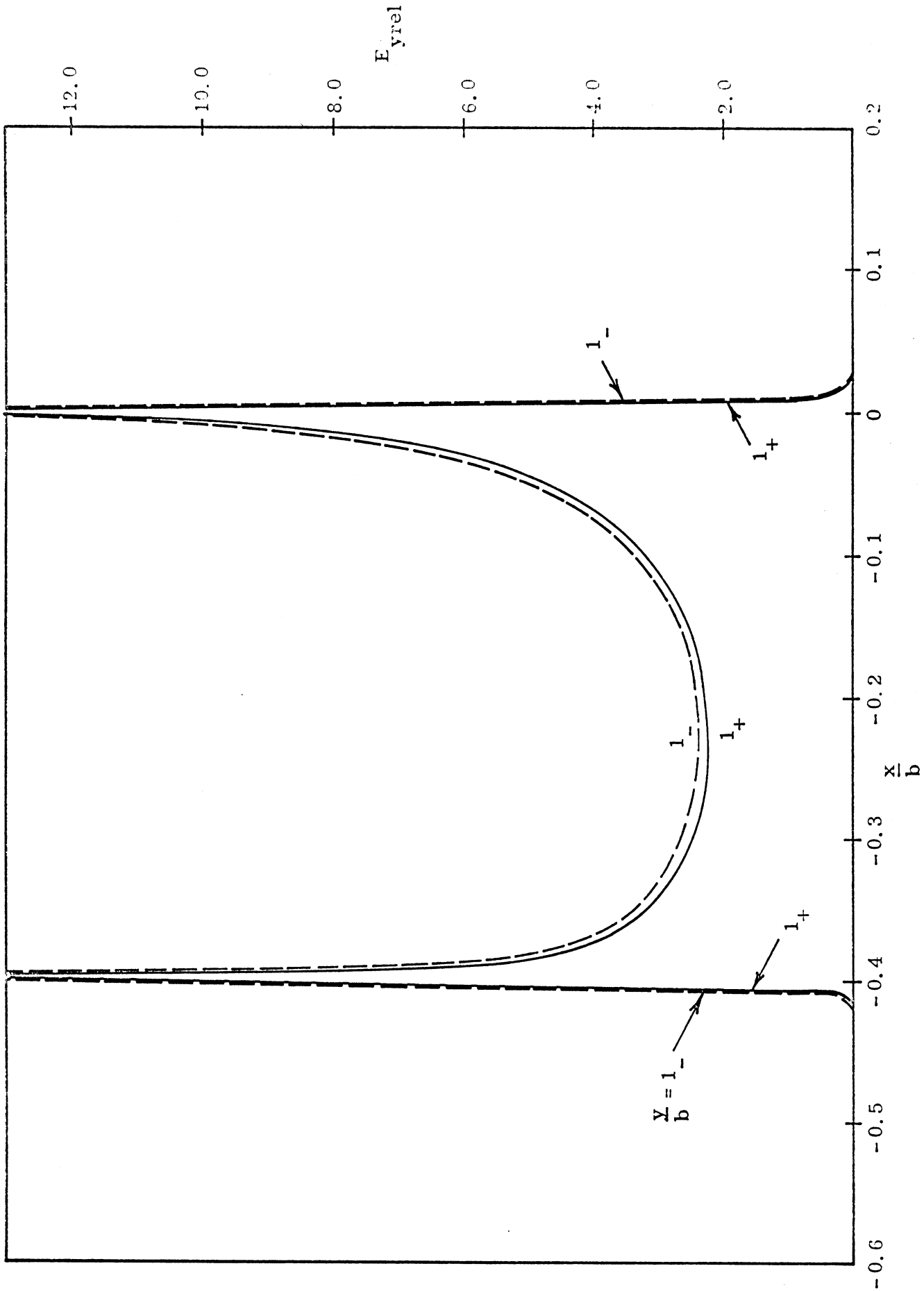

Fig. 3-6-b: E_{yrel} on $\frac{Y}{b} = 1_-$ and 1_+ lines for the case of $\frac{a}{b} = 0.2$, $\frac{d}{b} = 0.2$.

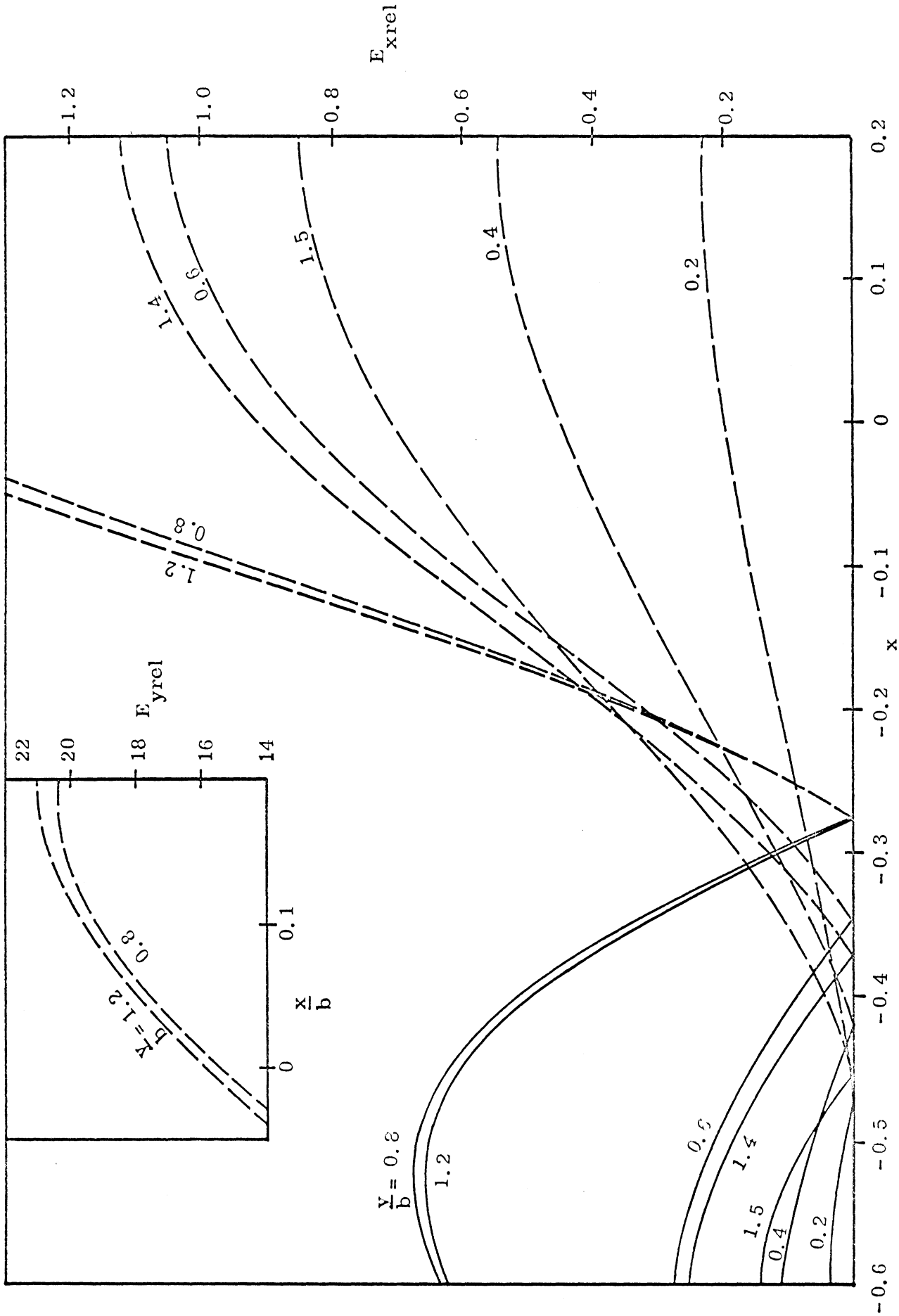

Fig. 3-6-c: E_{xrel} on $\frac{Y}{b}$= 0, 0.2, 0.4, 0.6, 0.8, 1.2, 1.4 and 1.5 lines for the case of $\frac{|a|}{b}$= 0.2, $\frac{d}{b}$= 0.2

(E_{xrel} on $\frac{Y}{b}$= 0 line is zero).

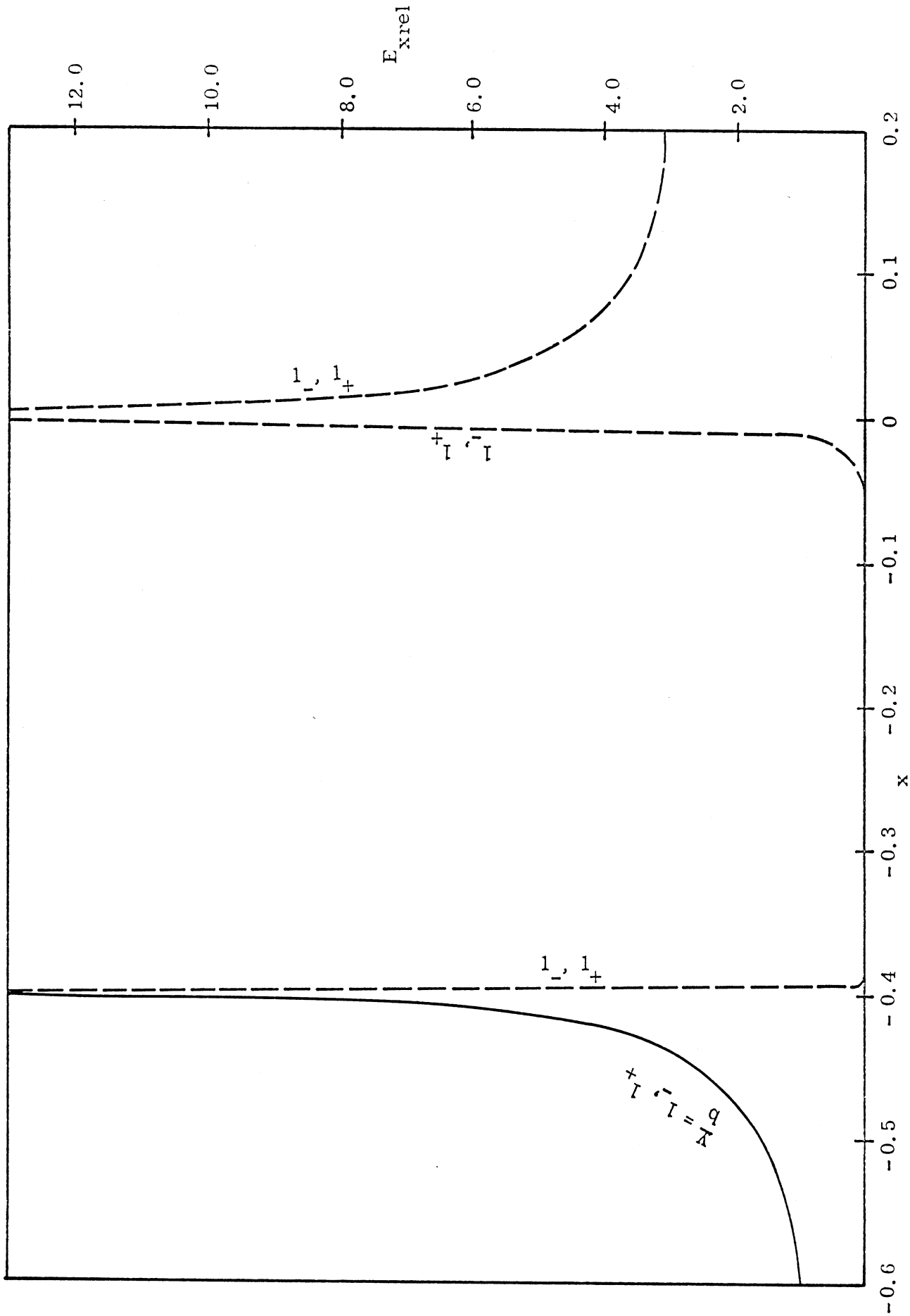

Fig. 3-6-d: E_{xrel} on $\frac{Y}{b} = 1_-$ and 1_+ lines for the case of $\frac{|a|}{b} = 0.2$, $\frac{d}{b} = 0.2$.

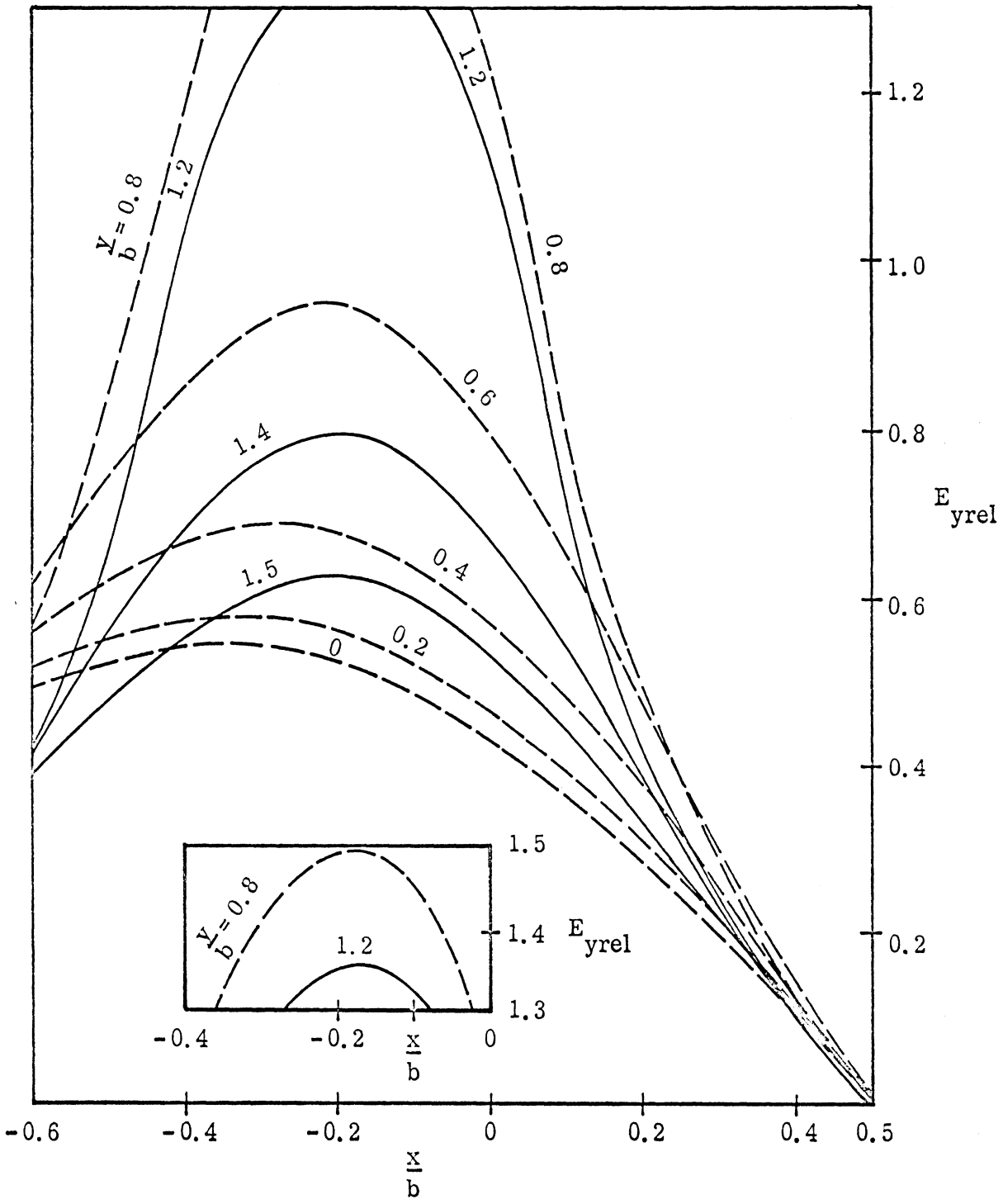

Fig. 3-7-a: E_{yrel} on $\frac{y}{b}$ = 0, 0.2, 0.4, 0.6, 0.8, 1.2, 1.4 and 1.5 lines for the case of $\frac{|a|}{b}$ = 0.2, $\frac{d}{b}$ = 0.5.

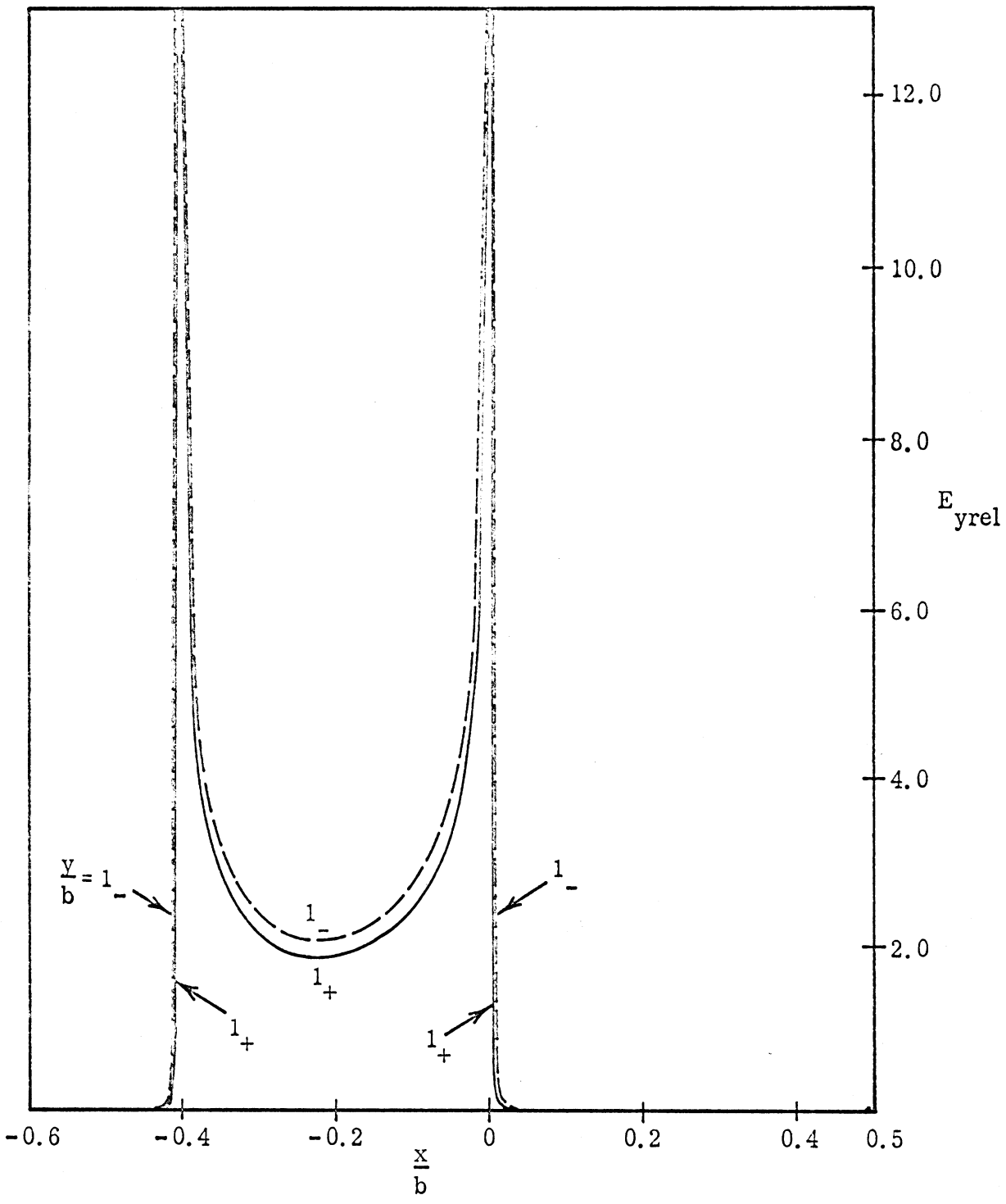

Fig. 3-7-b: E_{yrel} on $\frac{y}{b} = 1_-$ and 1_+ lines for the case of $\frac{|a|}{b} = 0.2$, $\frac{d}{b} = 0.5$.

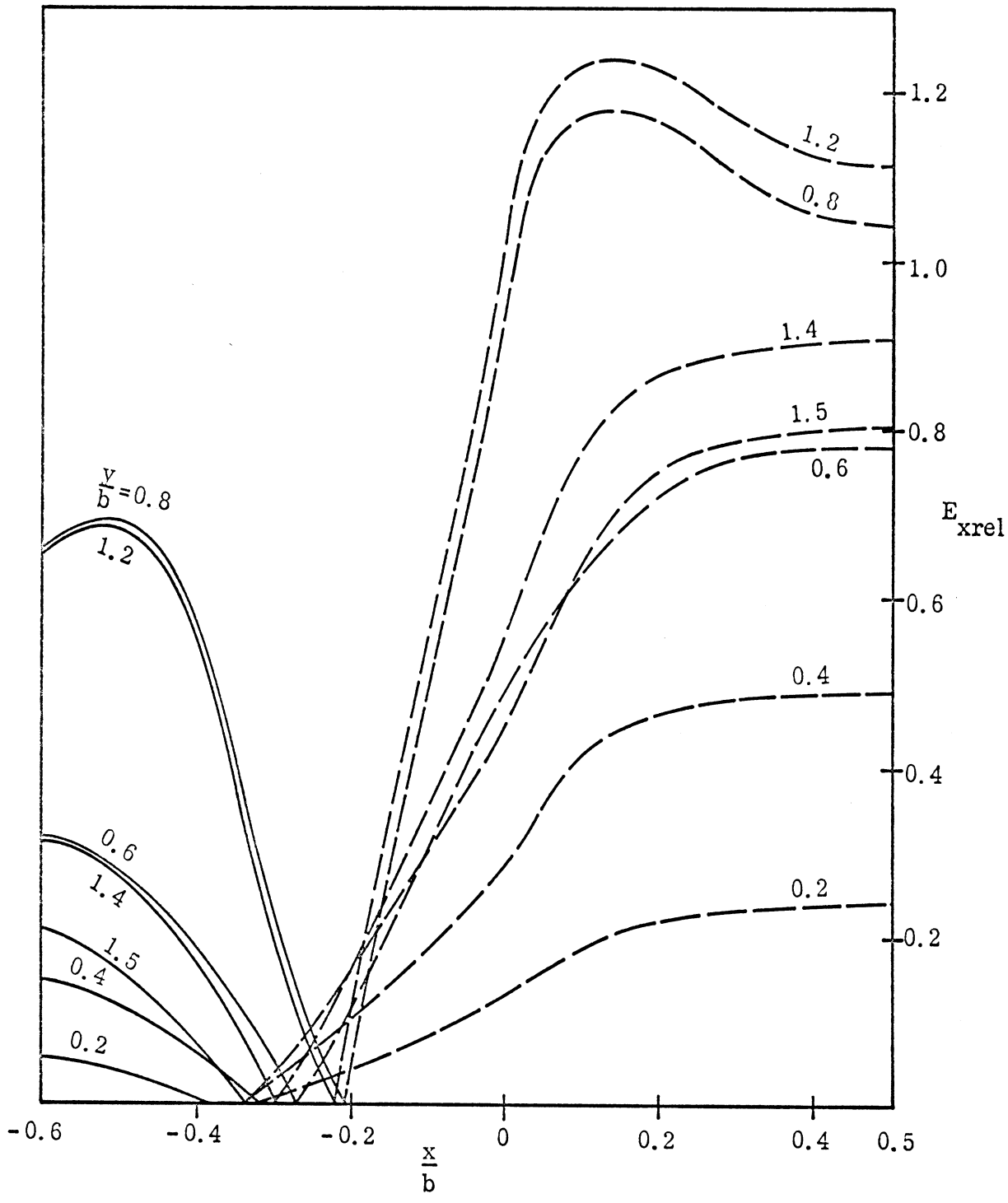

Fig. 3-7-c: E_{xrel} on $\frac{y}{b}=0$, 0.2, 0.4, 0.6, 0.8, 1.2, 1.4 and 1.5 lines for the case of $\frac{|a|}{b}=0.2$, $\frac{d}{b}=0.5$ (E_{xrel} on $\frac{y}{b}=0$ line is zero).

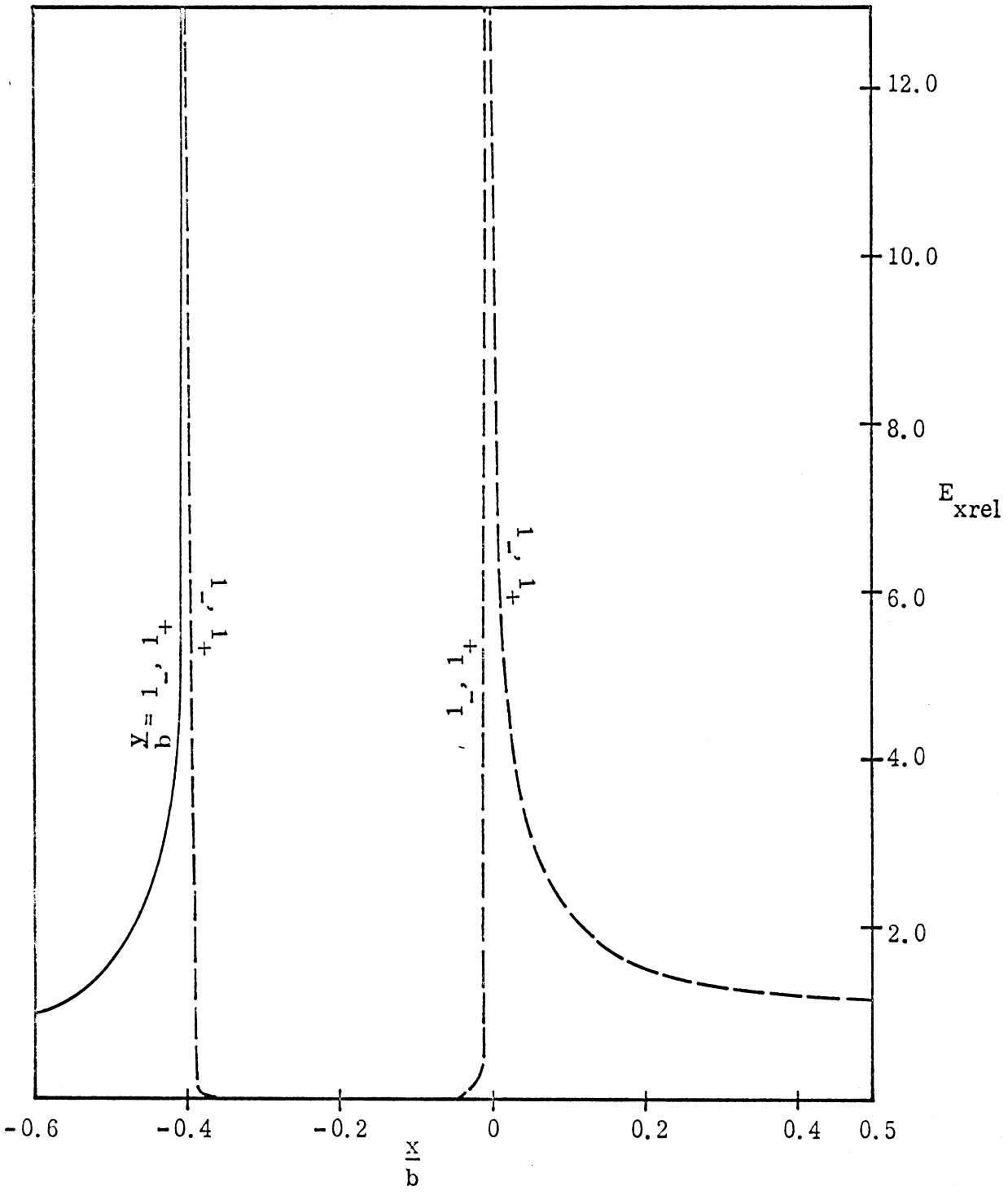

Fig. 3-7-d: E_{xrel} on $\frac{y}{b} = 1_-$ and 1_+ lines for the case of $\frac{|a|}{b} = 0.2$, $\frac{d}{b} = 0.5$.

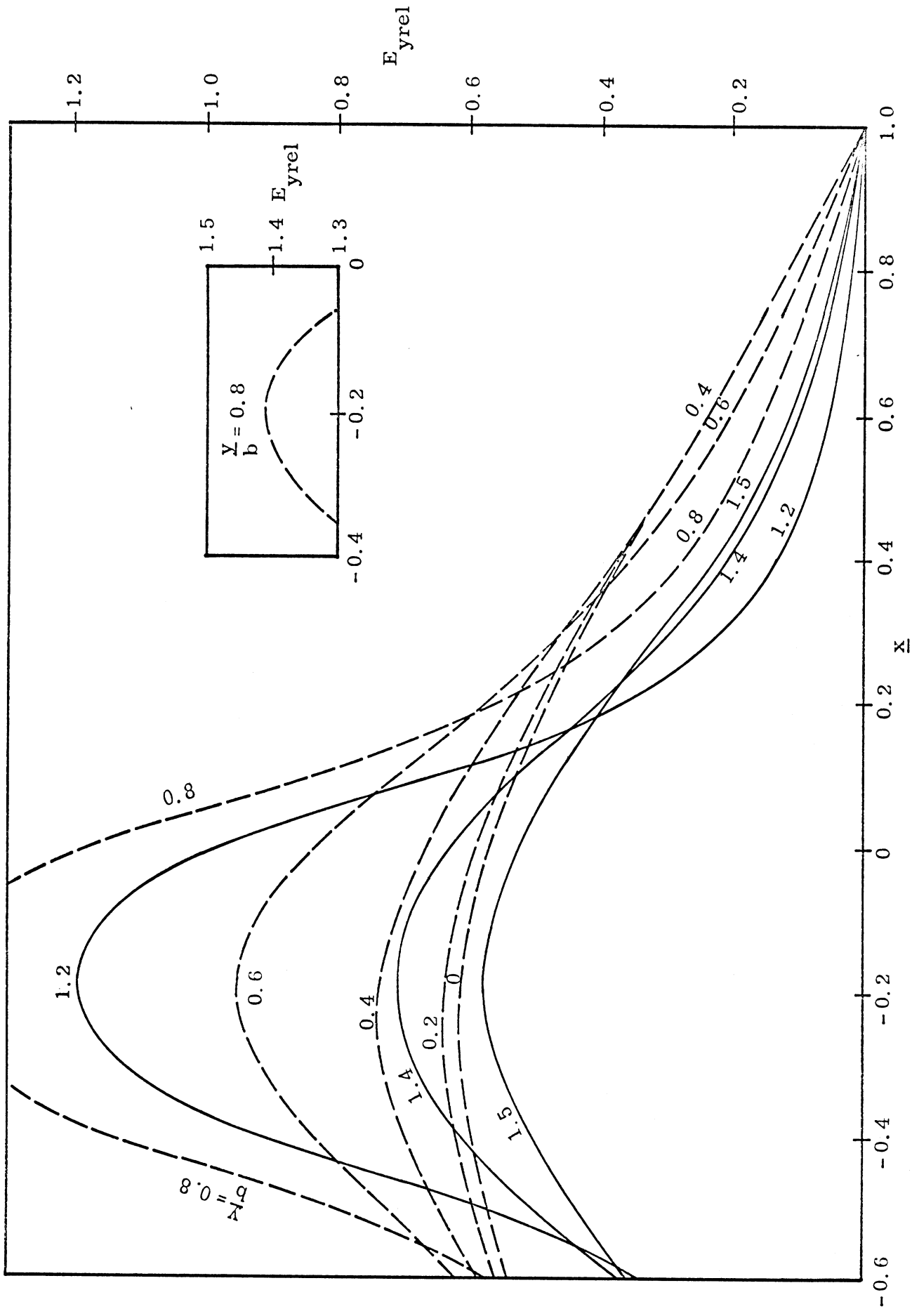

Fig. 3-8-a: E_{yrel} on $\frac{Y}{b} = 0, 0.2, 0.4, 0.6, 0.8, 1.0, 1.2, 1.4$ and 1.5 lines for the case of $\frac{|a|}{b} = 0.2$, $\frac{d}{b} = 1.0$.

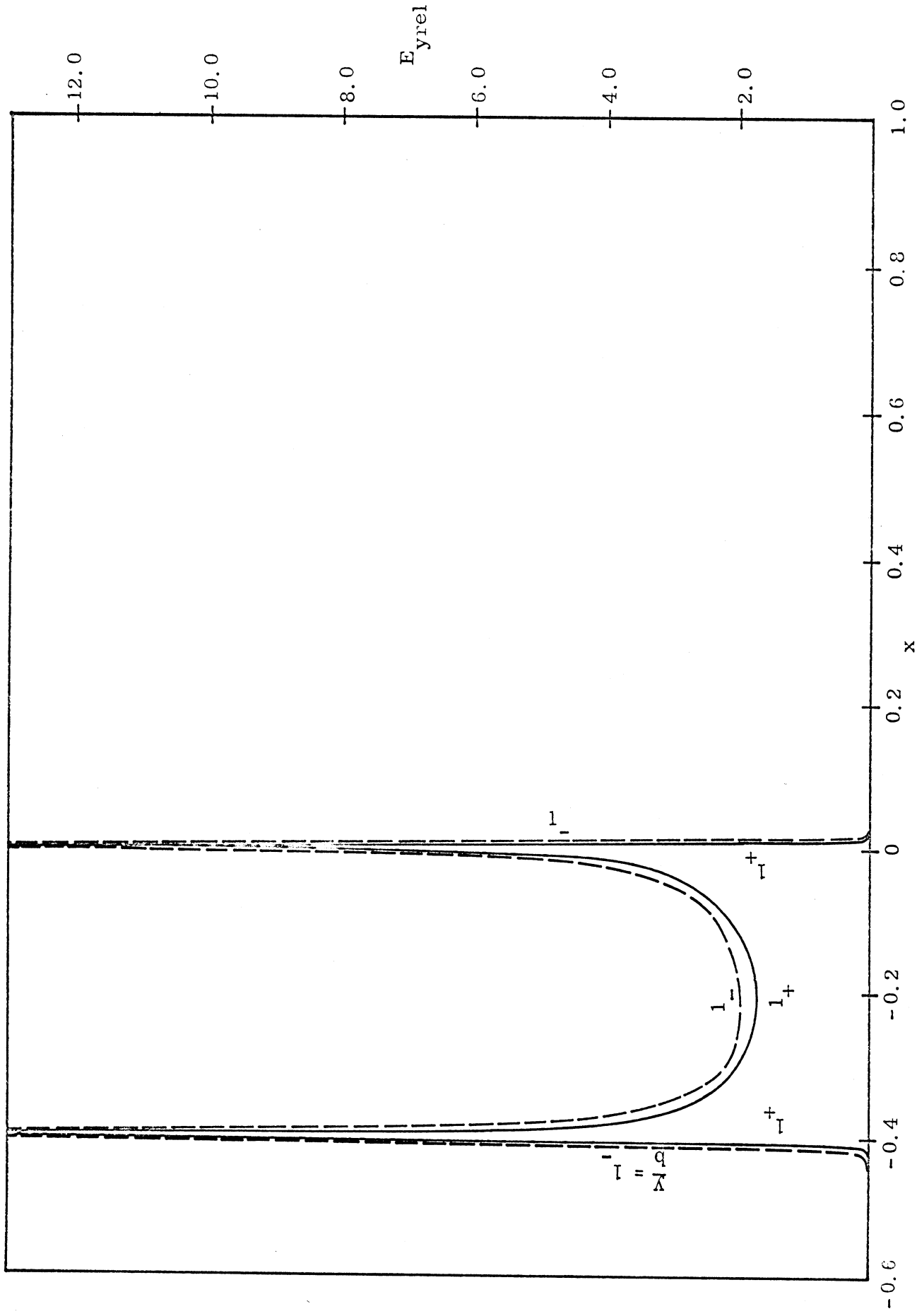

Fig. 3-8-b: E_{yrel} on $\frac{Y}{b} = l_-$ and l_+ lines for the case of $\frac{|a|}{b} = 0.2$, $\frac{d}{b} = 1.0$.

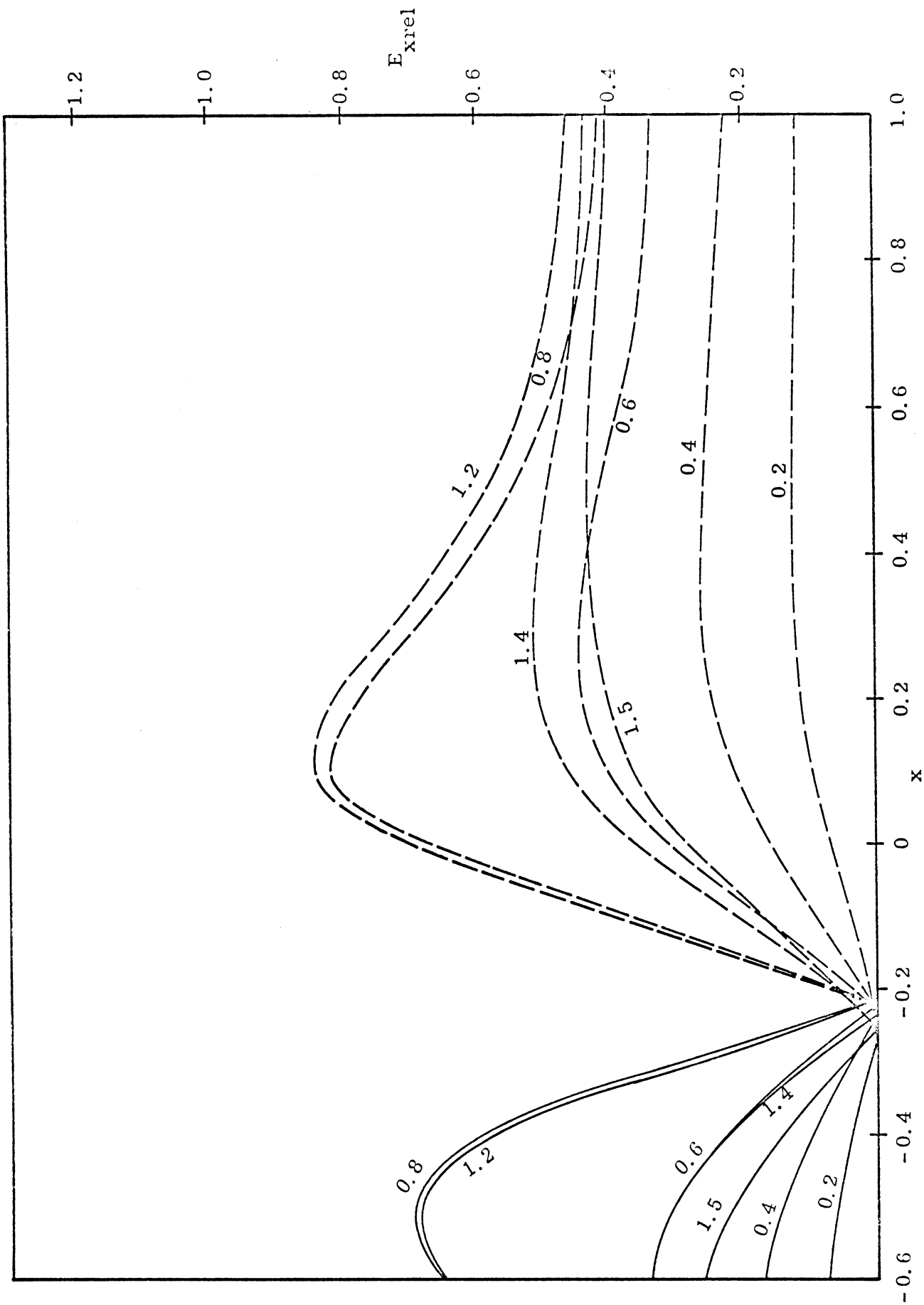

Fig. 3-8-c: E_{xrel} on $\frac{y}{b} = 0$, 0.2, 0.4, 0.6, 0.8, 1.2, 1.4 and 1.5 lines for the case of $\frac{|a|}{b} = 0.2$, $\frac{d}{b} = 1.0$

(E_{xrel} on $\frac{y}{b} = 0$ line is zero).

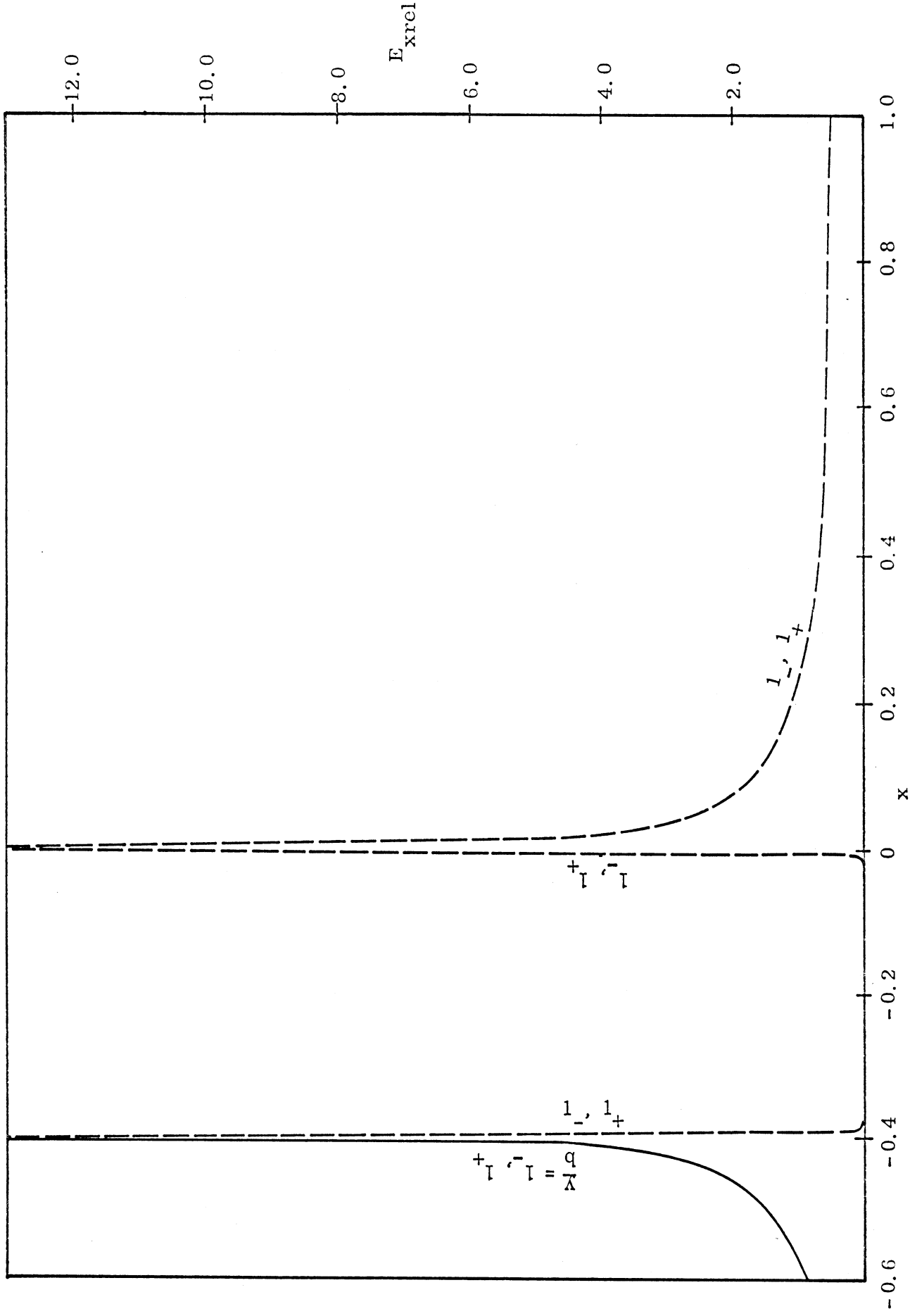

Fig. 3-8-d: E_{xrel} on $\frac{y}{b} = l_-$ and l_+ lines for the case of $\frac{|a|}{b} = 0.2$, $\frac{d}{b} = 1.0$.

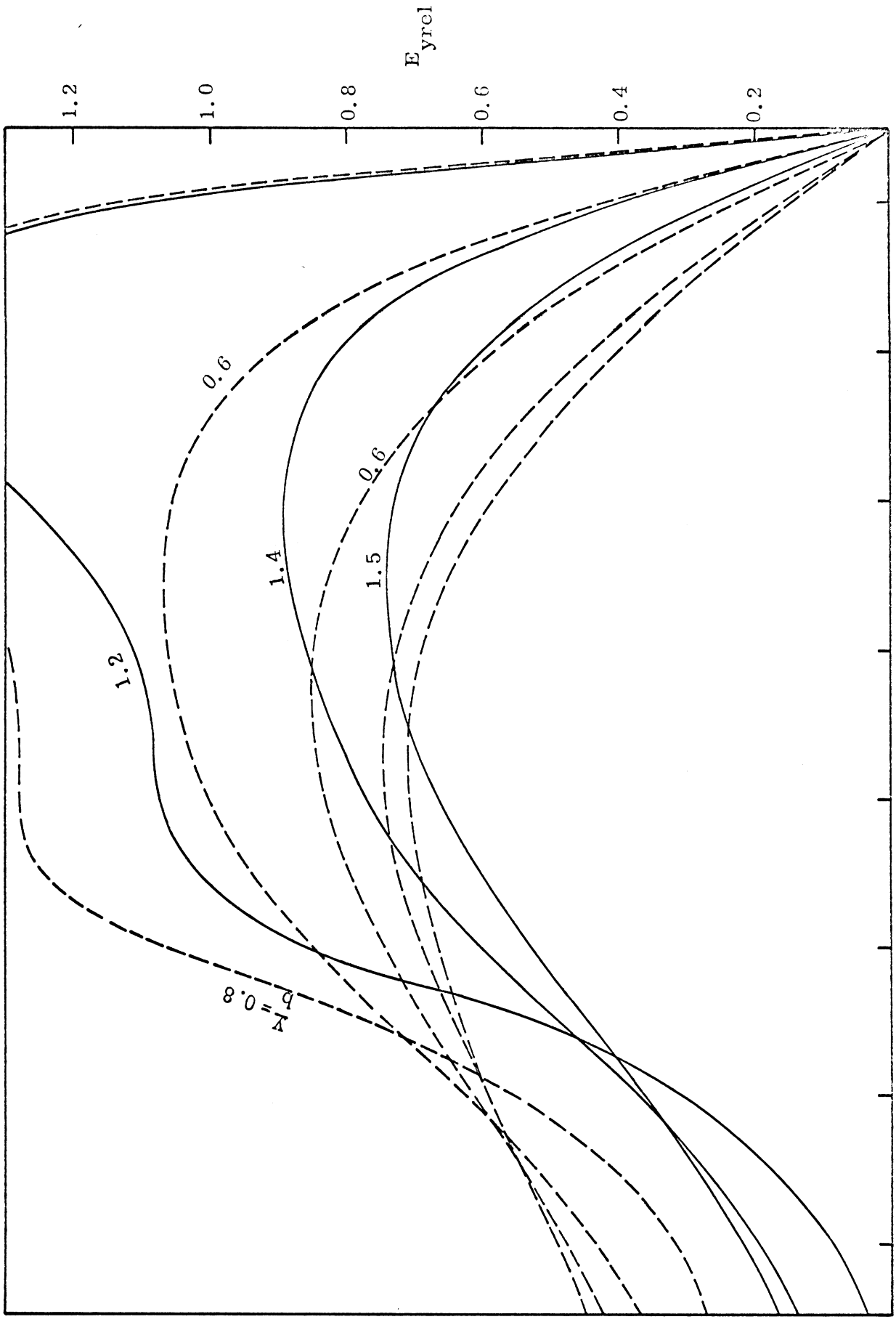

Fig. 3-9-a: E_{yrel} on $\frac{Y}{b}$ = 0, 0.2, 0.4, 0.6, 0.8, 1.2, 1.4 and 1.5 lines for the case of $\frac{|a|}{b}$ = 0.5, $\frac{d}{b}$ = 0.1.

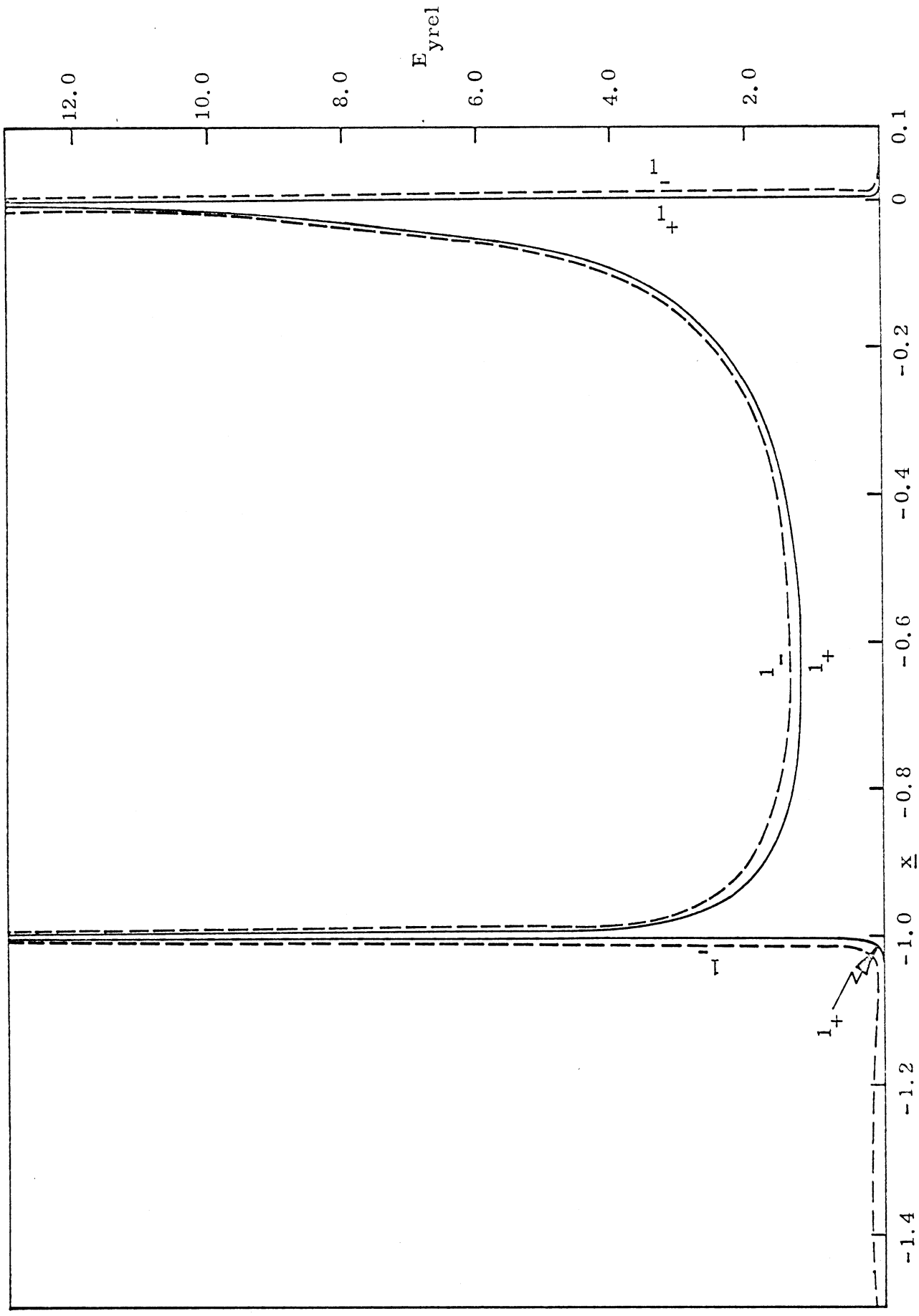

Fig. 3-9-b: E_{yrel} on $\frac{Y}{b} = 1_-$ and 1_+ lines for the case of $\frac{|a|}{b} = 0.5$, $\frac{d}{b} = 1.0$.

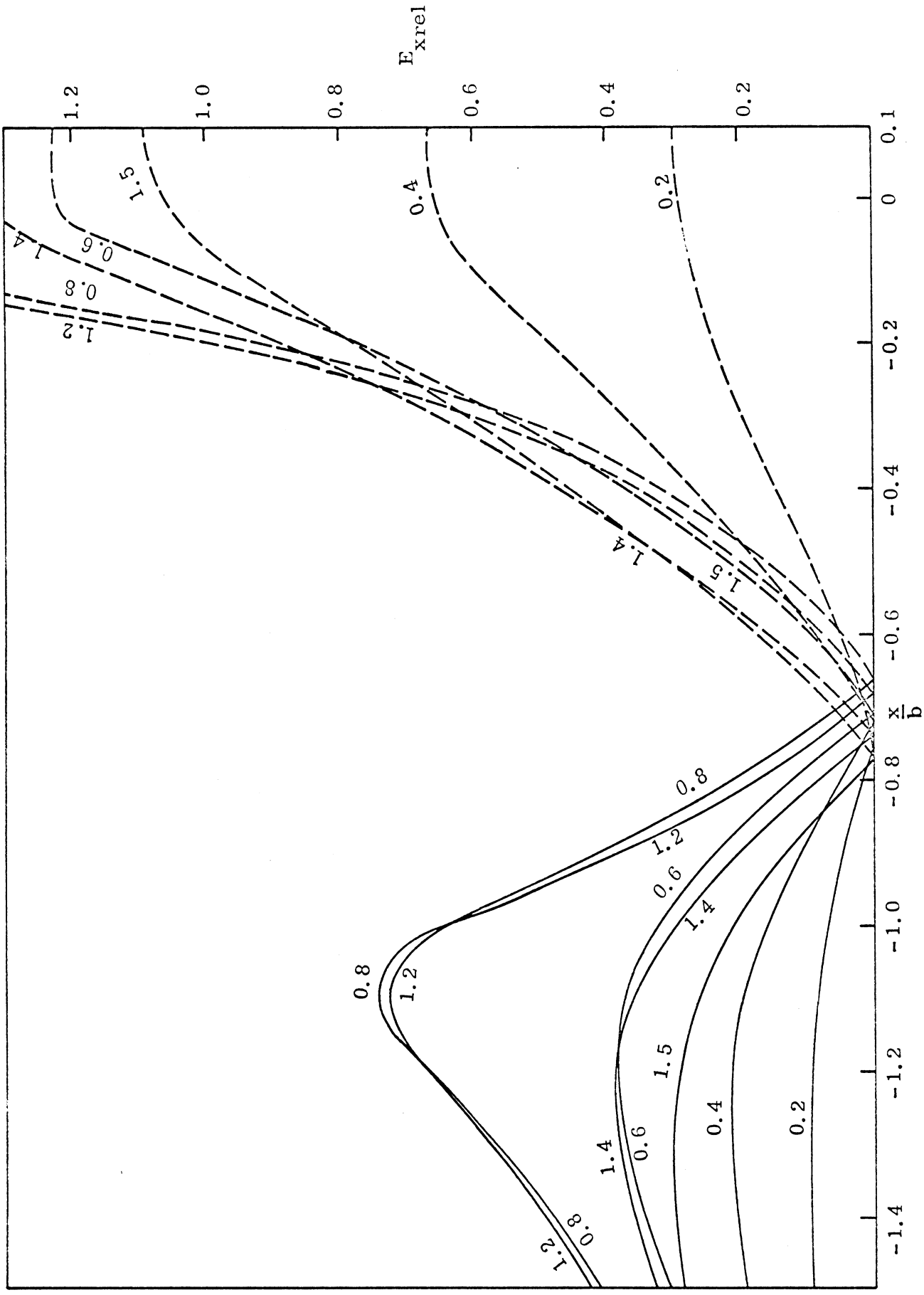

Fig. 3-9-c: E_{xrel} on $\frac{Y}{b} = 0$, 0.2, 0.4, 0.6, 0.8, 1.2, 1.4 and 1.5 for the case of $\frac{|a|}{b} = 0.5$, $\frac{d}{b} = 0.1$.
E_{xrel} on $\frac{Y}{b} = 0$ is zero.

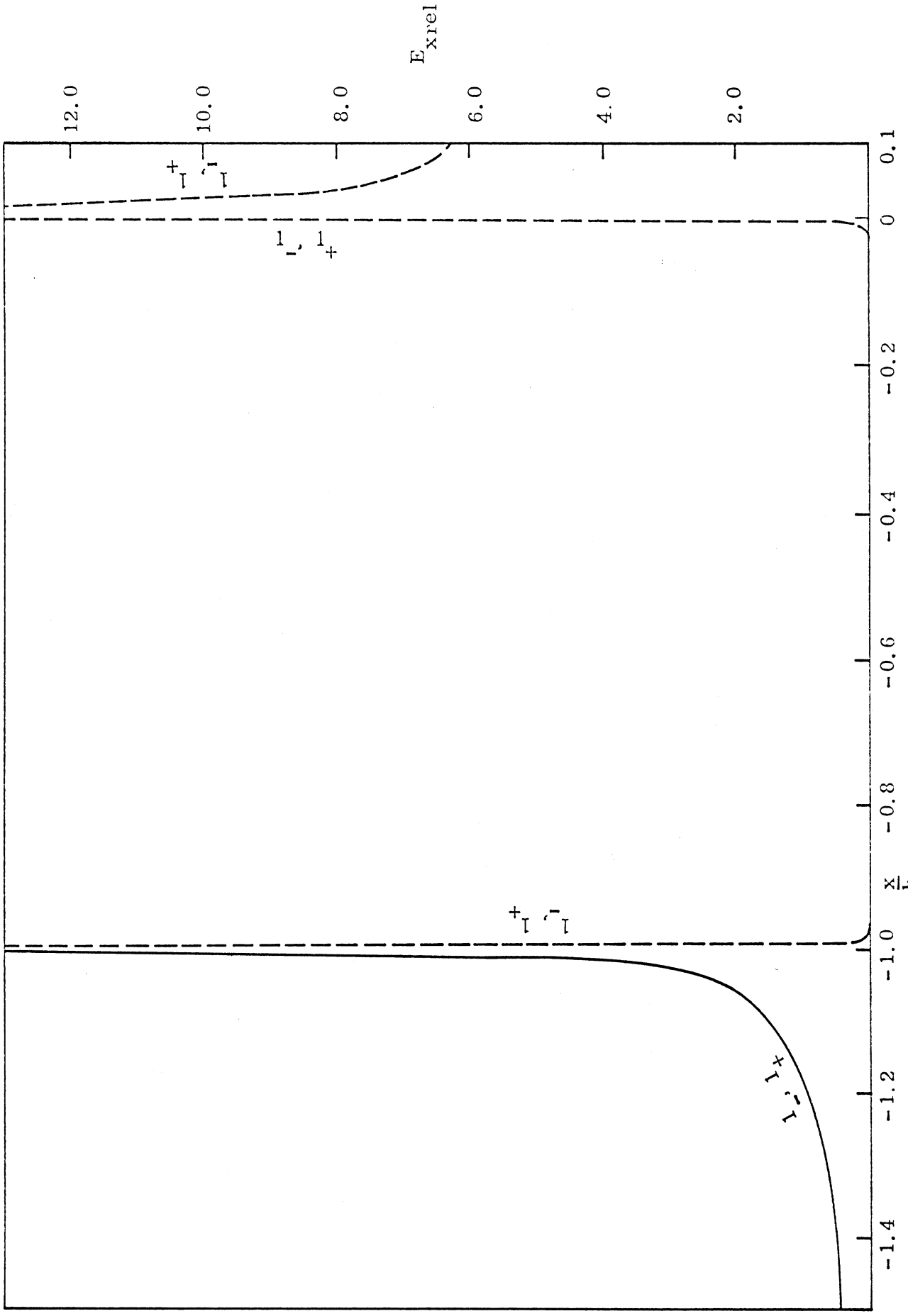

Fig. 3-9-d: E_{xrel} on $\frac{y}{b} = l_-$ and l_+ lines for the case of $\frac{|a|}{b} = 0.5$, $\frac{d}{b} = 0.1$. E_{xrel} on $\frac{y}{b} = 0$ is zero.

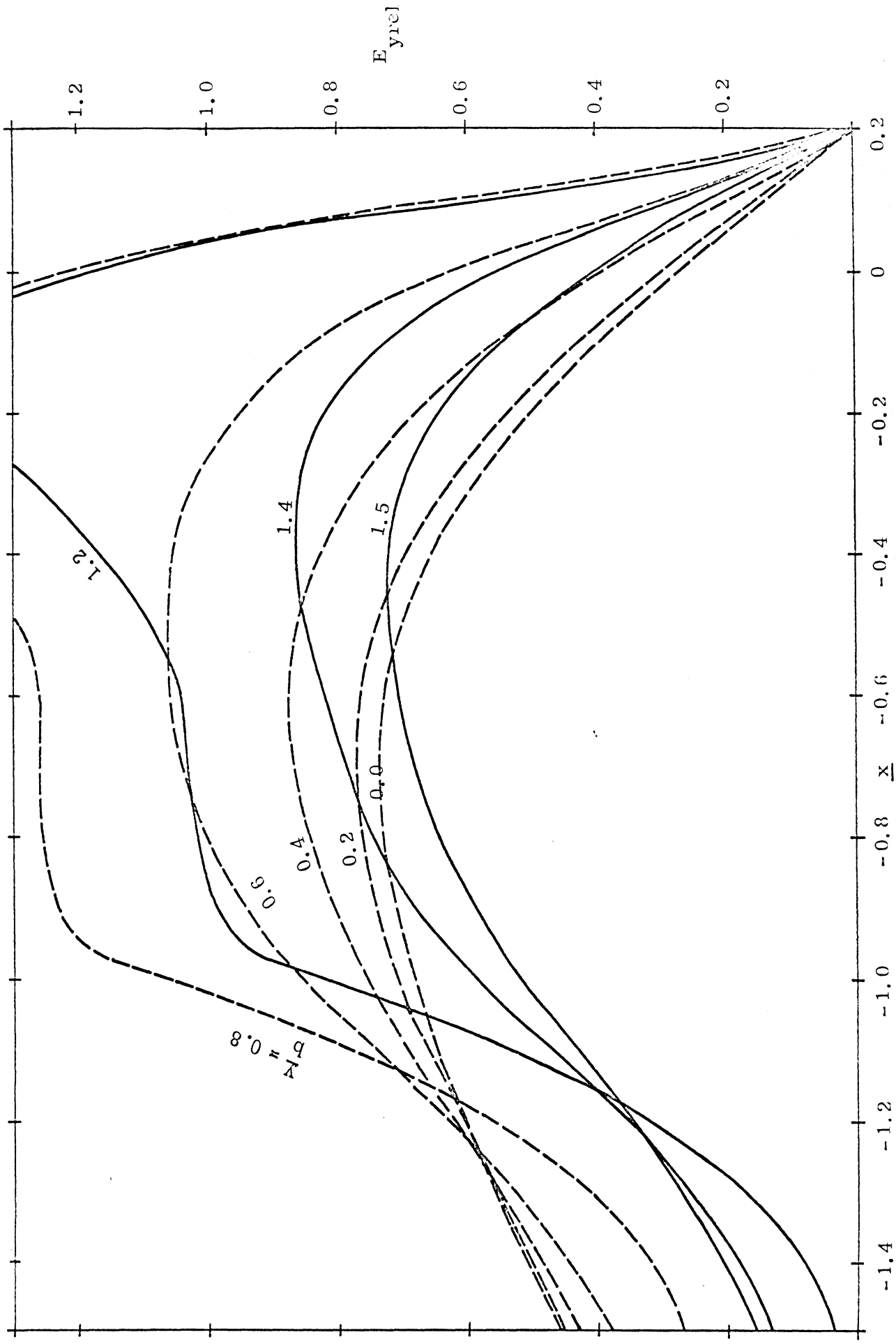

Fig. 3-10-a: E_{yrel} on $\frac{Y}{b} = 0$, 0.2, 0.4, 0.6, 0.8, 1.2, 1.4 and 1.5 lines for the case of $\frac{|a|}{b} = 0.5$, $\frac{d}{b} = 0.2$.

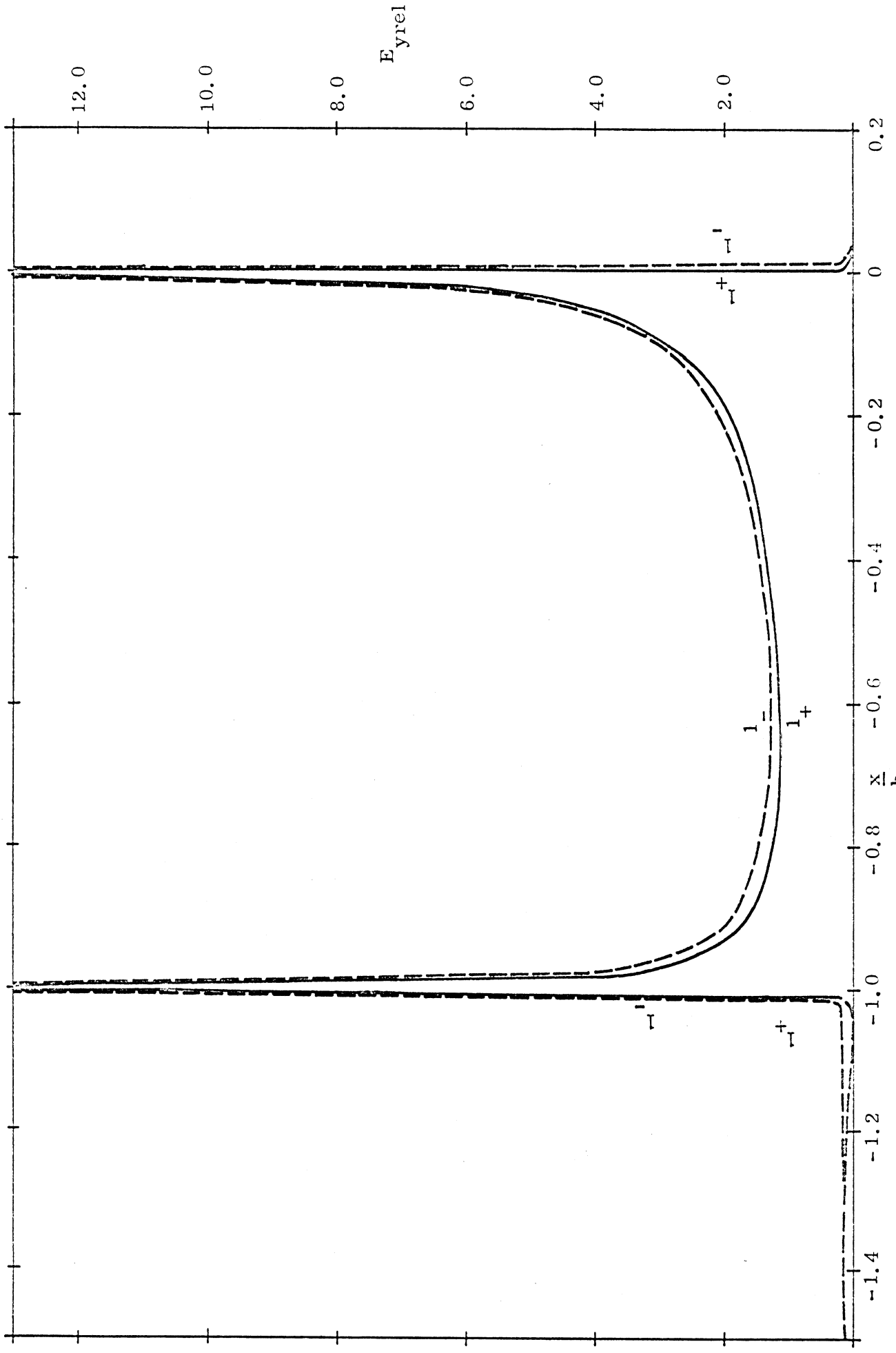

Fig. 3-10-b: E_{yrel} on $\frac{y}{b} = l_-$ and l_+ lines for the case of $\frac{|a|}{b} = 0.5$, $\frac{d}{b} = 0.2$.

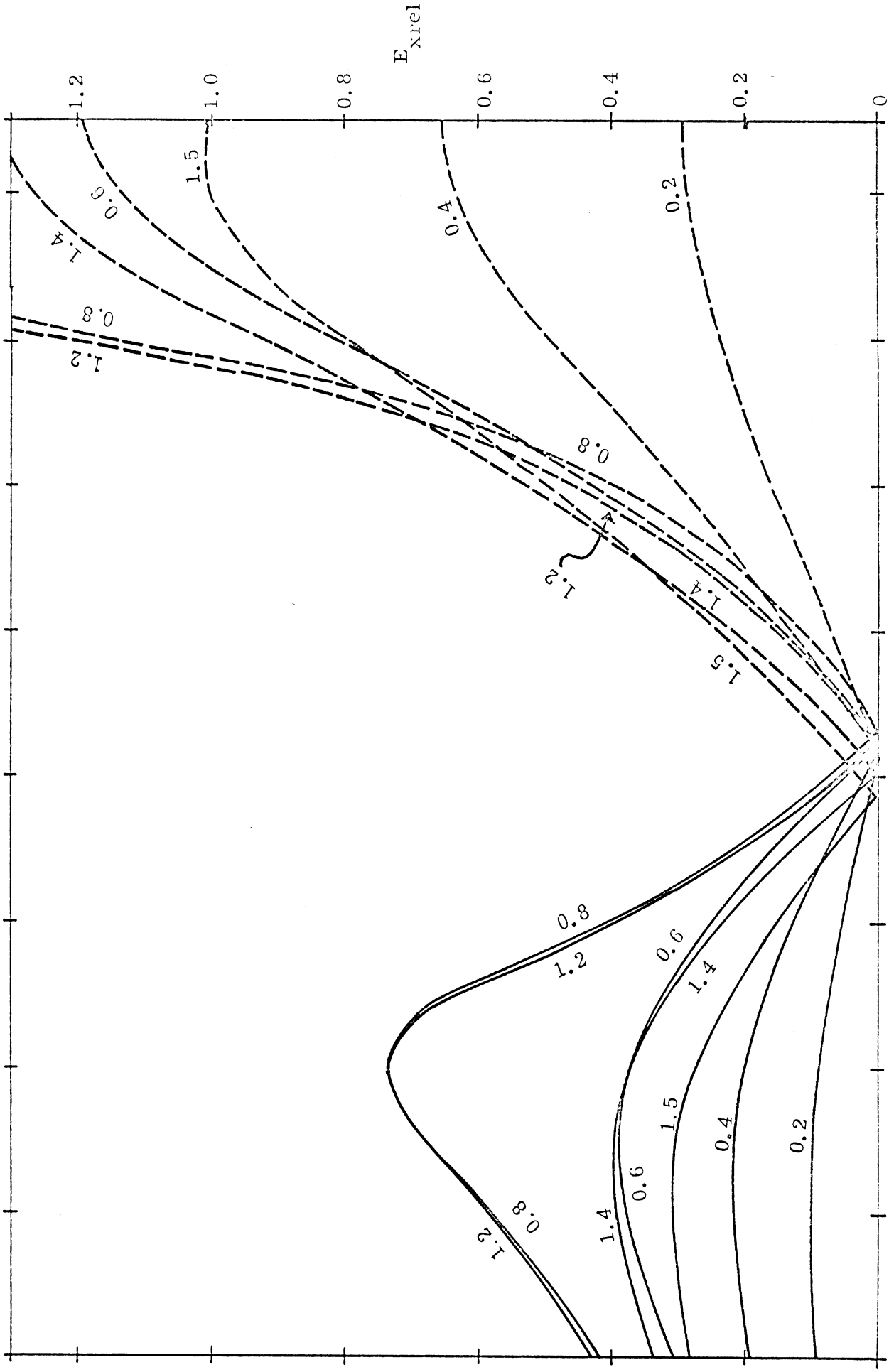

Fig. 3-10-c: E_{xrel} on $\frac{Y}{b} = 0$, 0.2, 0.4, 0.6, 0.8, 1.2, 1.4 and 1.5 lines for the case of $\frac{|a|}{b} = 0.5$, $\frac{d}{b} = 0.2$.
E_{xrel} on $\frac{Y}{b} = 0$ is zero.

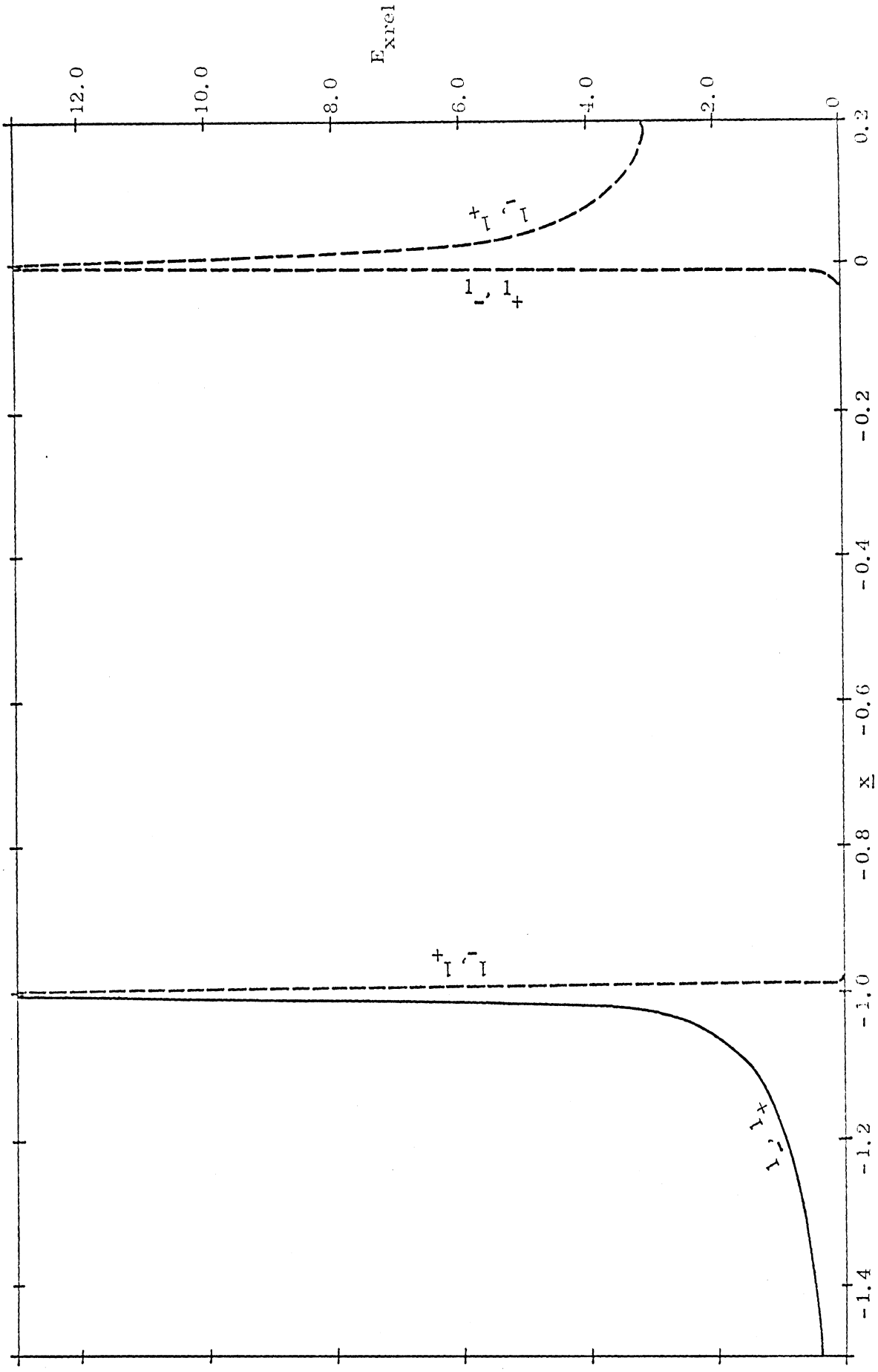

Fig. 3-10-d: E_{xrel} on $\frac{Y}{b} = l_-$ and l_+ lines for the case of $\frac{|a|}{b} = 0.5$, $\frac{d}{b} = 0.2$. E_{xrel} on $\frac{Y}{b} = 0$ is zero.

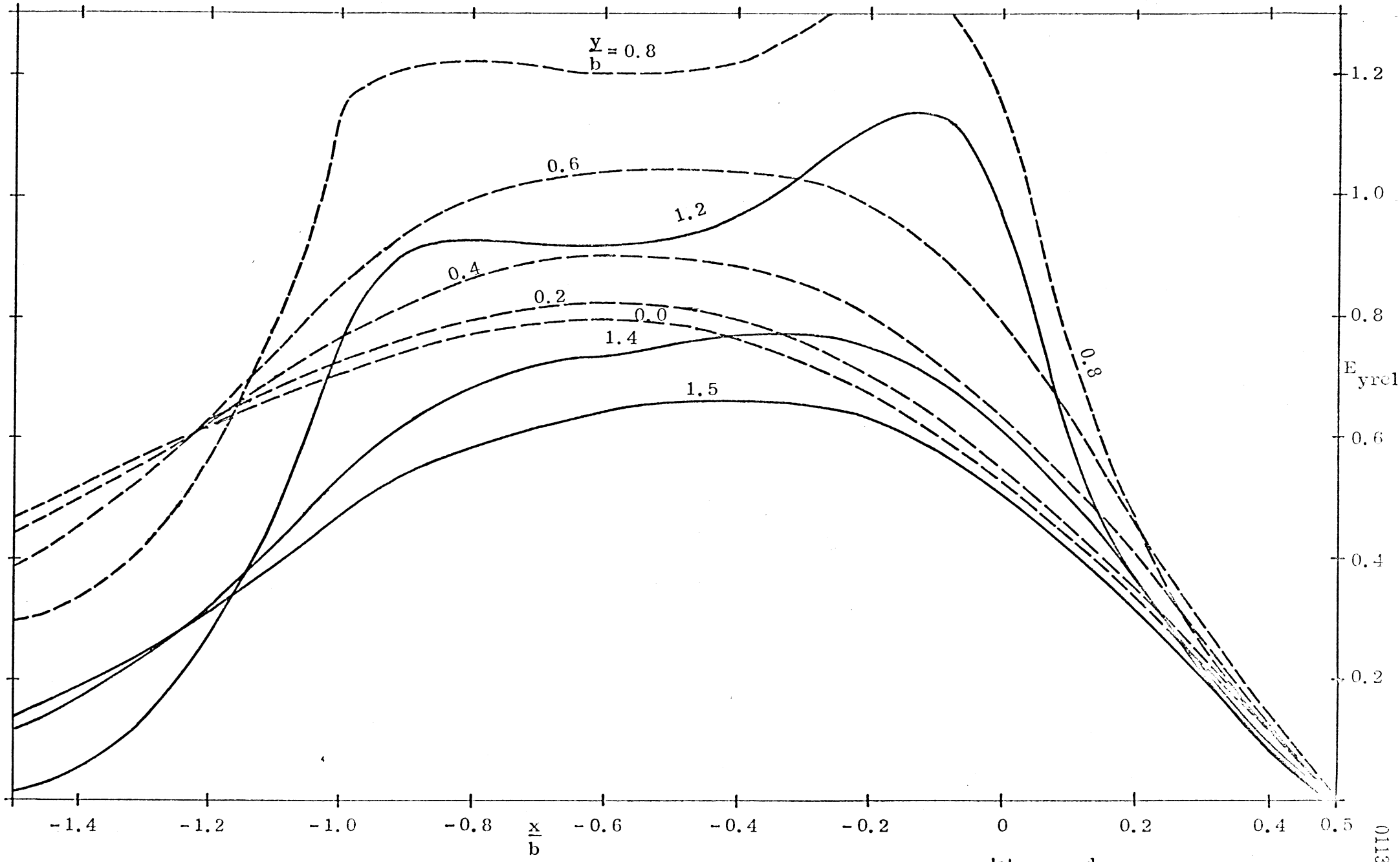

Fig. 3-11-a: E_{yrel} on $\frac{y}{b} = 0$, 0.2, 0.4, 0.6, 0.8, 1.2, 1.4 and 1.5 lines for the case of $\frac{|a|}{b} = 0.5$, $\frac{d}{b} = 0.5$.

011323-1-T

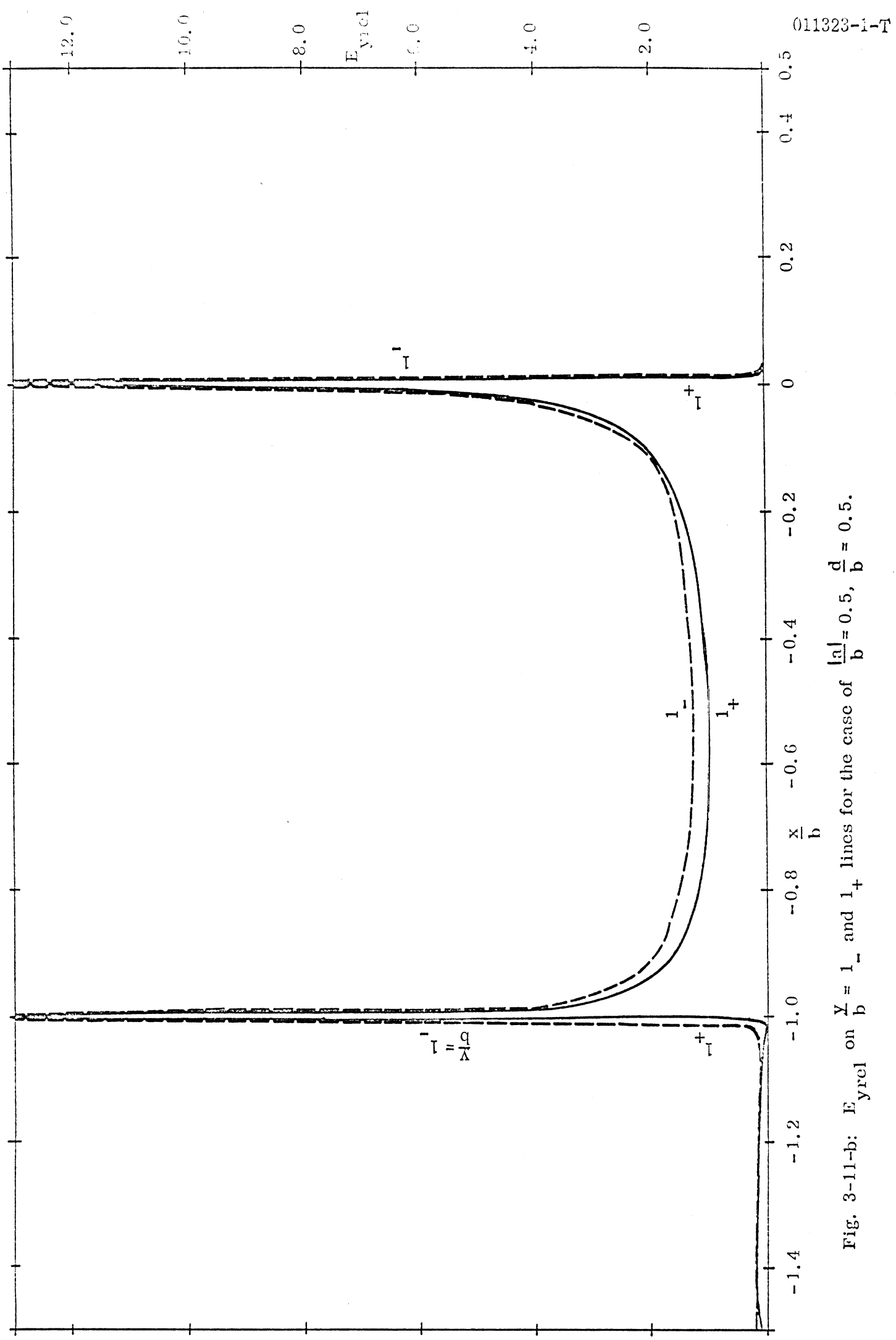

Fig. 3-11-b: E_{yrel} on $\frac{Y}{b} = 1_-$ and 1_+ lines for the case of $\frac{|a|}{b} = 0.5$, $\frac{d}{b} = 0.5$.

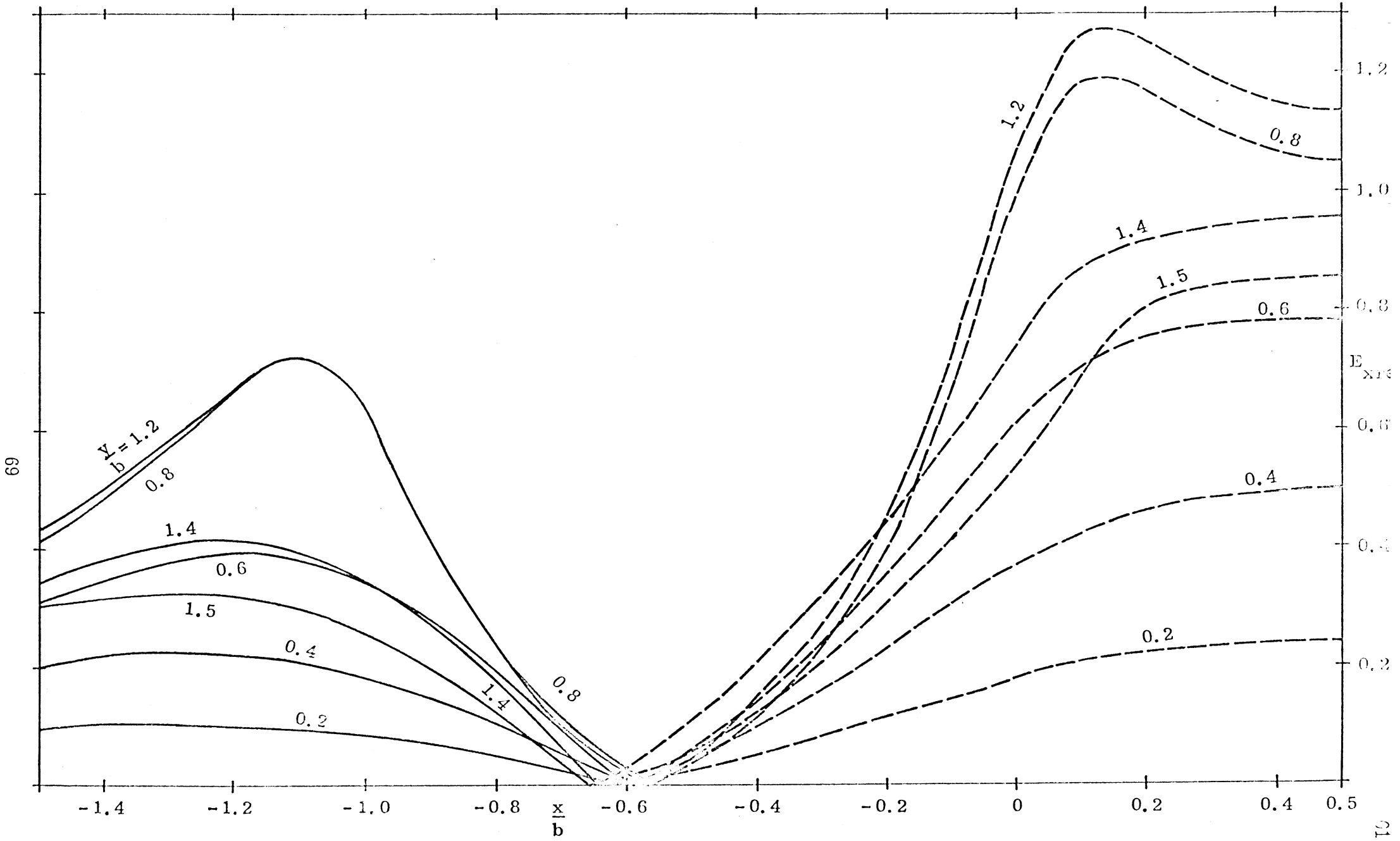

Fig. 3-11-c: E_{xrel} on $\frac{y}{b}$ = 0, 0.2, 0.4, 0.6, 0.8, 1.2, 1.4, 1.5 lines for the case of $\frac{|a|}{b}$ = 0.5, $\frac{d}{b}$ = 0.5.

E_{xrel} on $\frac{y}{b}$ = 0 is zero.

011323-1-T

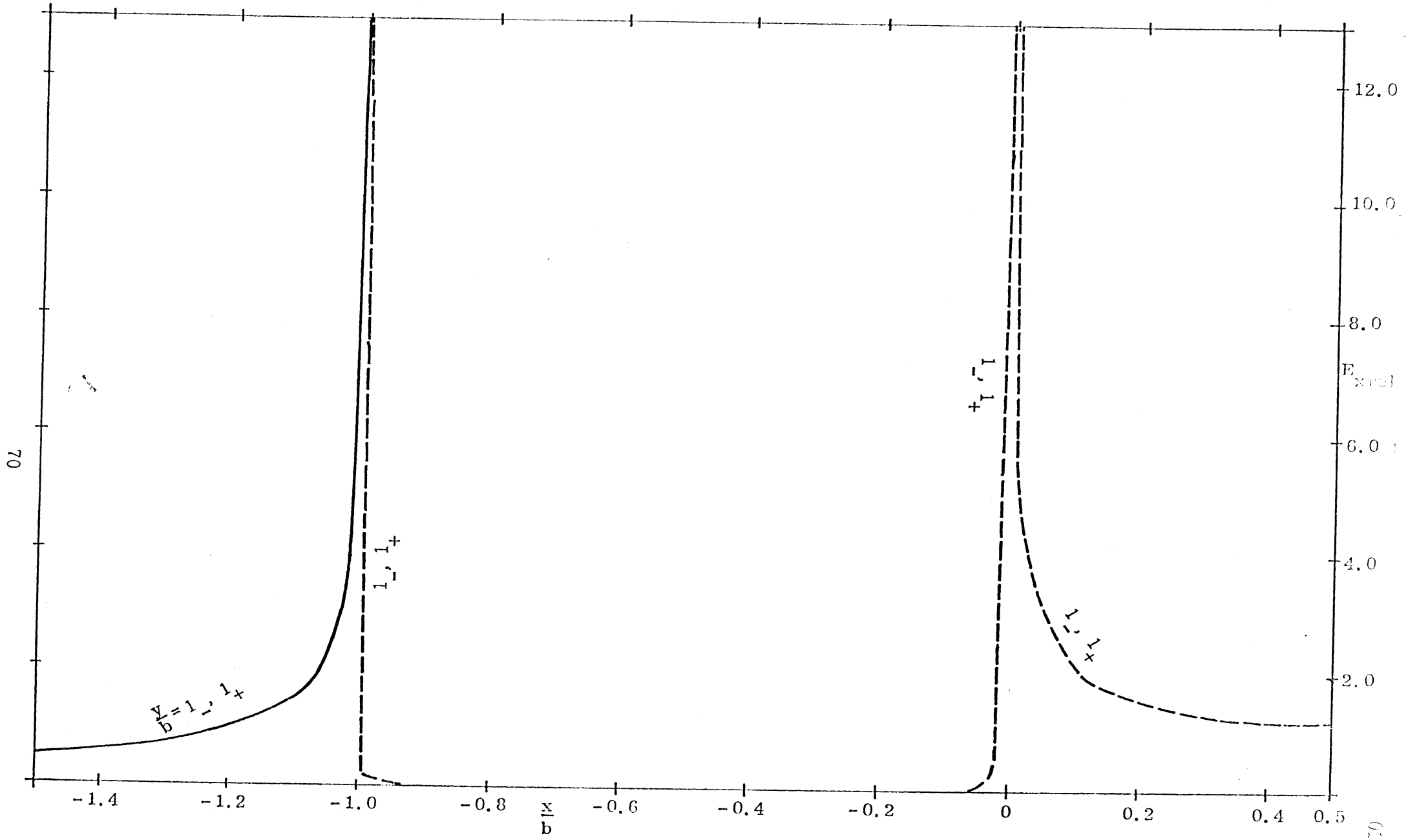

Fig. 3-11-d: E_{xrel} on $\frac{y}{b} = 1_-$ and 1_+ lines for the case of $\frac{|a|}{b} = 0.5$, $\frac{d}{b} = 0.5$. E_{xrel} on $\frac{y}{b} = 0$ is zero.

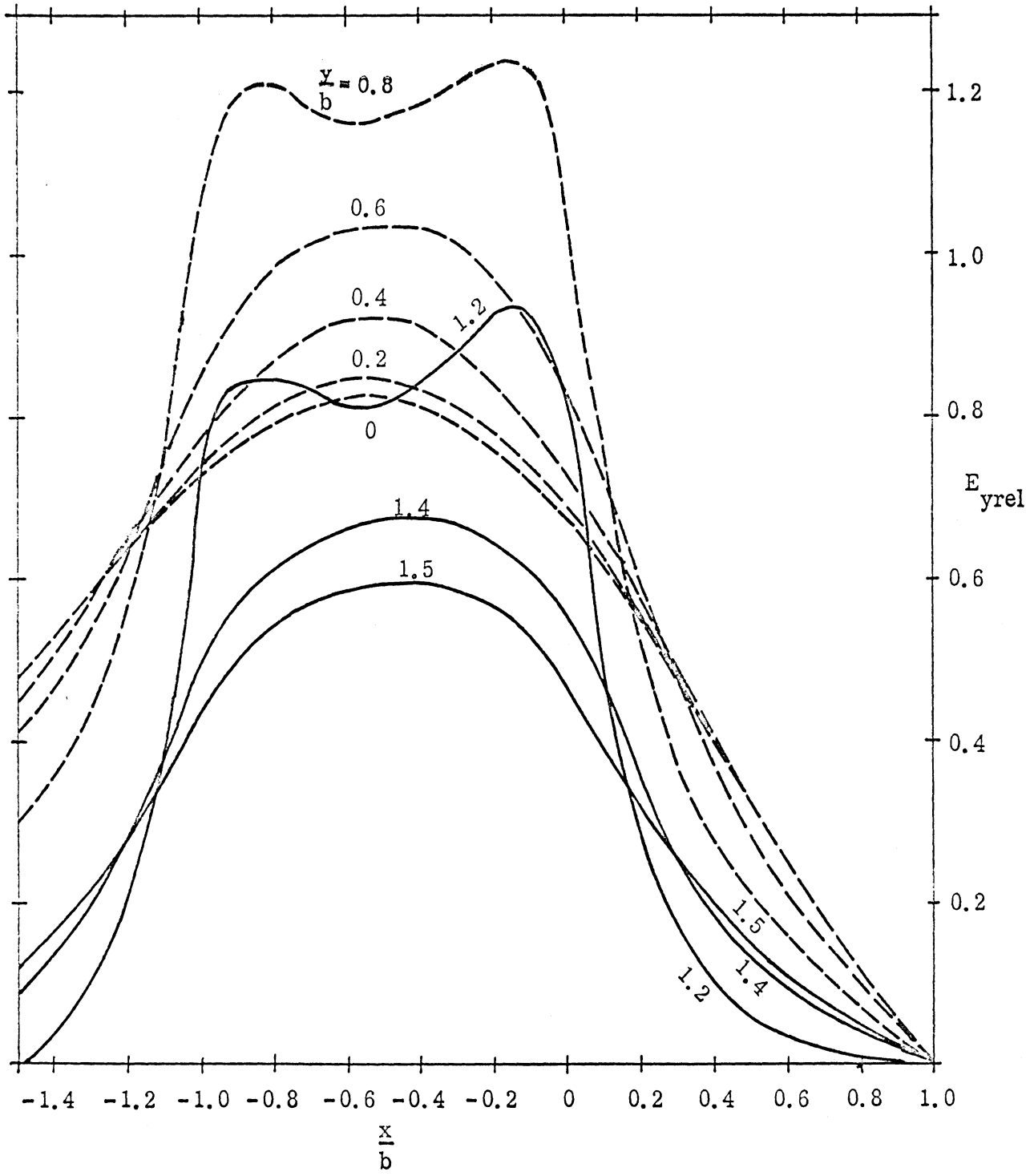

Fig. 3-12-a: E_{yrel} on $\frac{y}{b}$ = 0, 0.2, 0.4, 0.6, 0.8, 1.2, 1.4 and 1.5 for the case of $\frac{|a|}{b}$ = 0.5, $\frac{d}{b}$ = 1.0.

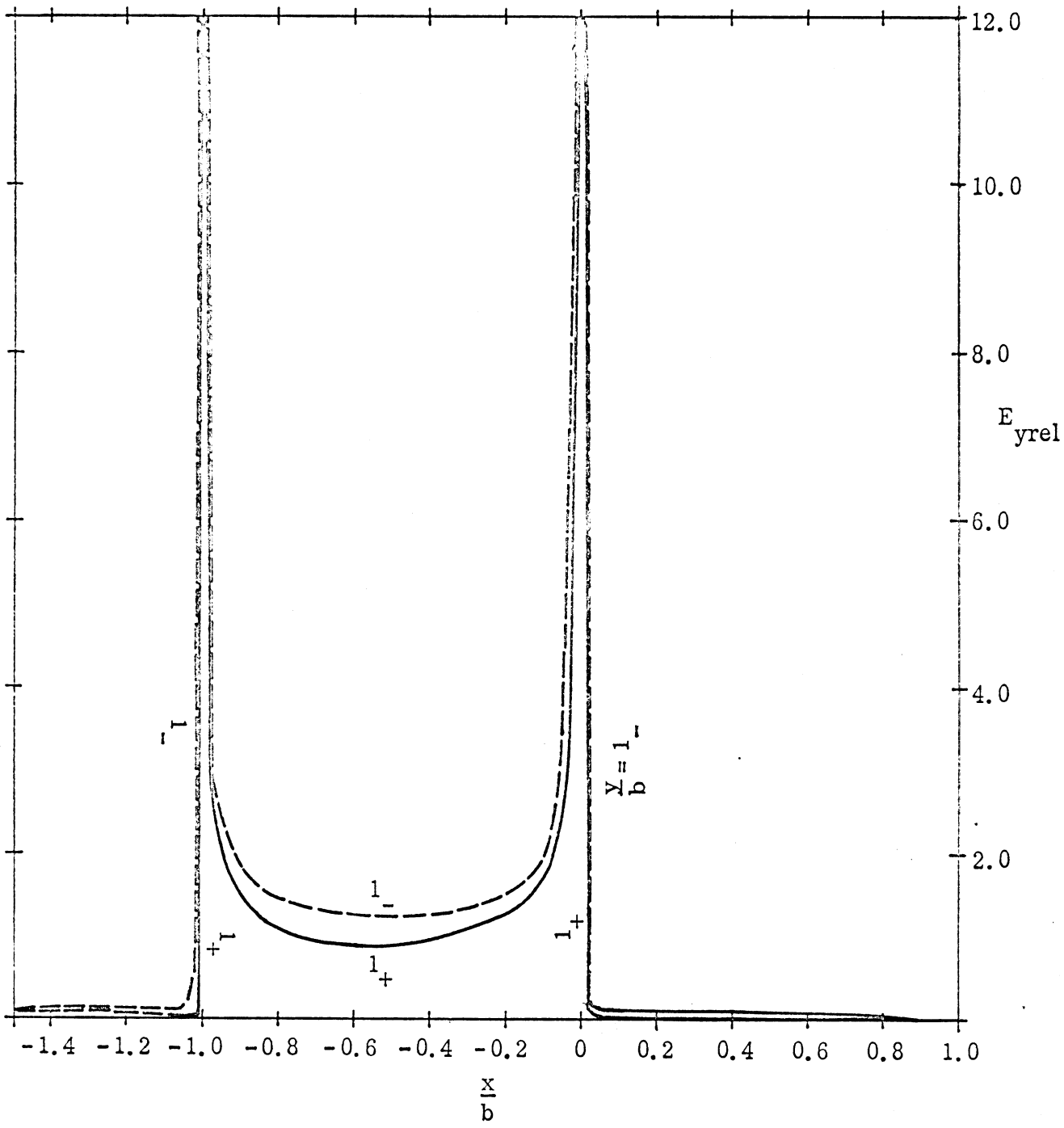

Fig. 3-12-b: E_{yrel} on $\frac{y}{b} = 1_-$ and 1_+ lines for the case of $\frac{|a|}{b} = 0.5$, $\frac{d}{b} = 1.0$.

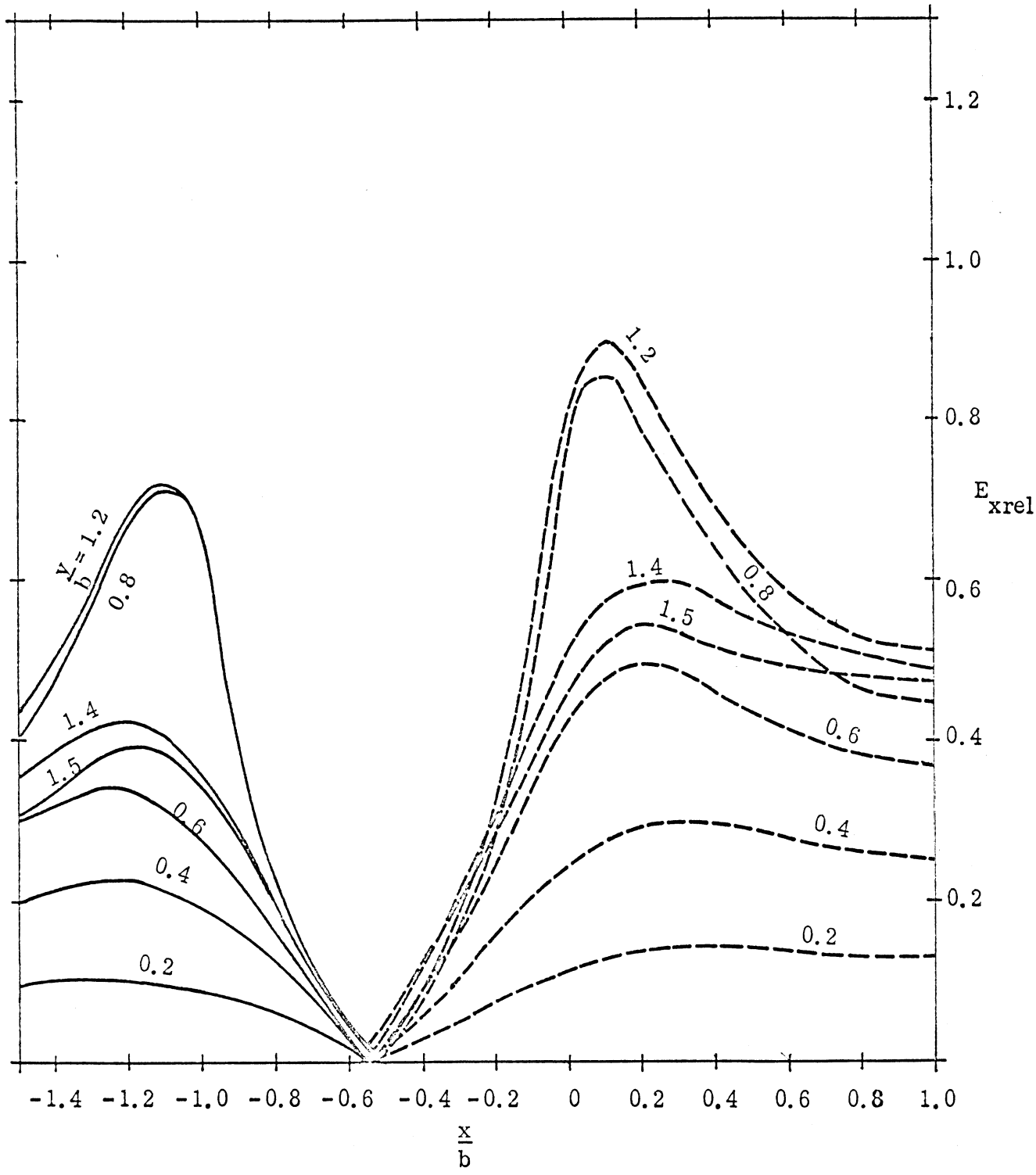

Fig. 3-12-c: E_{xrel} on $\frac{y}{b}$ = 0, 0.2, 0.4, 0.6, 0.8, 1.2, 1.4 and 1.5 lines for the case of $\frac{|a|}{b}$ = 0.5, $\frac{d}{b}$ = 1.0. (E_{xrel} on $\frac{y}{b}$ = 0 line is zero).

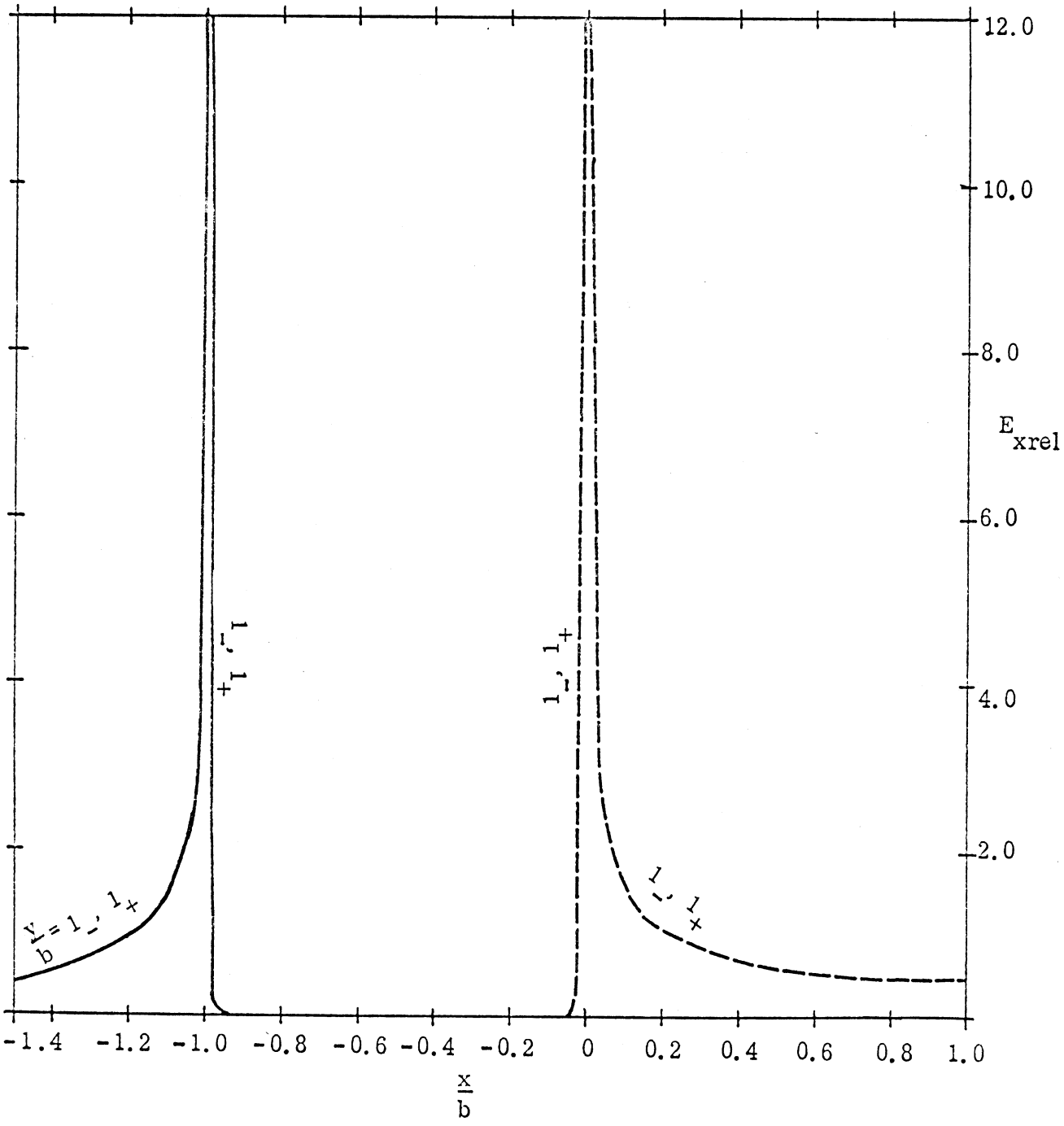

Fig. 3-12-d: E_{xrel} on $\frac{y}{b} = l_-$ and l_+ lines for the case of $\frac{|a|}{b} = 0.5$, $\frac{d}{b} = 1.0$.

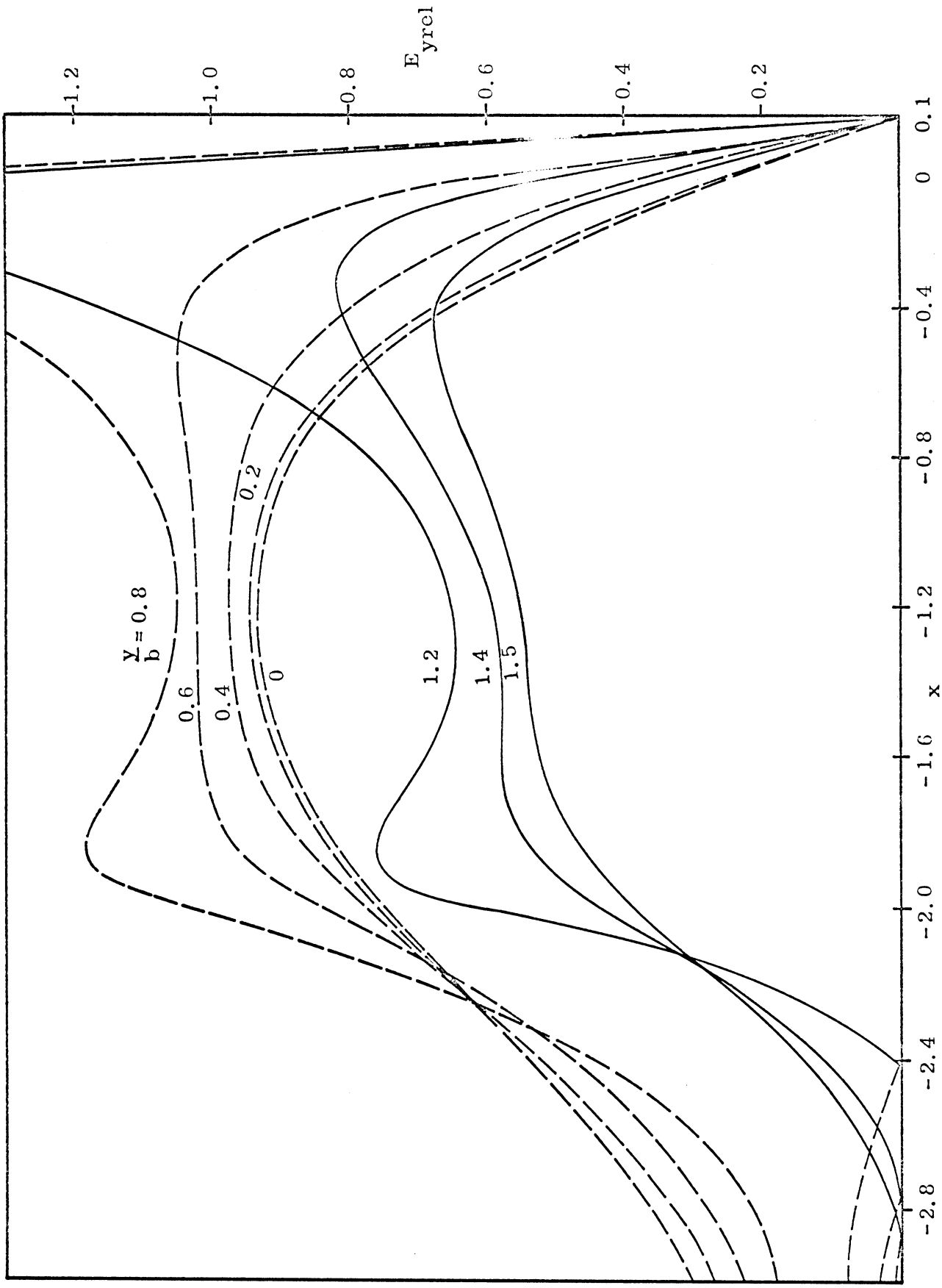

Fig. 3-13-a: E_{yrel} on $\frac{y}{b}$ = 0, 0.2, 0.4, 0.6, 0.8, 1.2, 1.4 and 1.5 lines for the case of $\frac{|a|}{b}$ = 1.0, $\frac{d}{b}$ = 0.1.

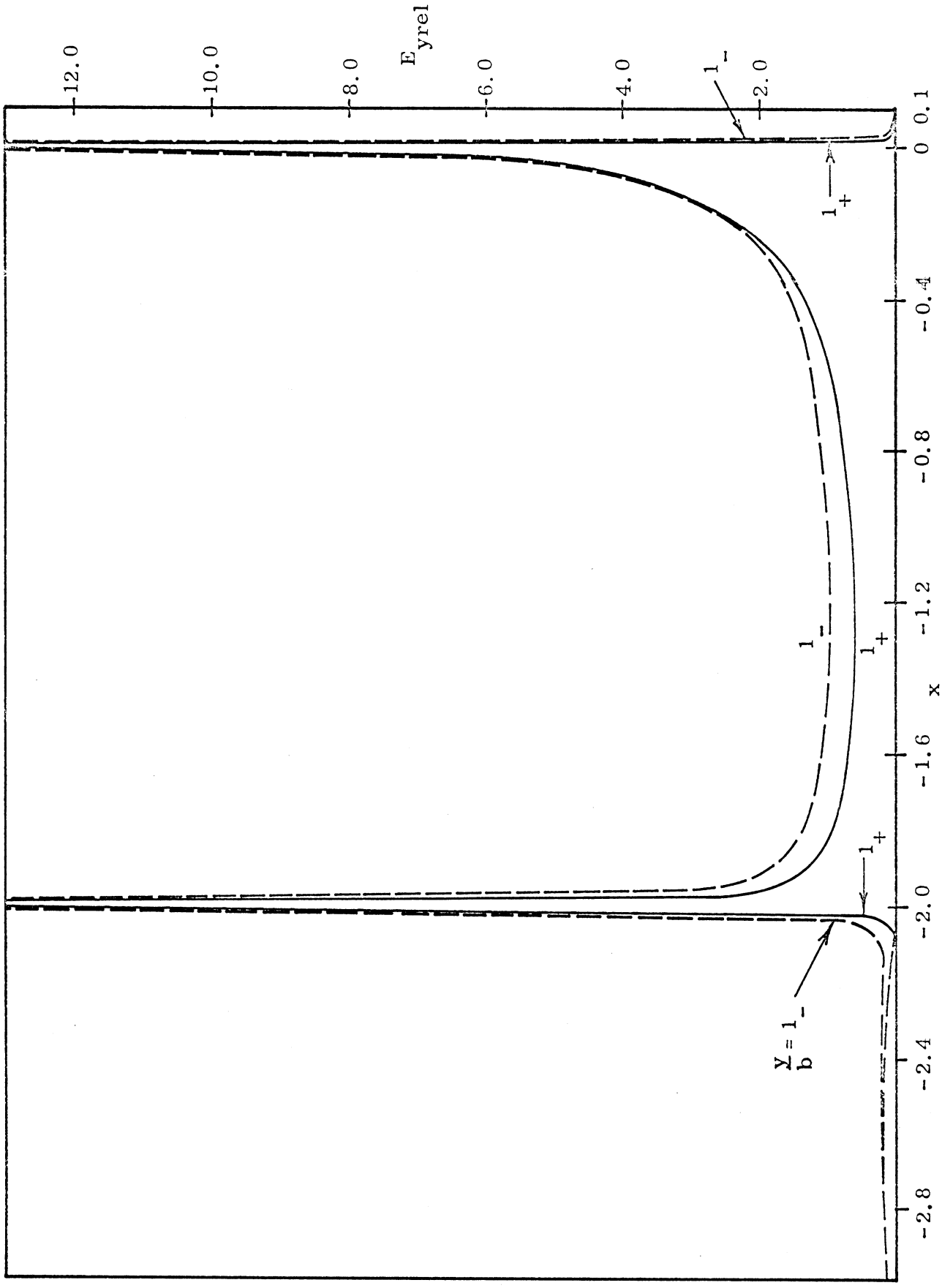

Fig. 3-13-b: E_{yrel} on $\frac{Y}{b} = l_-$ and l_+ lines for the case of $\frac{|a|}{b} = 1.0$, $\frac{d}{b} = 0.1$.

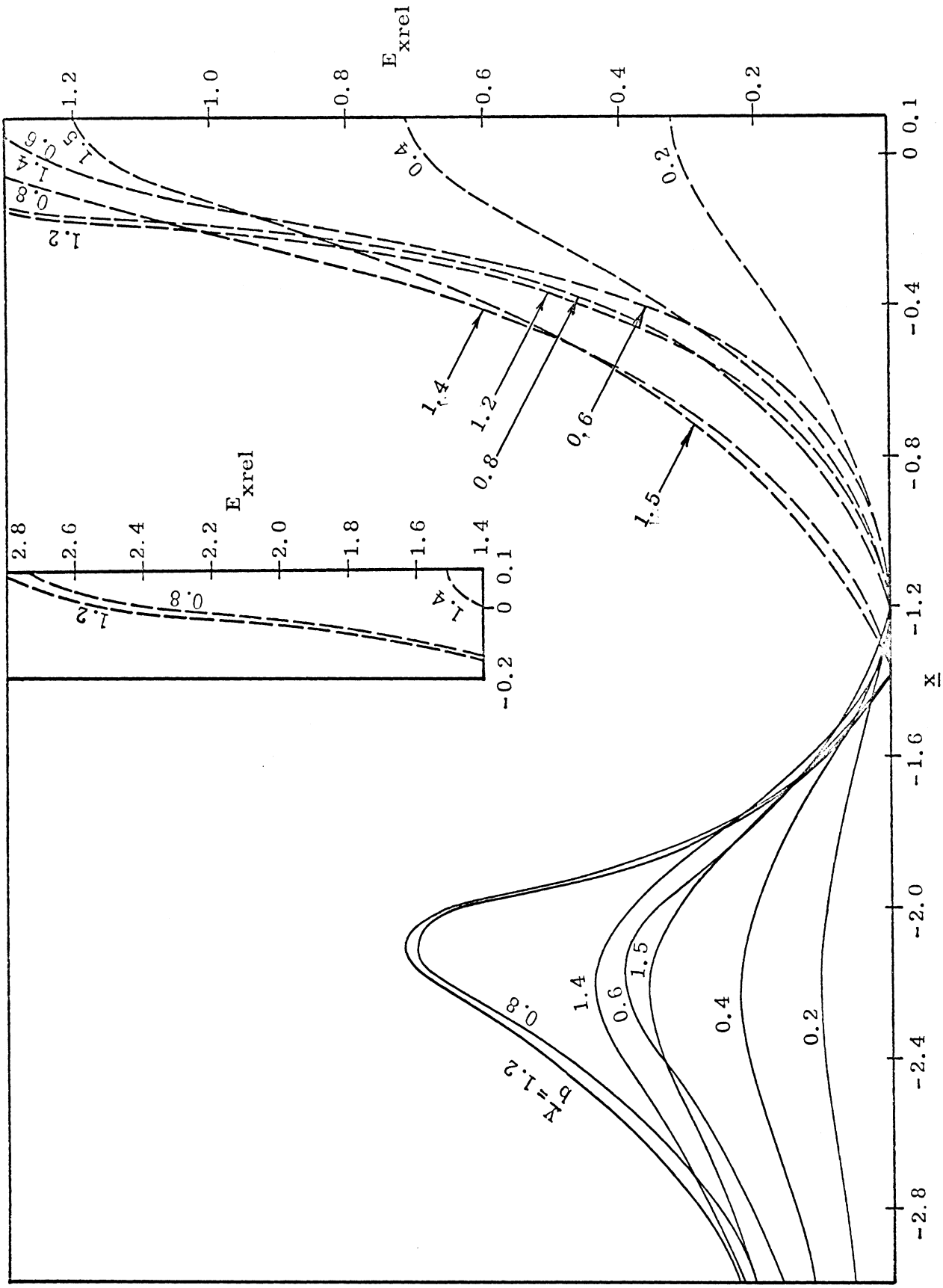

Fig. 3-13-c: E_{xrel} on $\frac{y}{b} = 0$, 0.2, 0.4, 0.6, 0.8, 1.2, 1.4 and 1.5 lines for the case of $\frac{|a|}{b} = 1.0$, $\frac{d}{b} = 0.1$

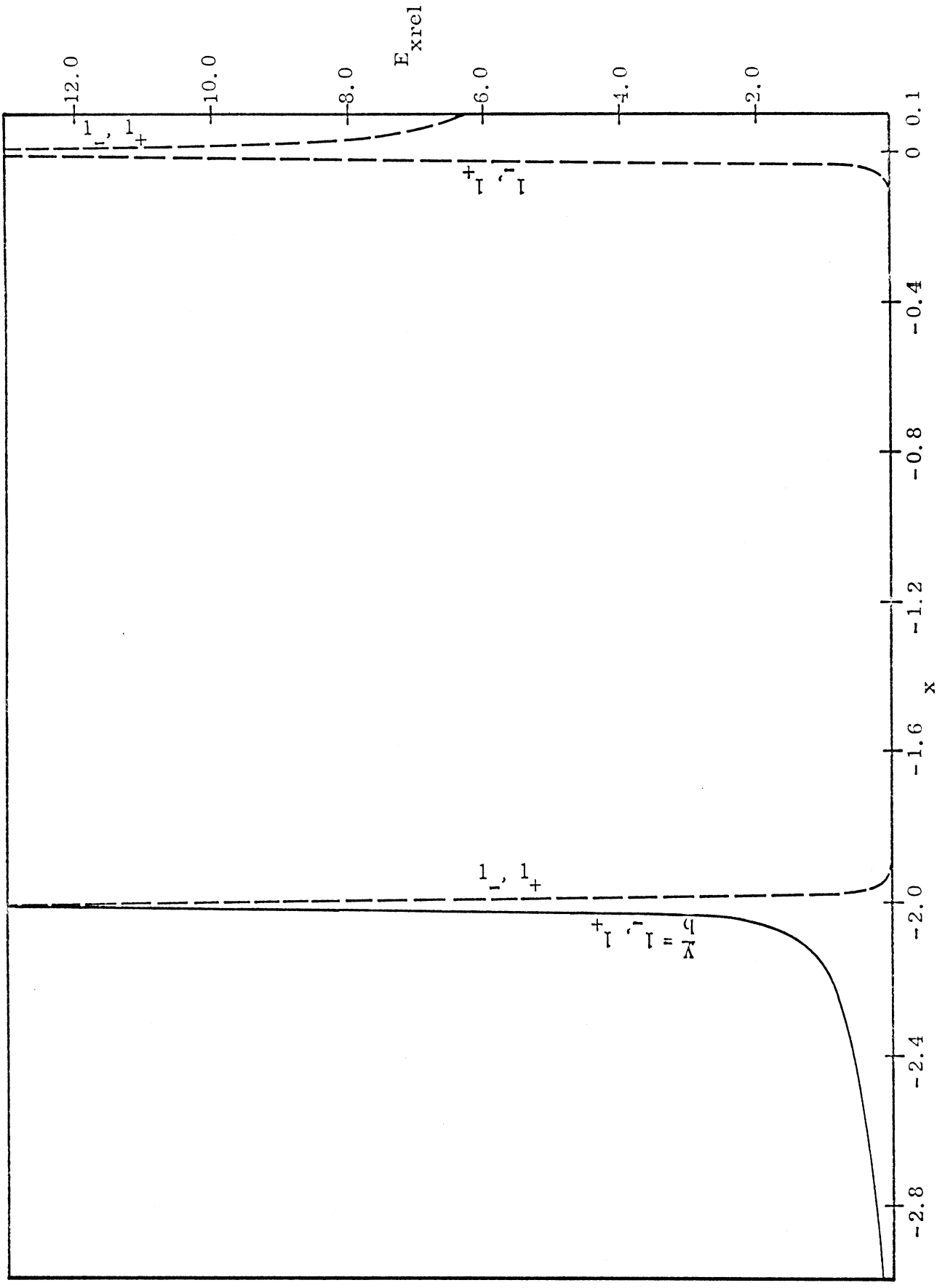

Fig. 3-13-d: E_{xrel} on $\frac{y}{b} = l_-$ and l_+ lines for the case of $\frac{|a|}{b} = 1.0$, $\frac{d}{b} = 0.1$.

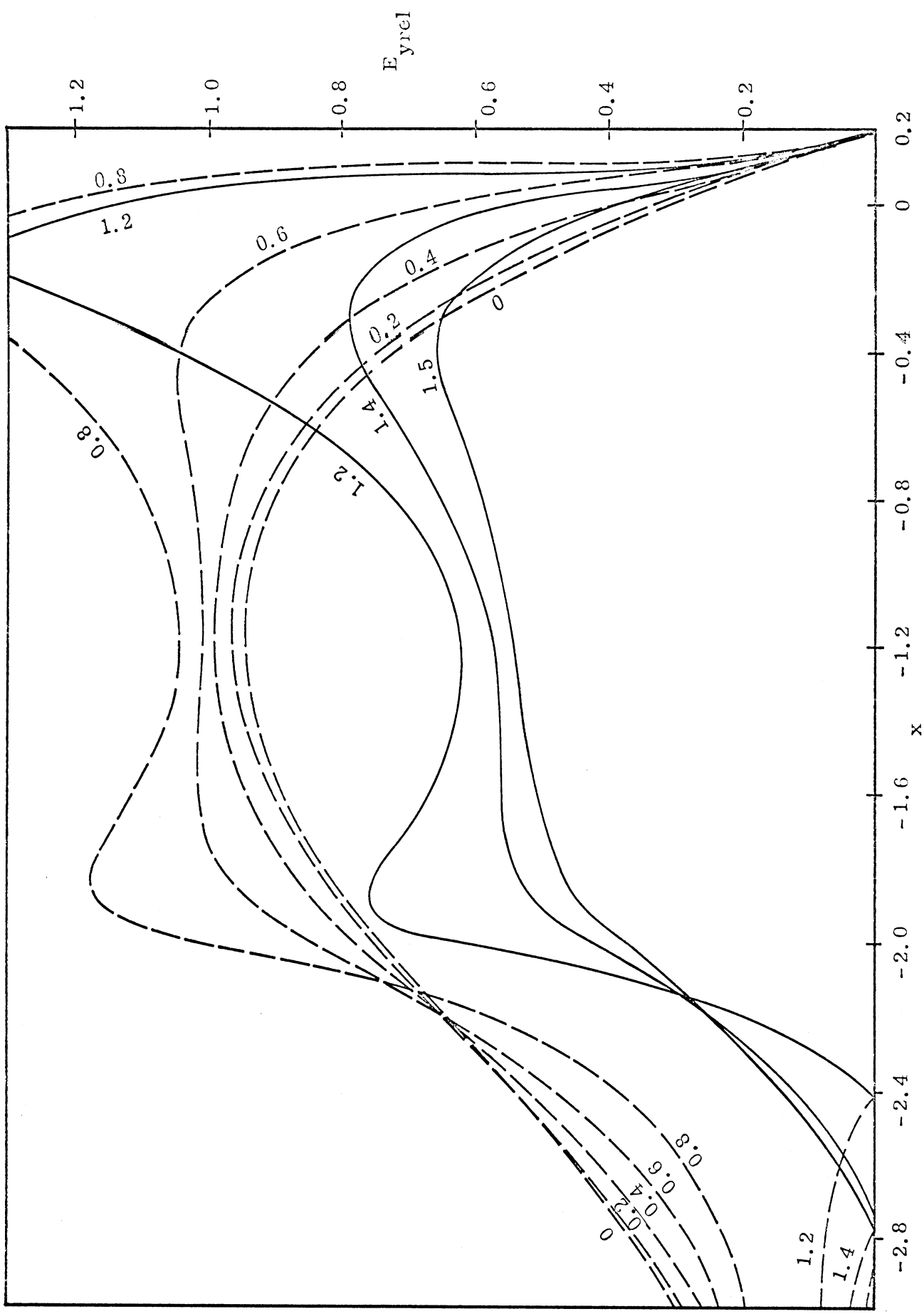

Fig. 3-14-a: E_{yrel} on $\frac{Y}{b} = 0, 0.2, 0.4, 0.6, 0.8, 1.2, 1.4$ and 1.5 lines for the case of $\frac{|z|}{b} = 1.0$, $\frac{d}{b} = 0.2$.

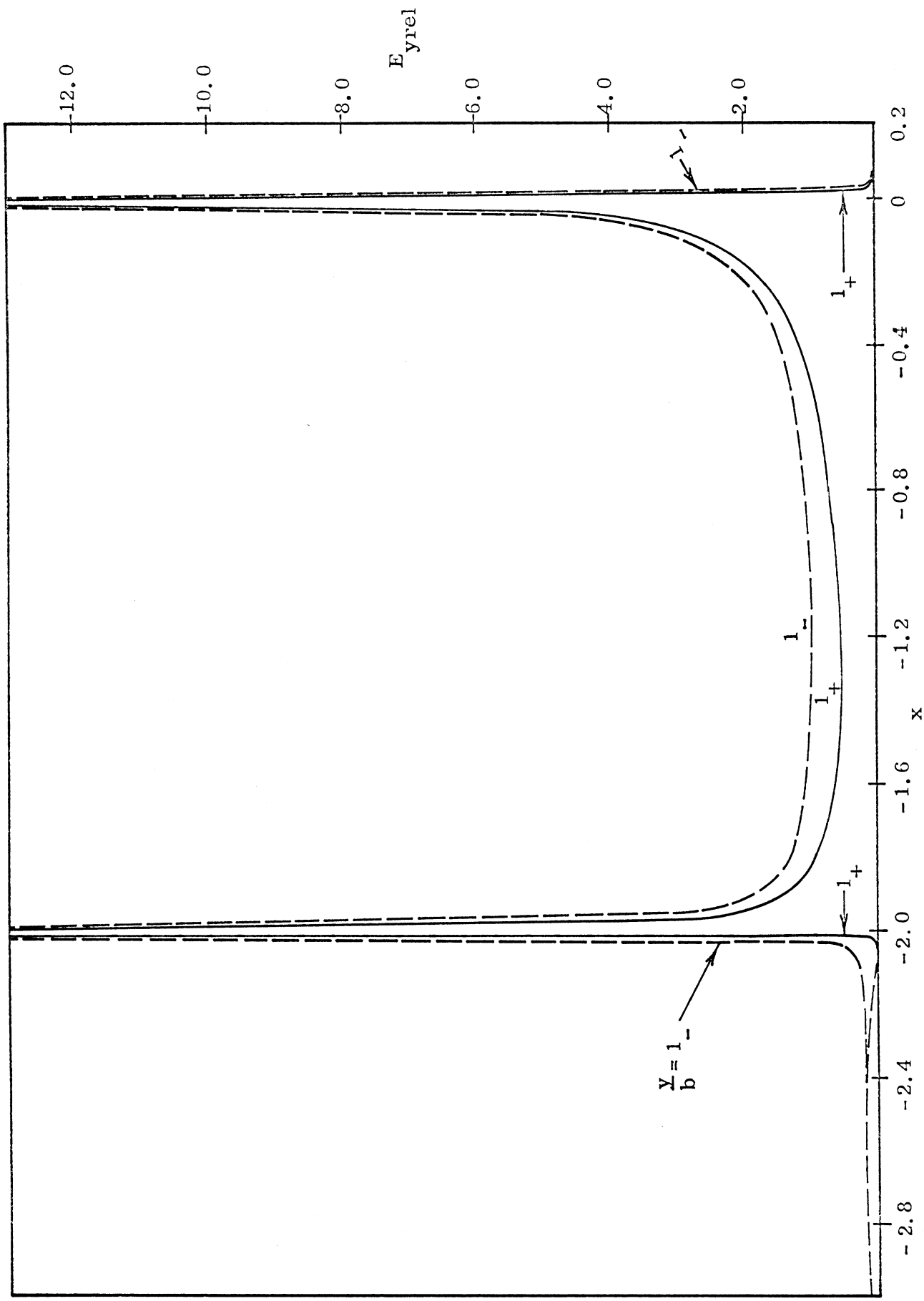

Fig. 3-14-b: E_{yrel} on $\frac{Y}{b} = l_-$ and l_+ lines for the case of $\frac{|a|}{b} = 1.0$, $\frac{d}{b} = 0.2$.

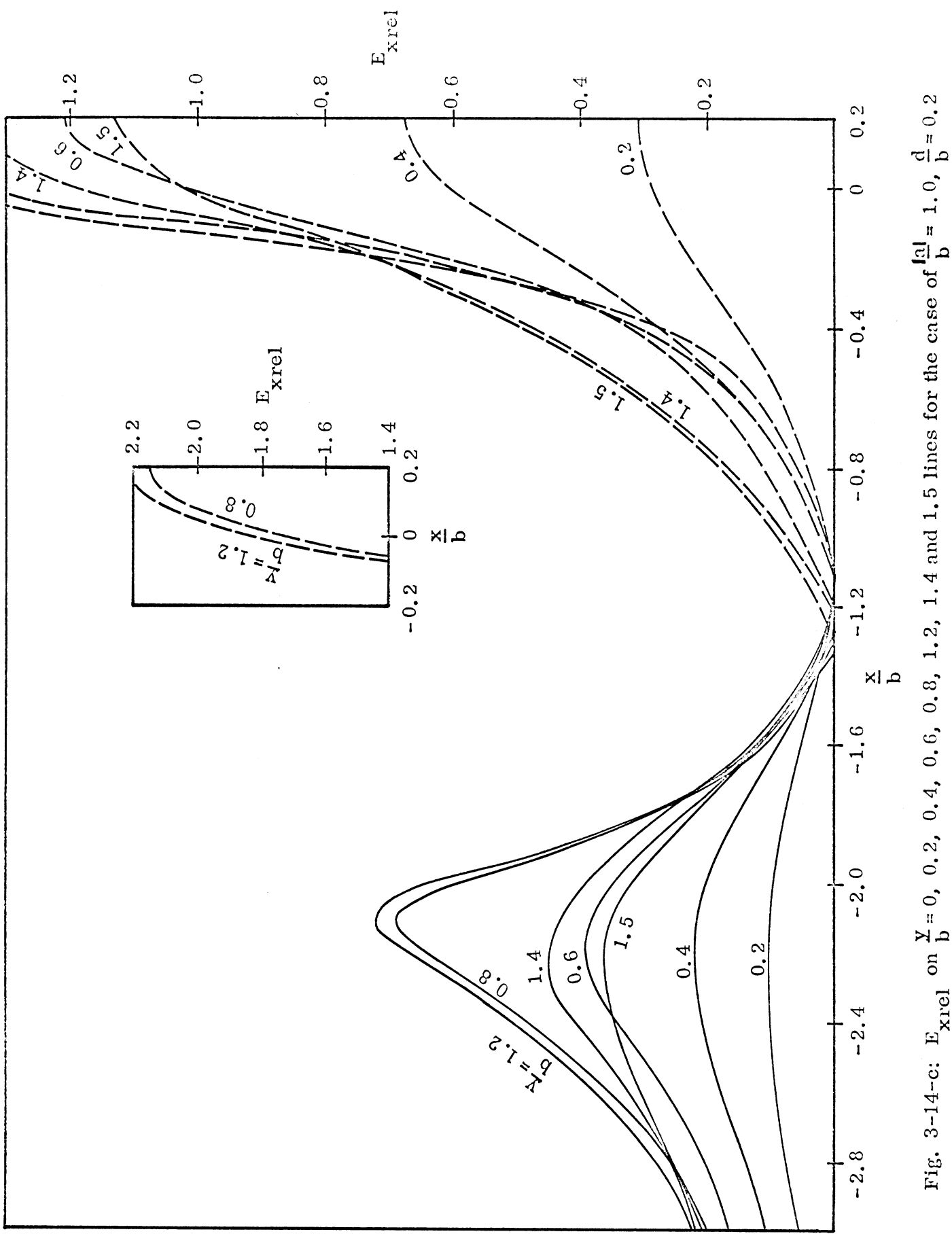

Fig. 3-14-c: E_{xrel} on $\frac{Y}{b} = 0$, 0.2, 0.4, 0.6, 0.8, 1.2, 1.4 and 1.5 lines for the case of $\frac{|a|}{b} = 1.0$, $\frac{d}{b} = 0.2$

(E_{xrel} on $\frac{Y}{b} = 0$ line is zero).

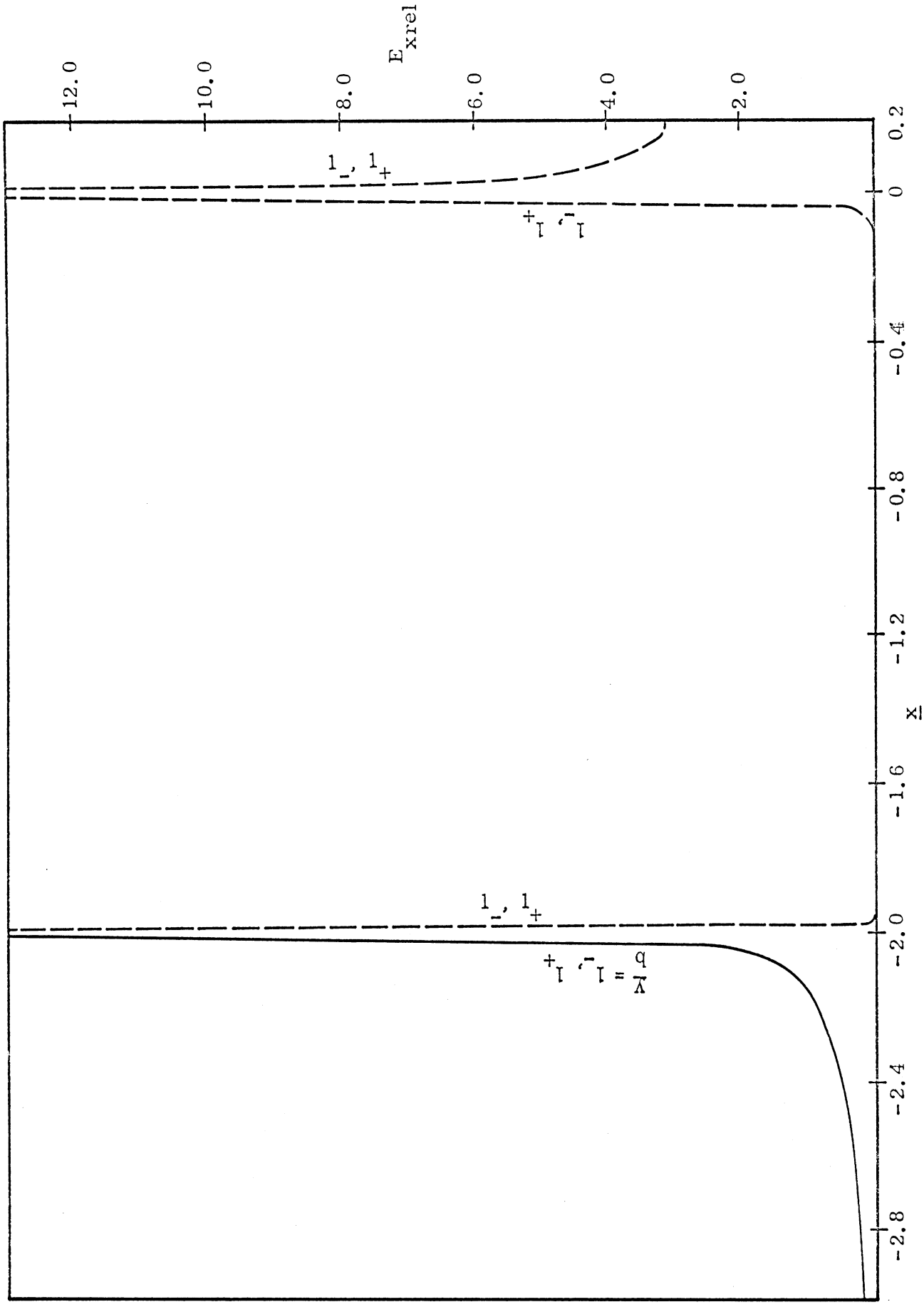

Fig. 3-14-d: E_{xrel} on $\frac{y}{b} = l_-$ and l_+ lines for the case of $\frac{|a|}{b} = 1.0$, $\frac{d}{b} = 0.2$.

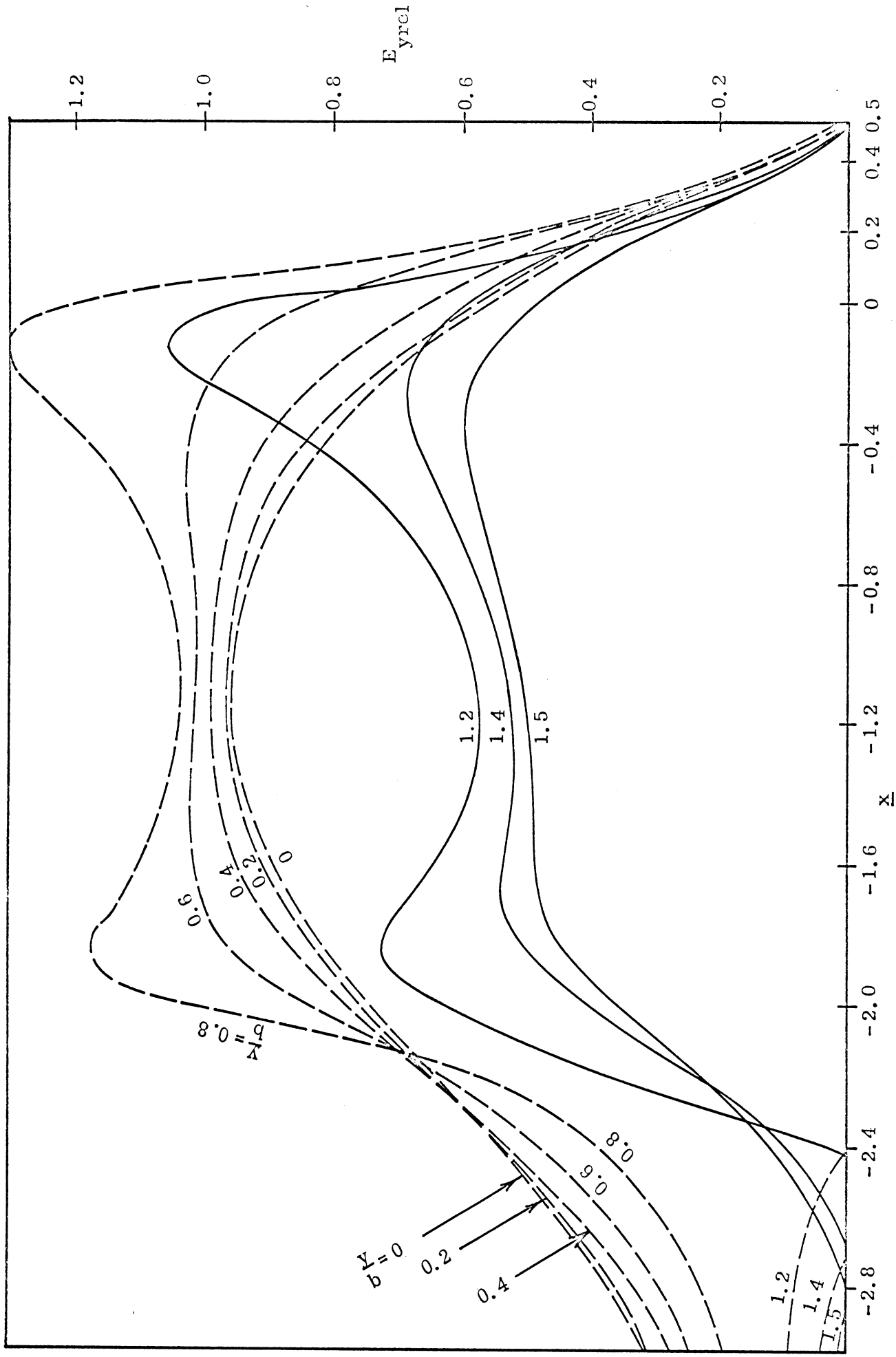

Fig. 3-15-a: E_{yrel} on $\frac{Y}{b} = 0$, 0.2, 0.4, 0.6, 0.8, 1.2, 1.4 and 1.5 lines for the case of $\frac{|a|}{b} = 1.0$, $\frac{d}{b} = 0.5$.

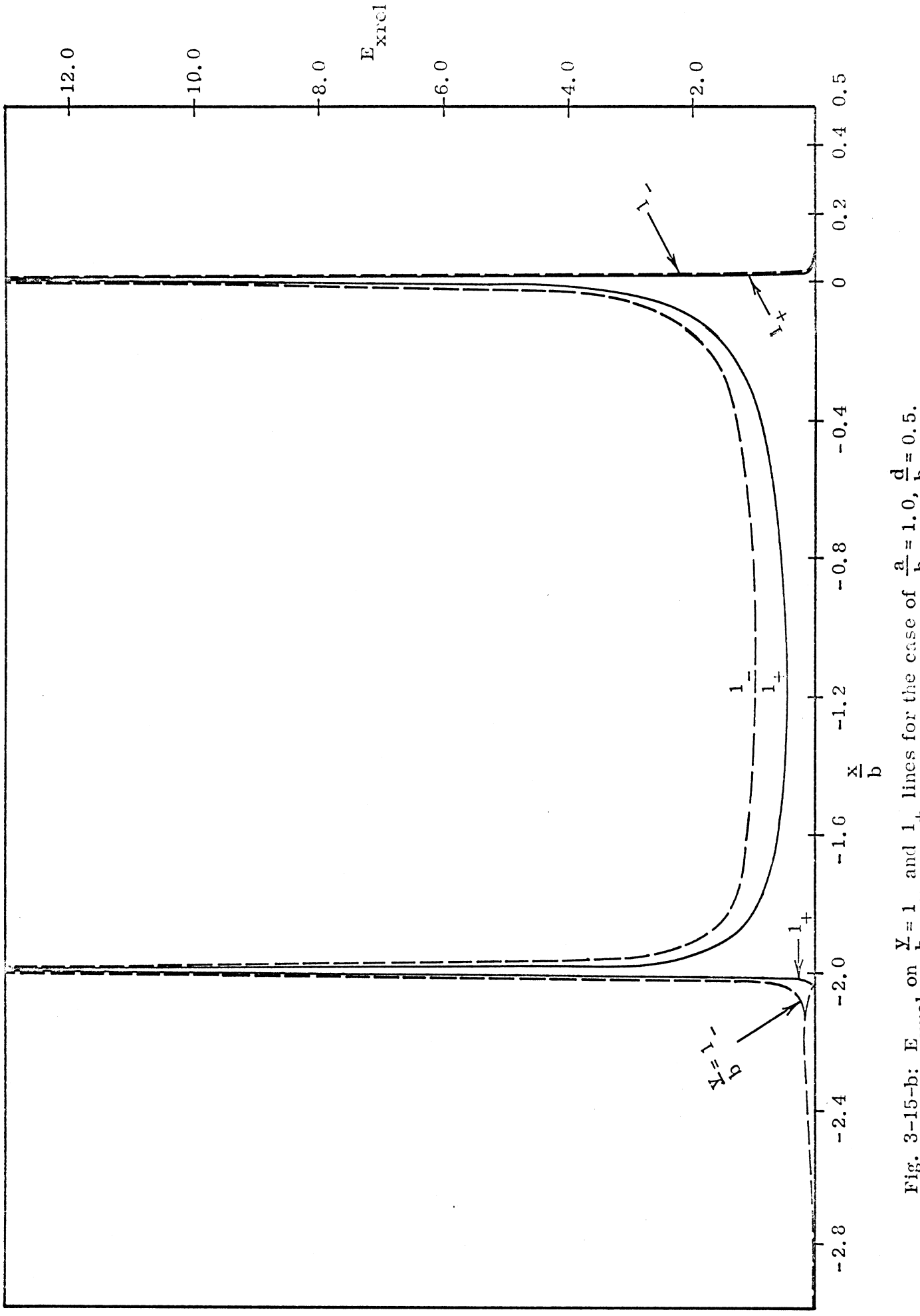

Fig. 3-15-b: E_{xrel} on $\frac{Y}{b} = l_-$ and l_+ lines for the case of $\frac{a}{b} = 1.0$, $\frac{d}{b} = 0.5$.

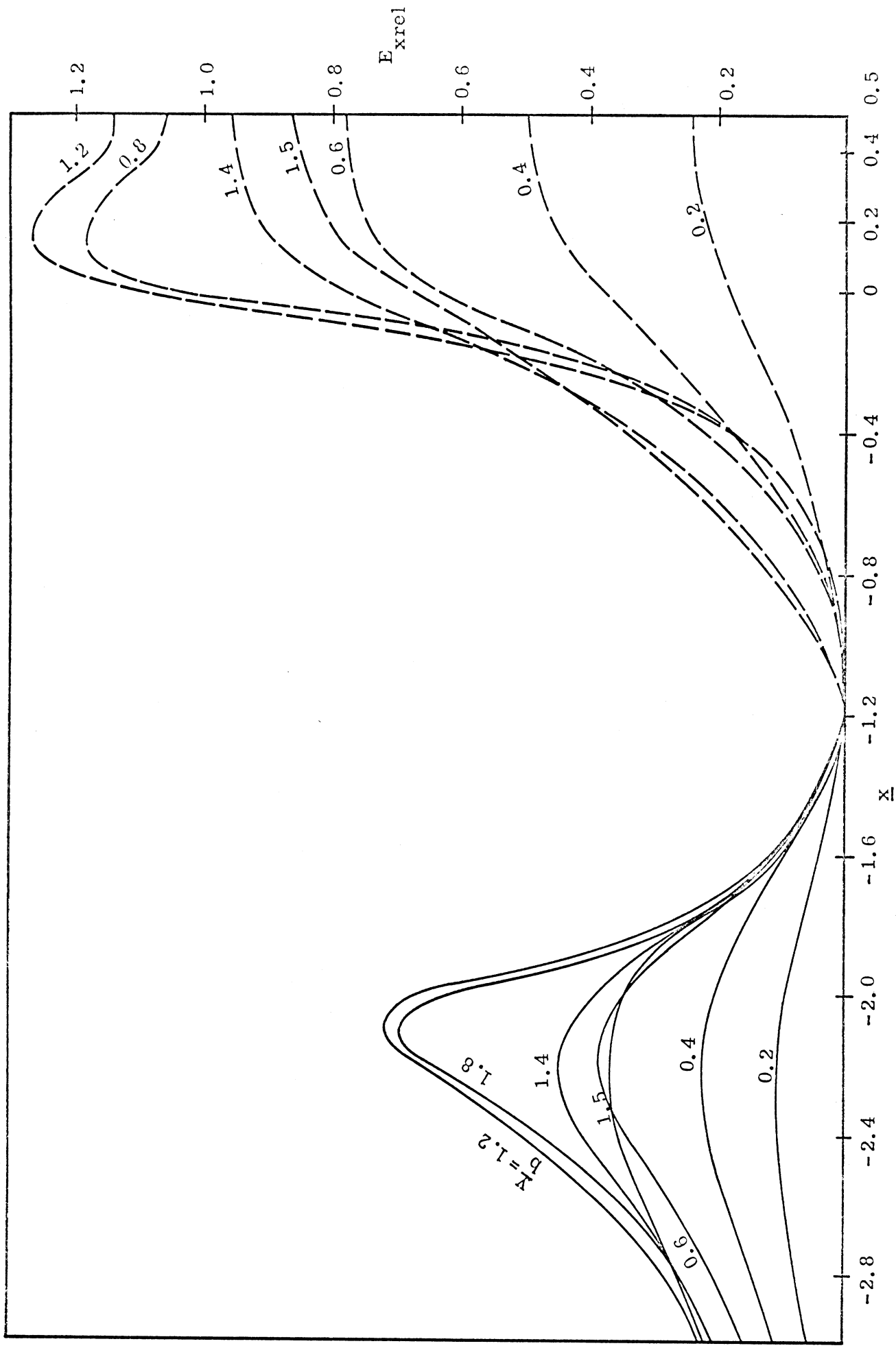

Fig. 3-15-c: E_{xrel} on $\frac{y}{b}$ = 0, 0.2, 0.4, 0.6, 0.8, 1.2, 1.4 and 1.5 lines for the case of $\frac{|a|}{b}$ = 1.0 and $\frac{d}{b}$ = 0.5 (E_{xrel} on $\frac{y}{b}$ = 0 line is zero).

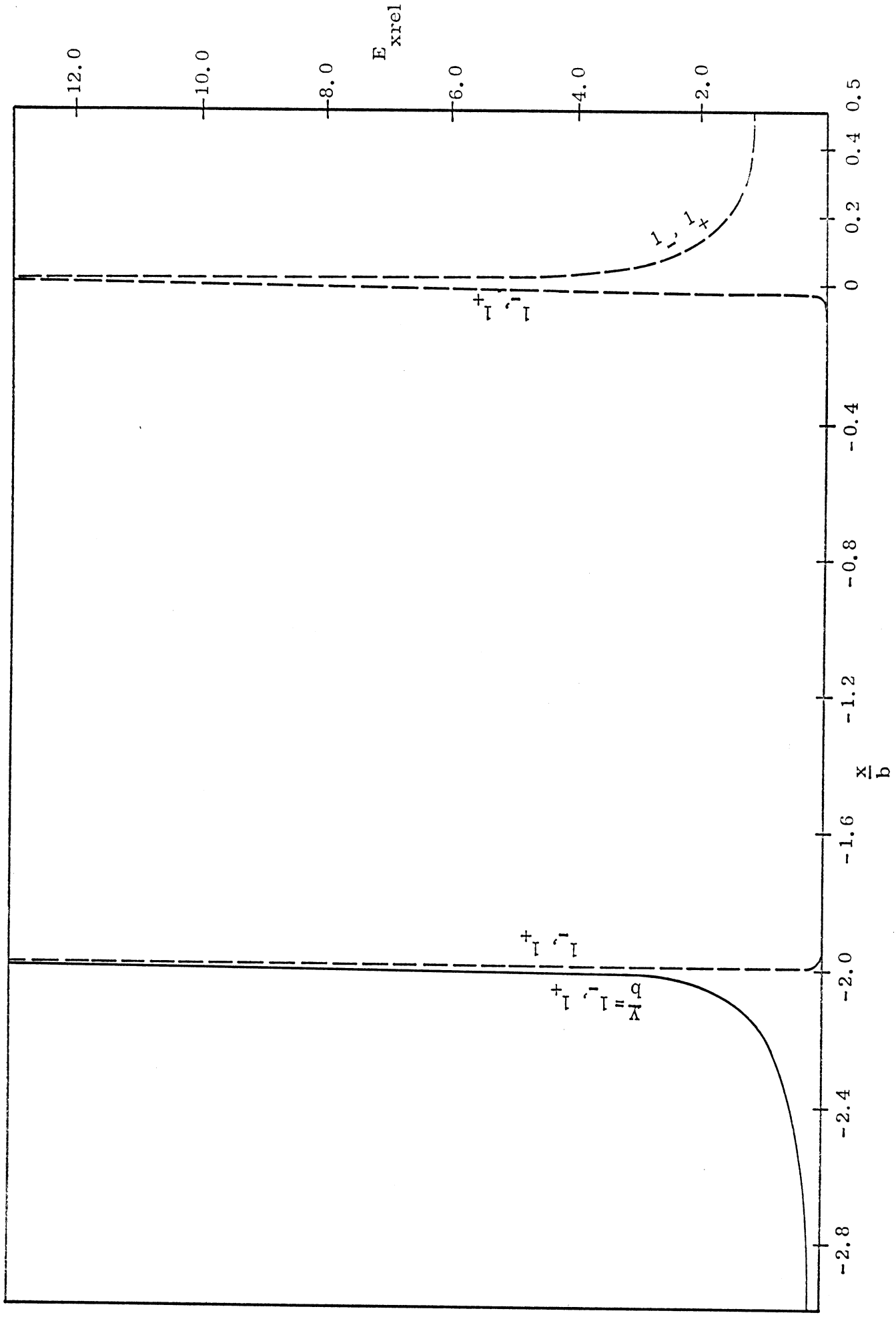

Fig. 3-15-d: E_{xrel} on $\frac{y}{b} = 1_-$ and 1_+ lines for the case of $\frac{|a|}{b} = 1.0$, $\frac{d}{b} = 0.5$.

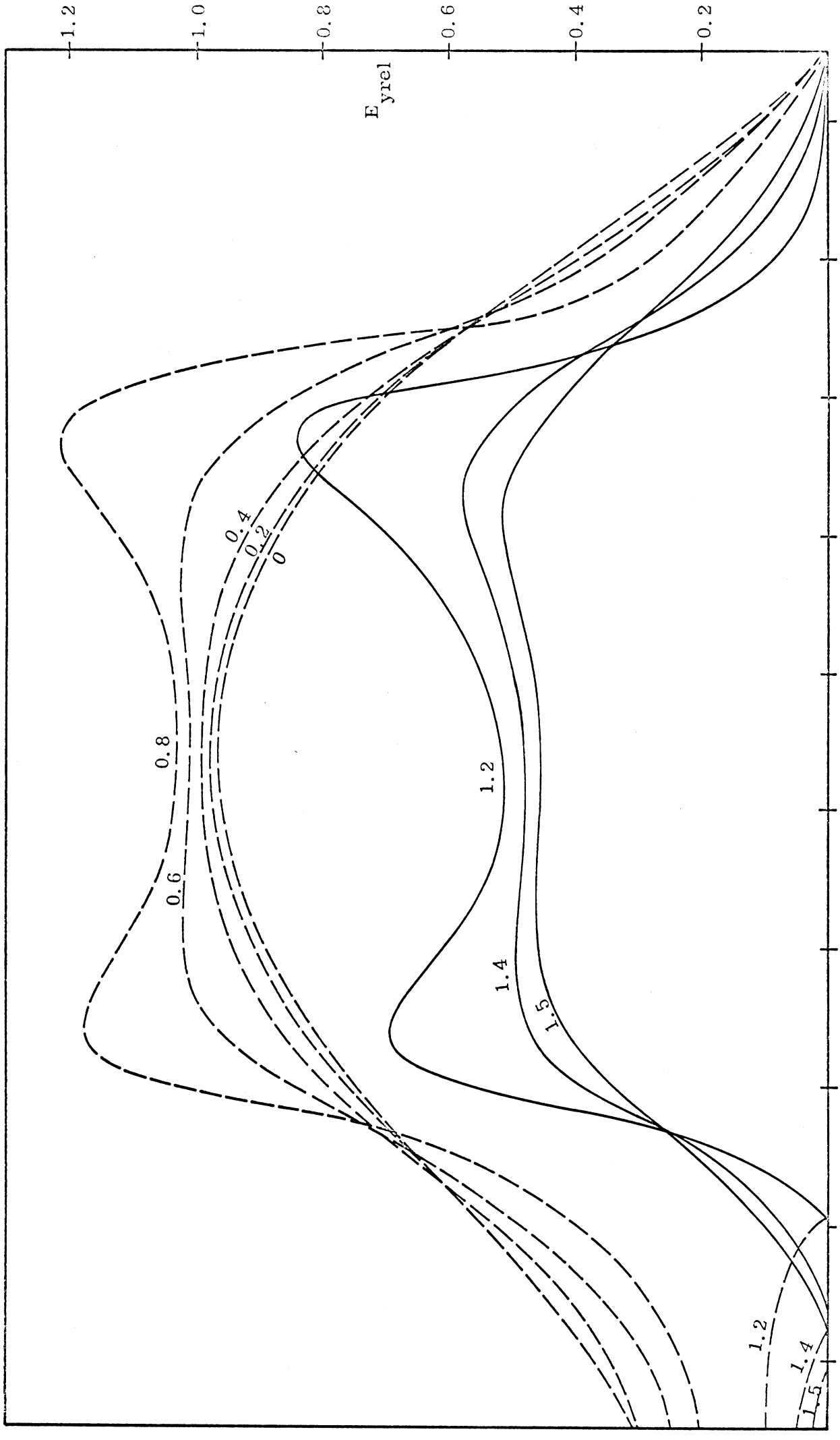

Fig. 3-16-a: E_{yrel} on $\frac{Y}{b} = 0,\ 0.2,\ 0.4,\ 0.6,\ 0.8,\ 1.2,\ 1.4$ and 1.5 lines for the case of $\frac{|a|}{b} = 1.0,\ \frac{d}{b} = 1.0$.

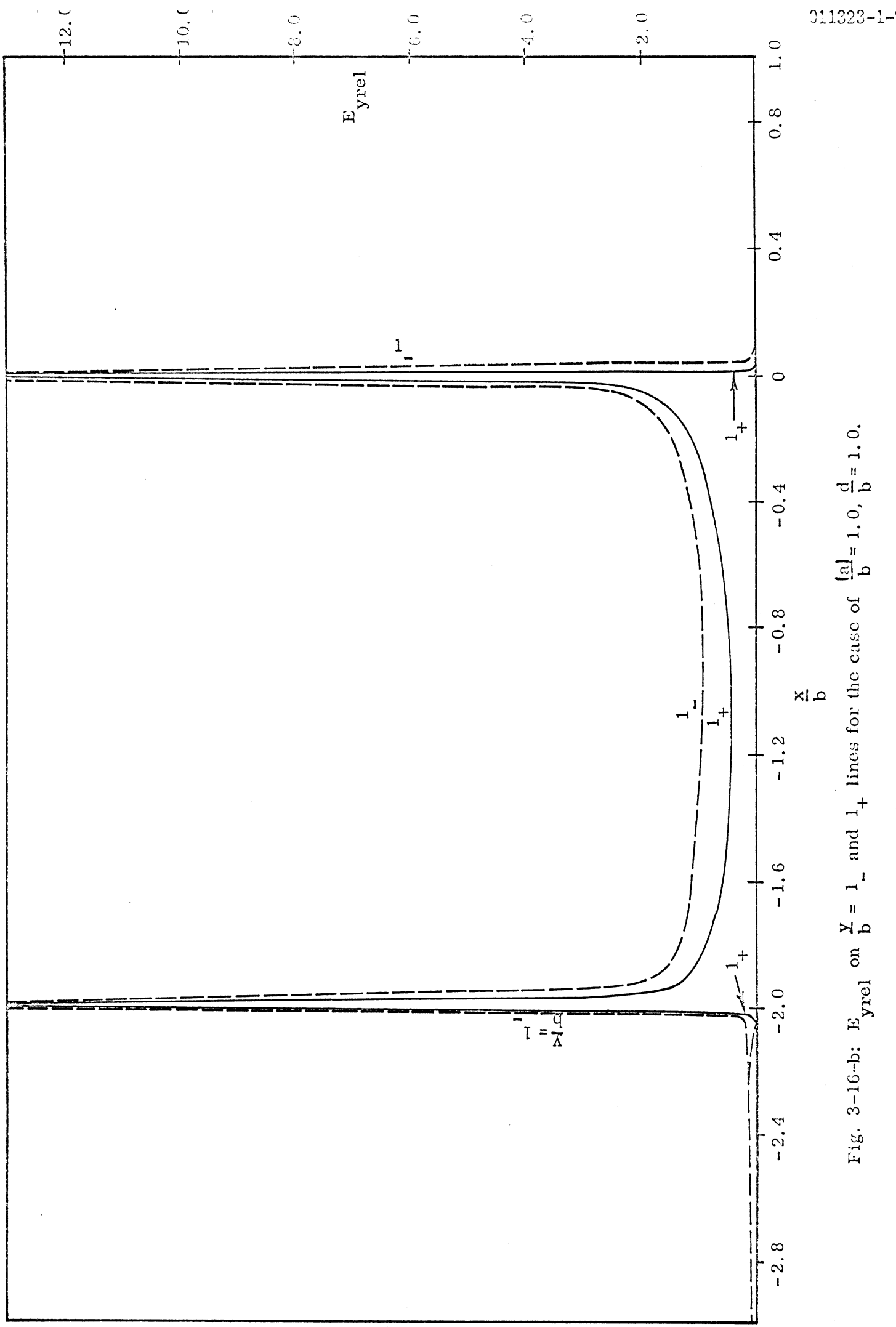

Fig. 3-16-b: E_{yrel} on $\frac{Y}{b} = 1_-$ and 1_+ lines for the case of $\frac{|a|}{b} = 1.0$, $\frac{d}{b} = 1.0$.

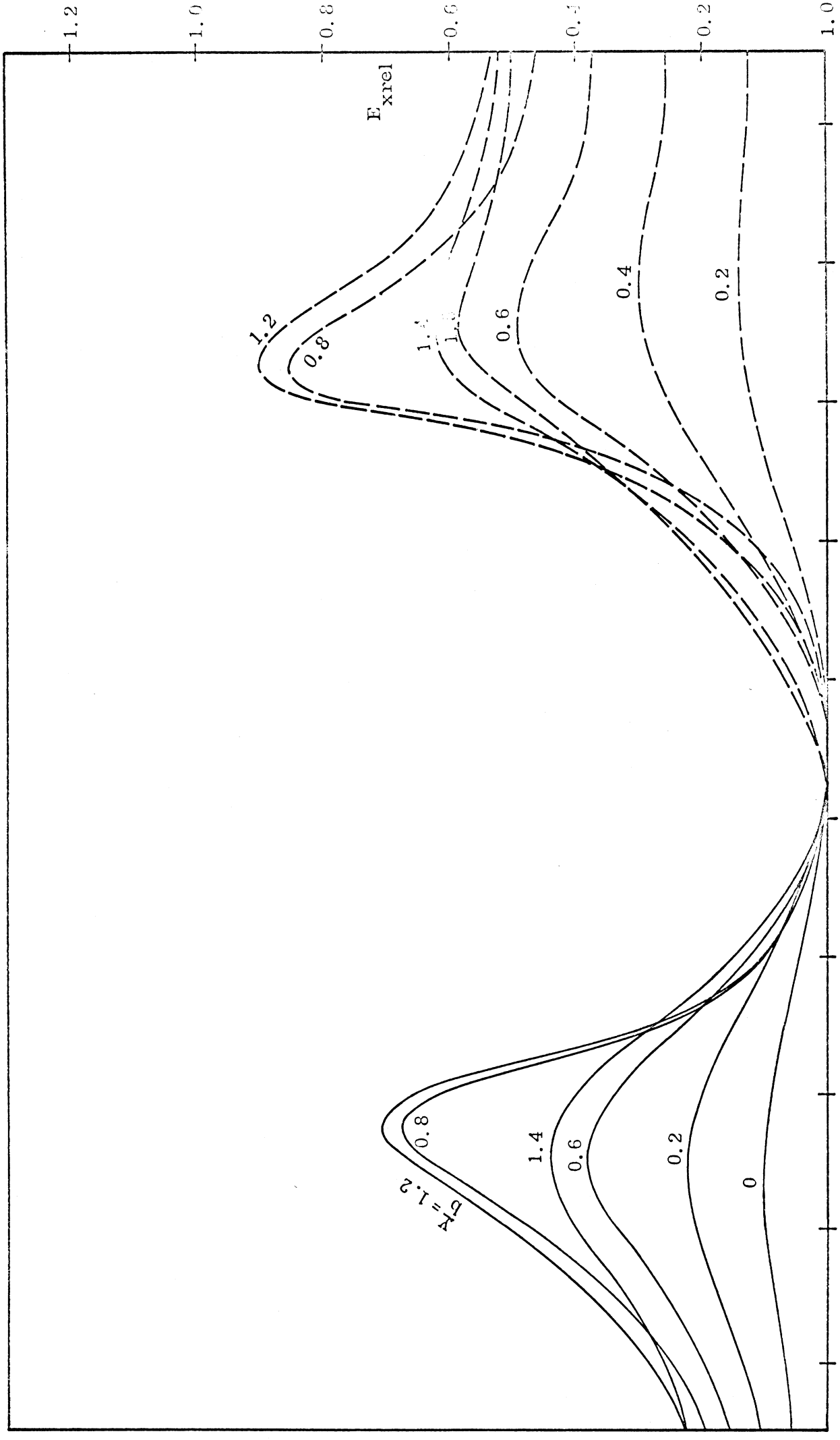

Fig. 3-16-c: E_{xrel} on $\frac{Y}{b}$ = 0, 0.2, 0.4, 0.6, 0.8, 1.2, 1.4 and 1.5 lines for the case of $\frac{|a|}{b}$ = 1.0, $\frac{d}{b}$ = 1.0 (E_{xrel} on $\frac{Y}{b}$ = 0 line is zero).

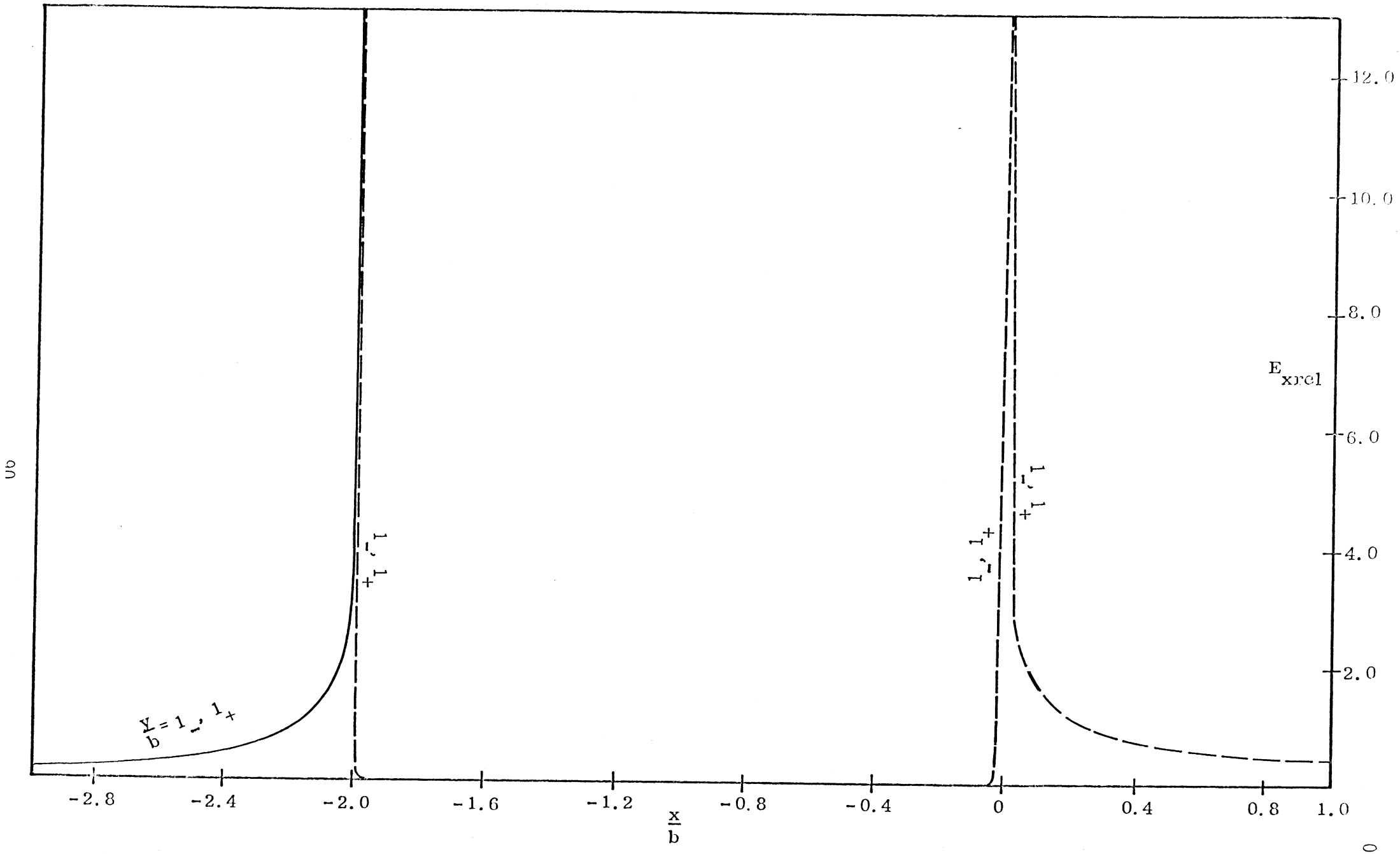

Fig. 3-16-d: E_{xrel} on $\frac{y}{b} = 1_-$ and 1_+ lines for the case of $\frac{|a|}{b} = 1.0$, $\frac{d}{b} = 1.0$.

011323-1-T

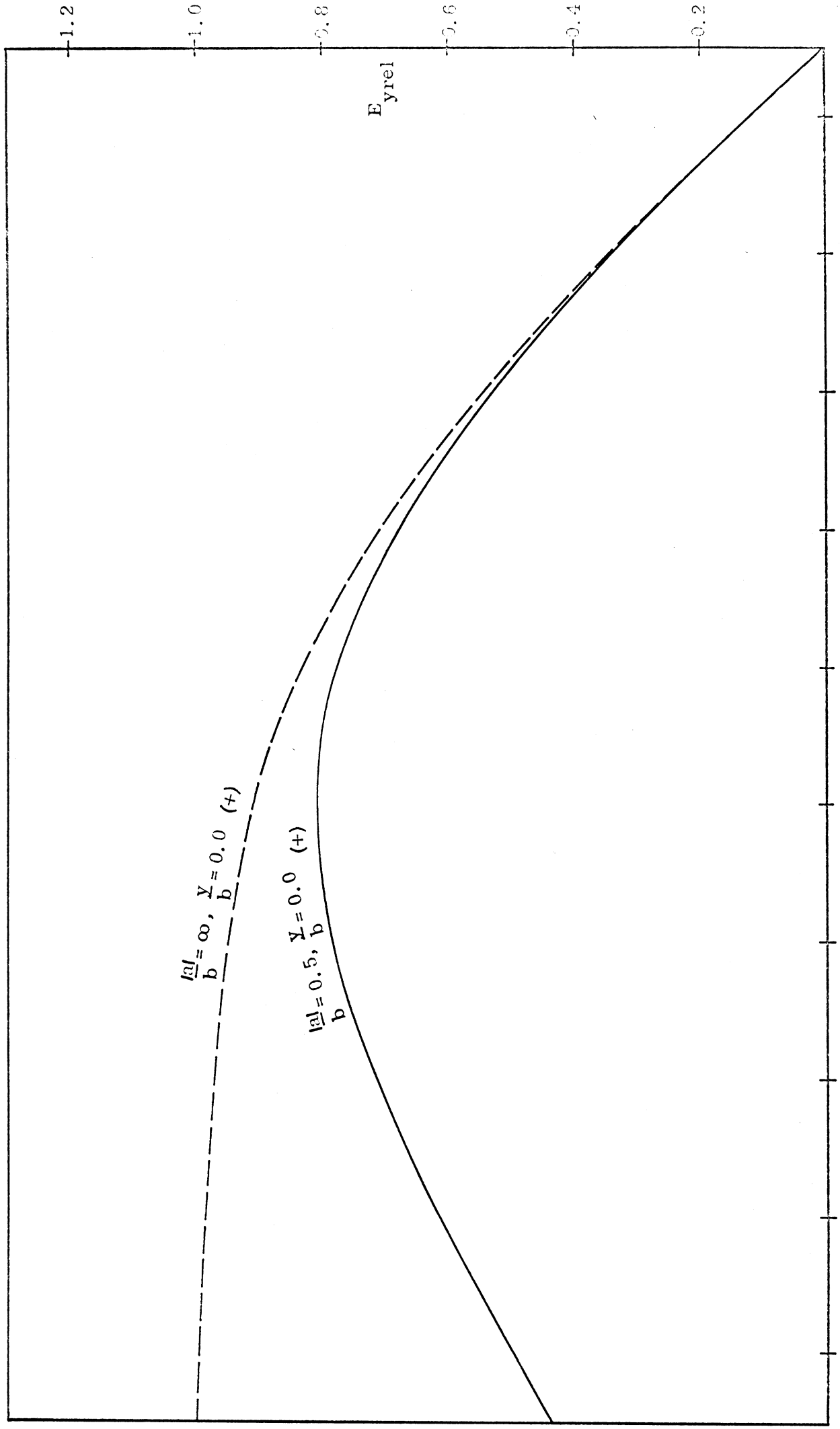

Fig. 3-17-1: Comparison of E_{yrel} on $\frac{y}{b} = 0$ line for the case of $\frac{d}{b} = 0.5$ between $\frac{|a|}{b} = 0.5$ and ∞.

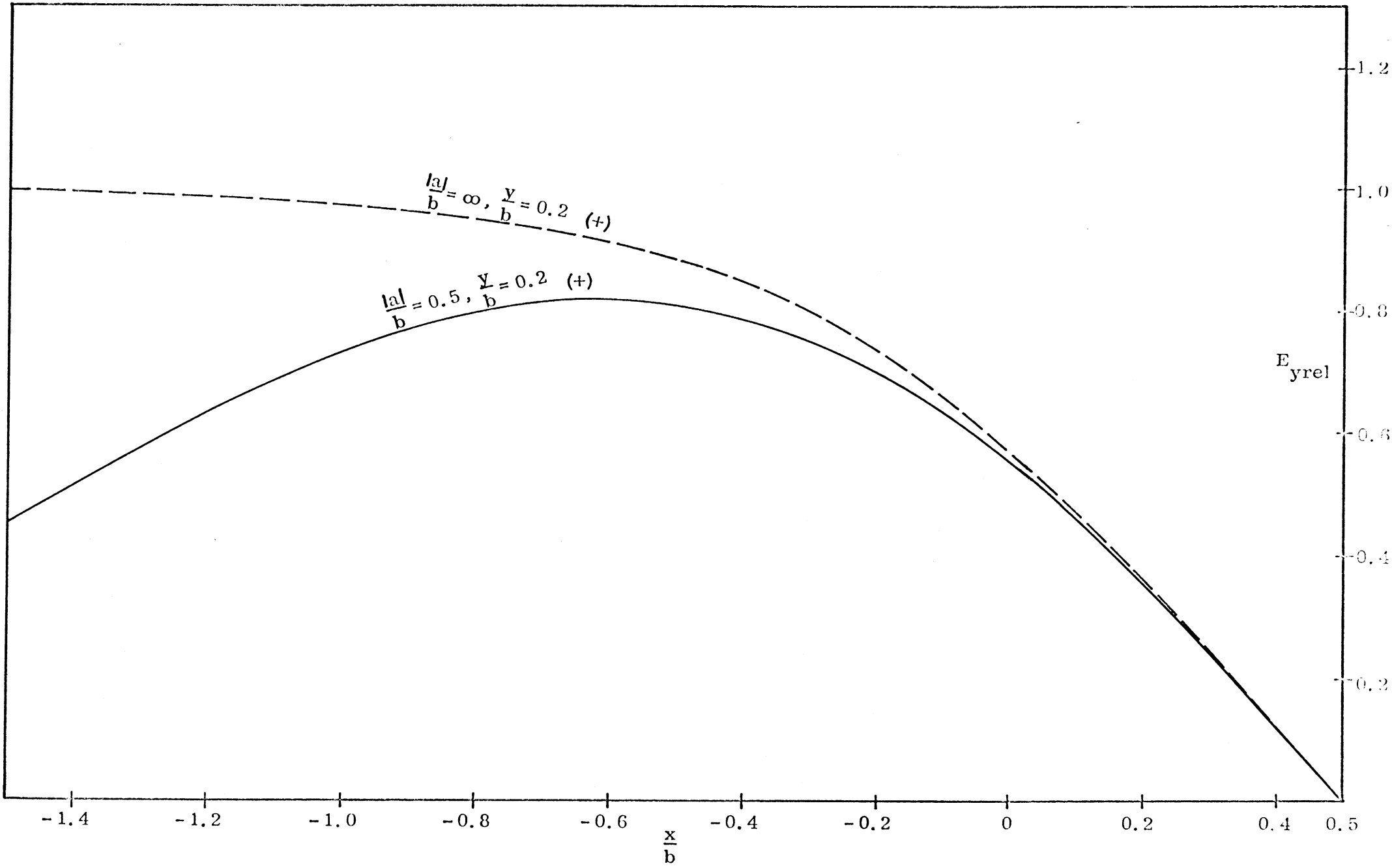

Fig. 3-17-2: Comparison of E_{yrel} on $\frac{y}{b} = 0.2$ line for the case of $\frac{d}{b} = 0.5$ between $\frac{|a|}{b} = 0.5$ and ∞.

01122-1-T

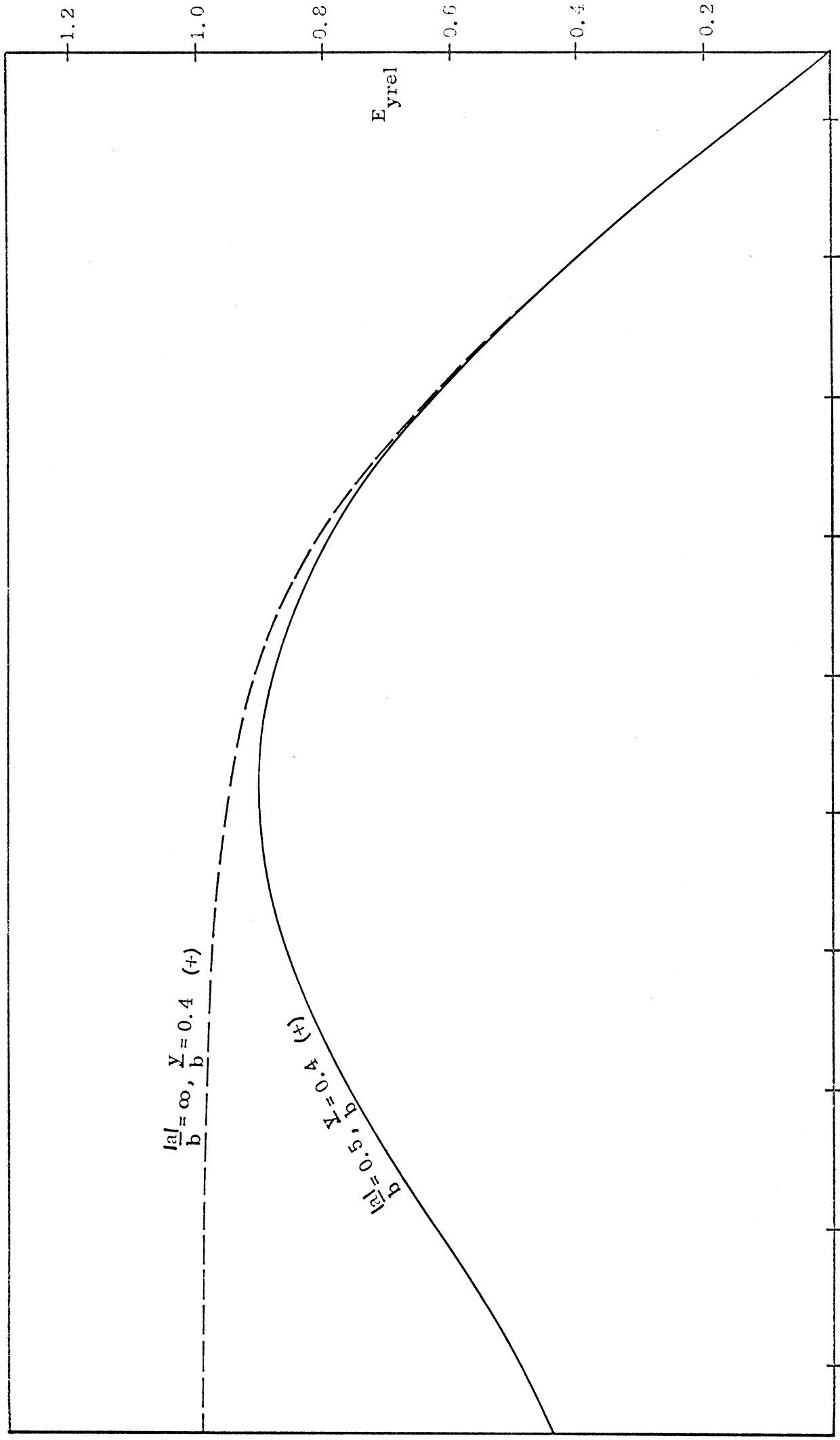

Fig. 3-17-3: Comparison of E_{yrel} on $\frac{Y}{b} = 0.4$ line for the case of $\frac{d}{b} = 0.5$ between $\frac{|a|}{b} = 0.5$ and ∞.

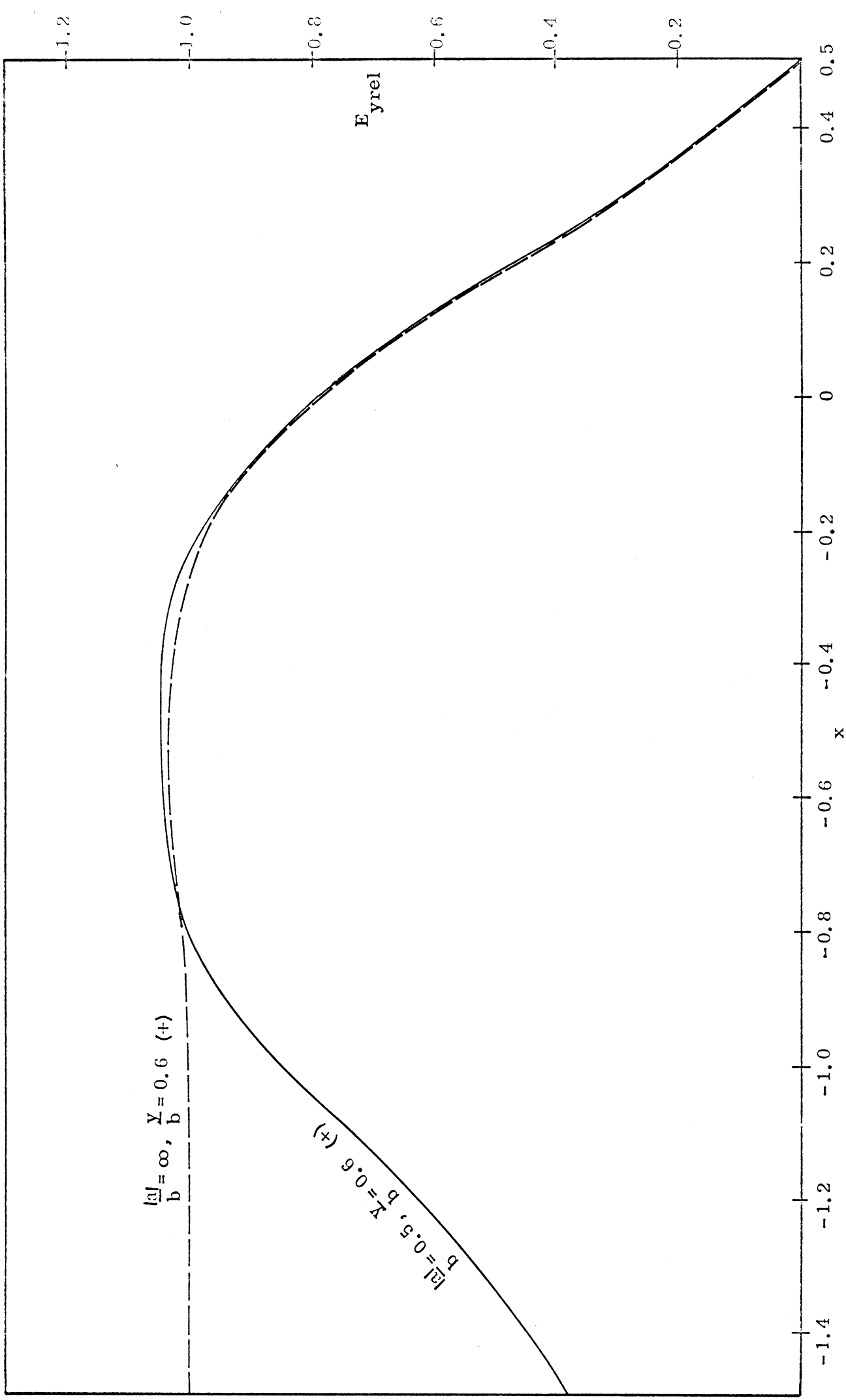

Fig. 3-17-4: Comparison of E_{yrel} on $\frac{Y}{b} = 0.6$ line for the case of $\frac{d}{b} = 0.5$ between $\frac{|a|}{b} = 0.5$ and ∞.

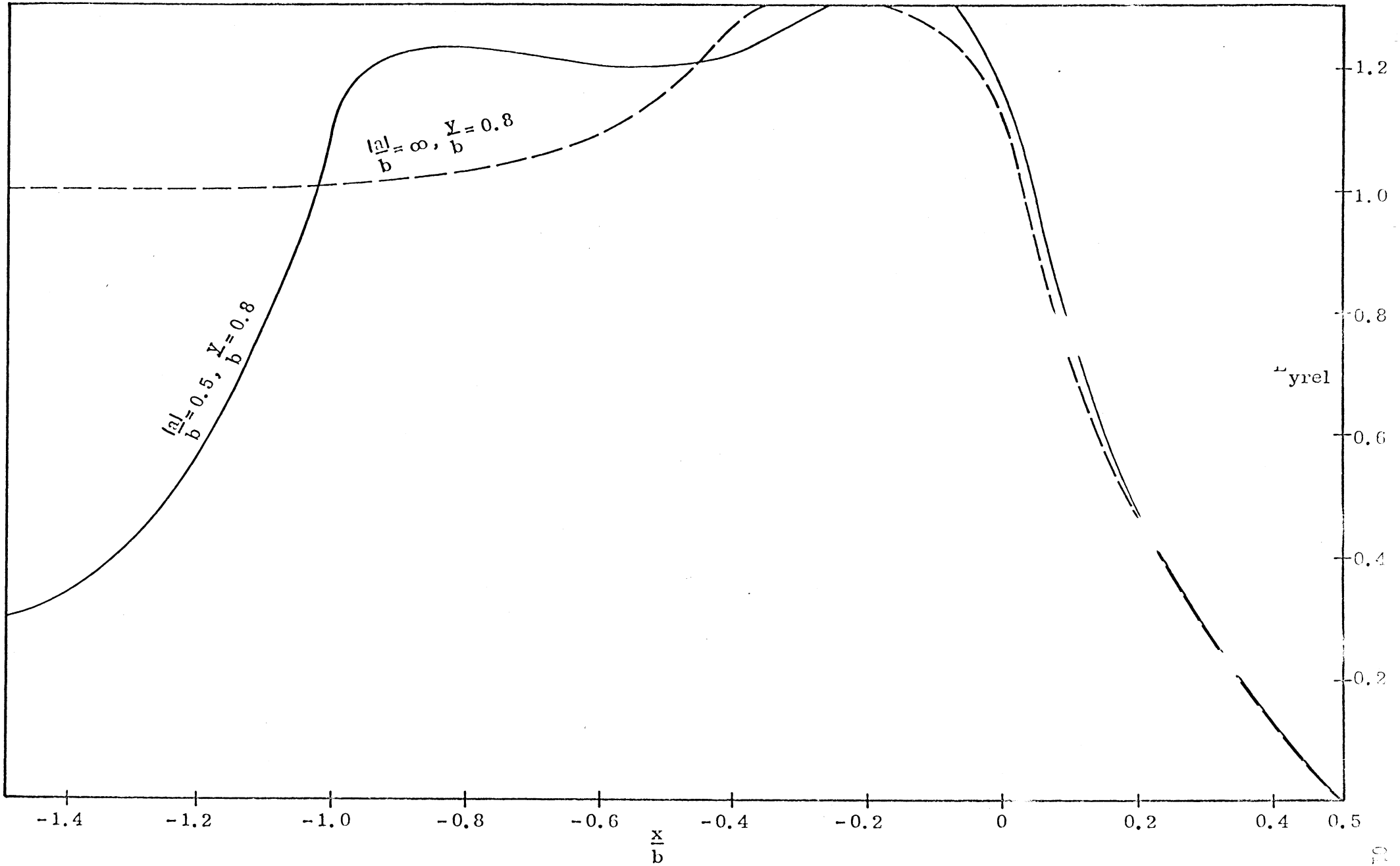

Fig. 3-17-5: Comparison of E_{yrel} on $\frac{y}{b} = 0.8$ line for the case of $\frac{d}{b} = 0.5$ between $\frac{|a|}{b} = 0.5$ and ∞.

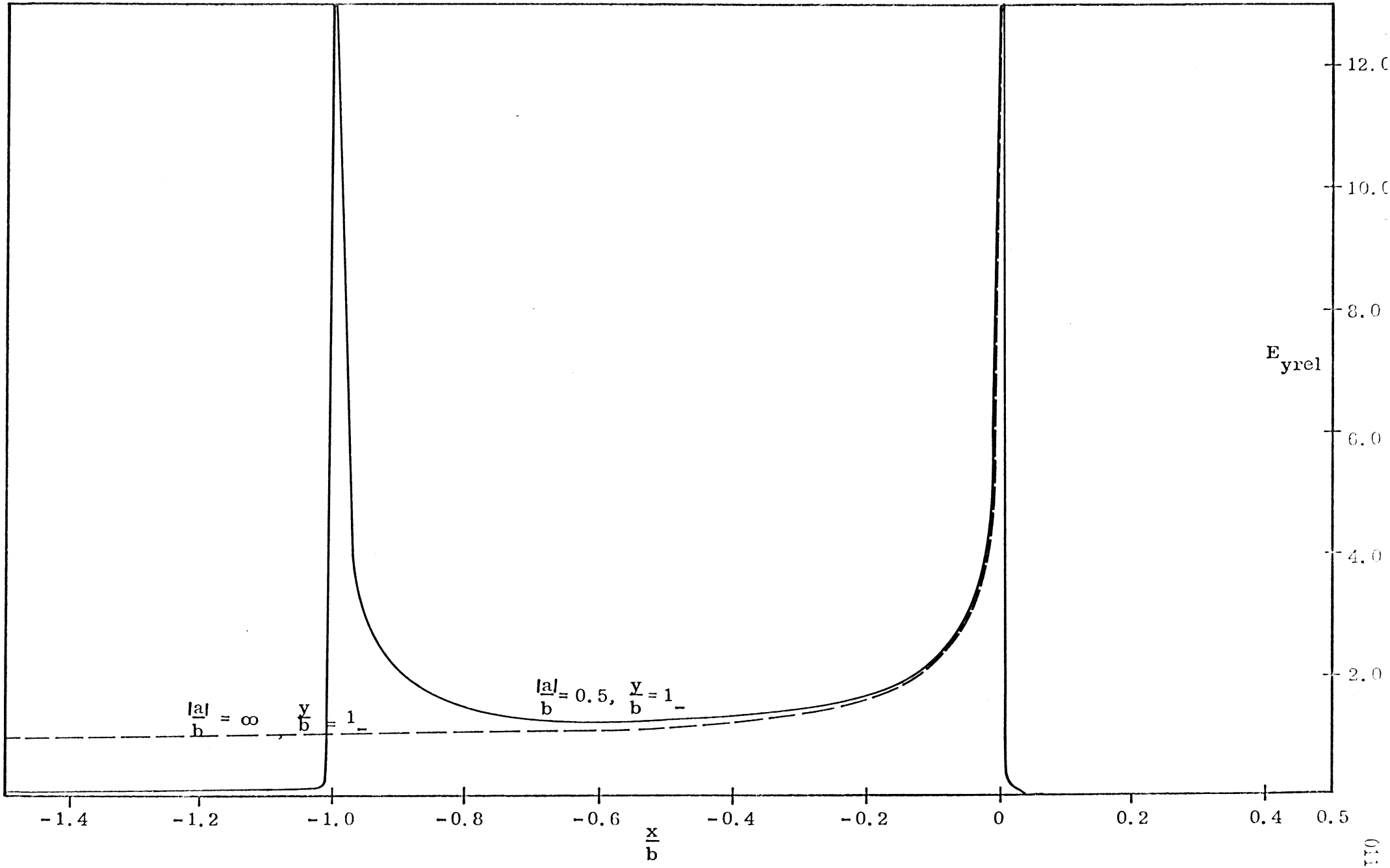

Fig. 3-17-6: Comparison of E_{yrel} on $\frac{y}{b} = 1_-$ line for the case of $\frac{d}{b} = 0.5$ between $\frac{|a|}{b} = 0.5$ and ∞.

011323-1-T

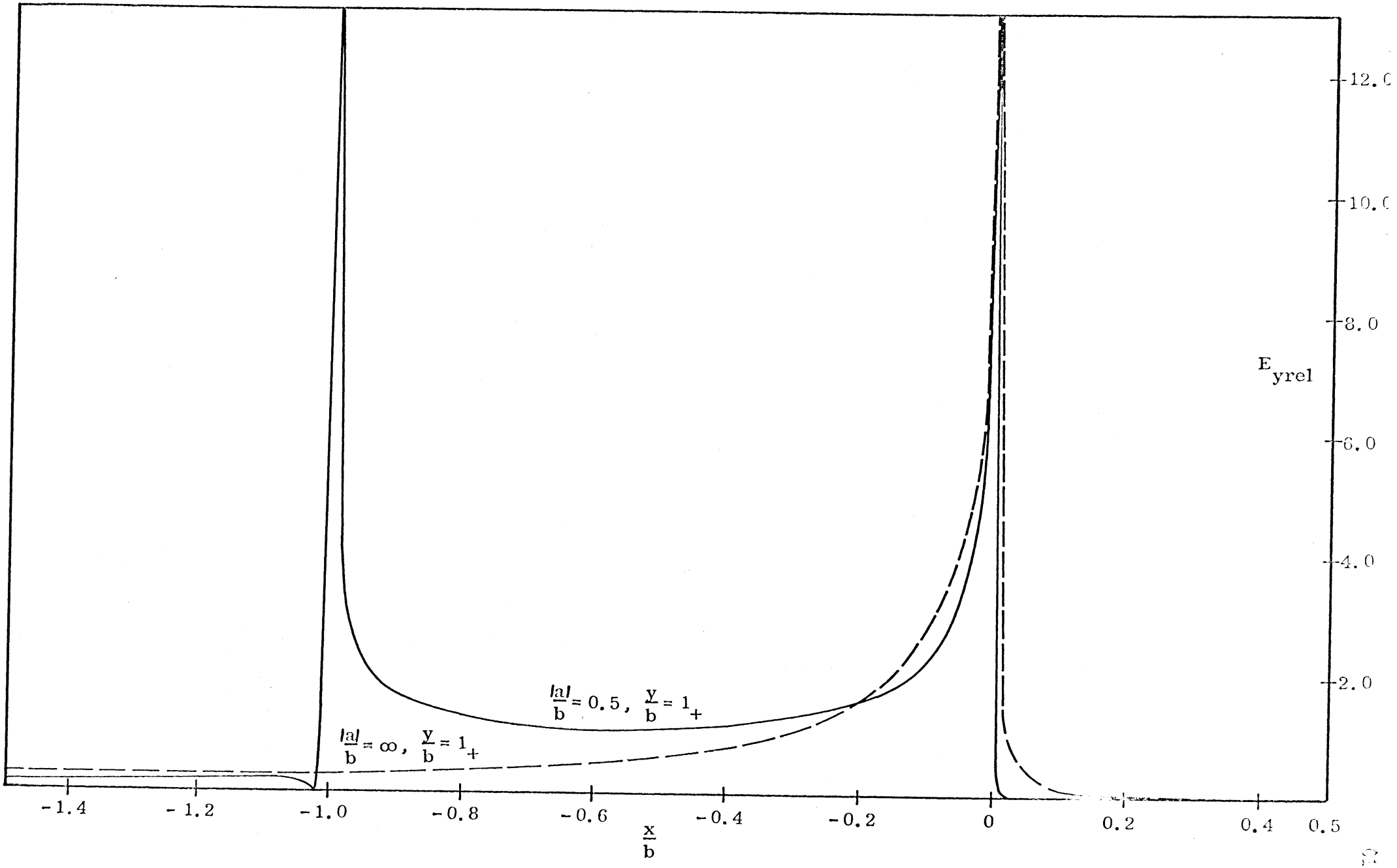

Fig. 3-17-7: Comparison of E_{yrel} on $\frac{y}{b} = 1_+$ line for the case of $\frac{d}{b} = 0.5$ between $\frac{|a|}{b} = 0.5$ and ∞.

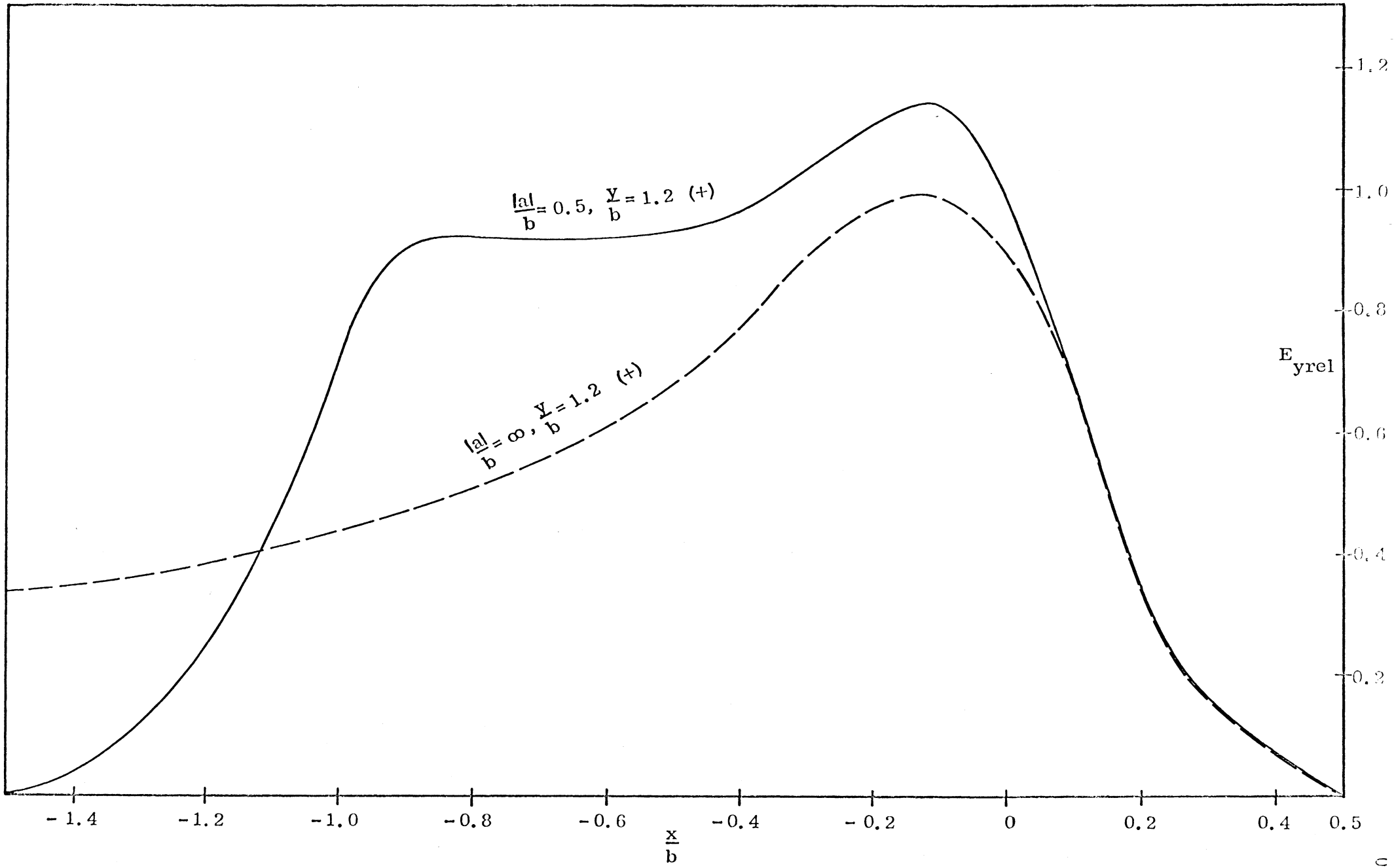

Fig. 3-17-8: Comparison of E_{yrel} on $\frac{y}{b} = 1.2$ line for the case of $\frac{d}{b} = 0.5$ between $\frac{|a|}{b} = 0.5$ and ∞.

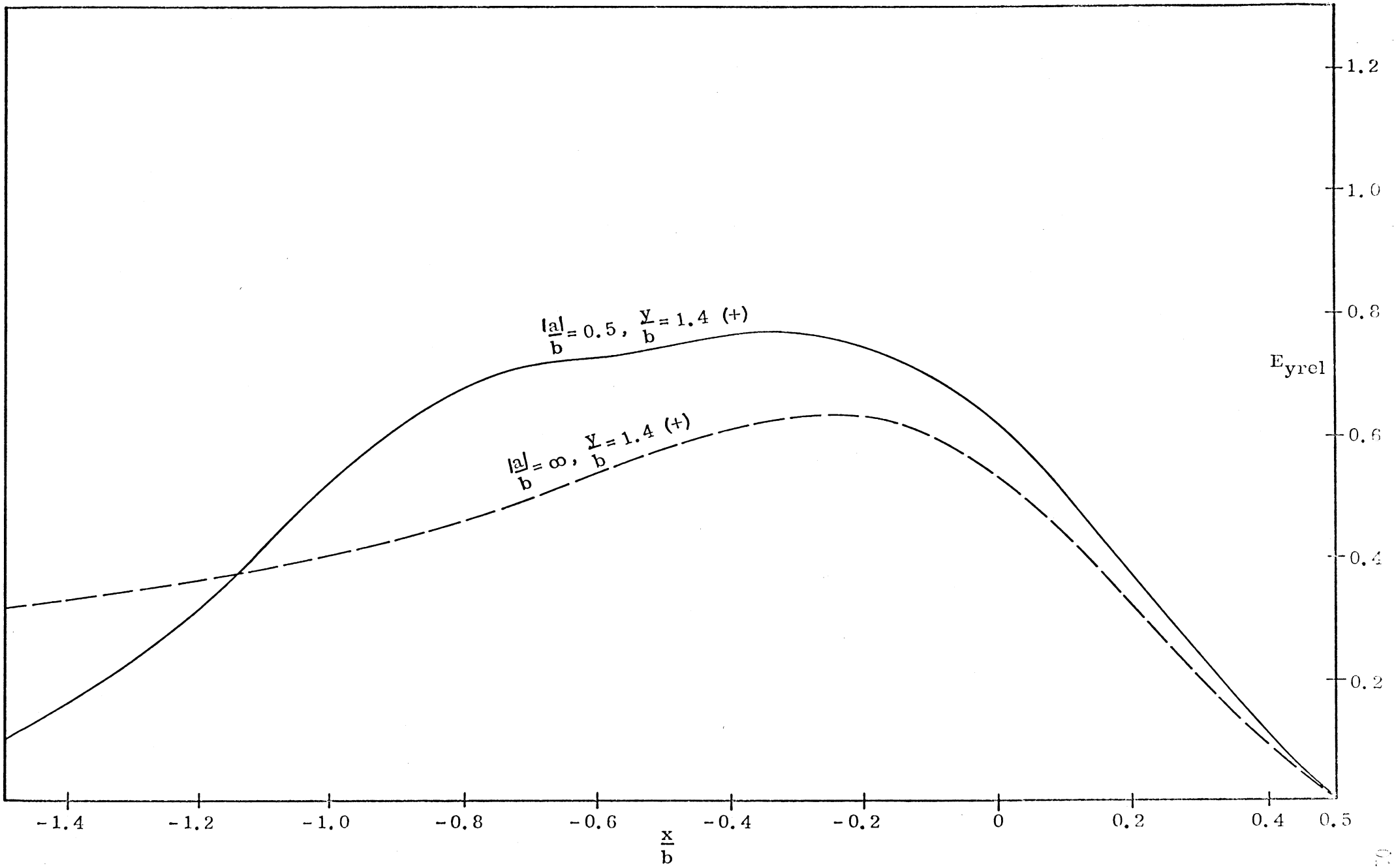

Fig. 3-17-9: Comparison of E_{yrel} on $\frac{y}{b} = 0.4$ line for the case of $\frac{d}{b} = 0.5$ between $\frac{|a|}{b} = 0.5$ and ∞.

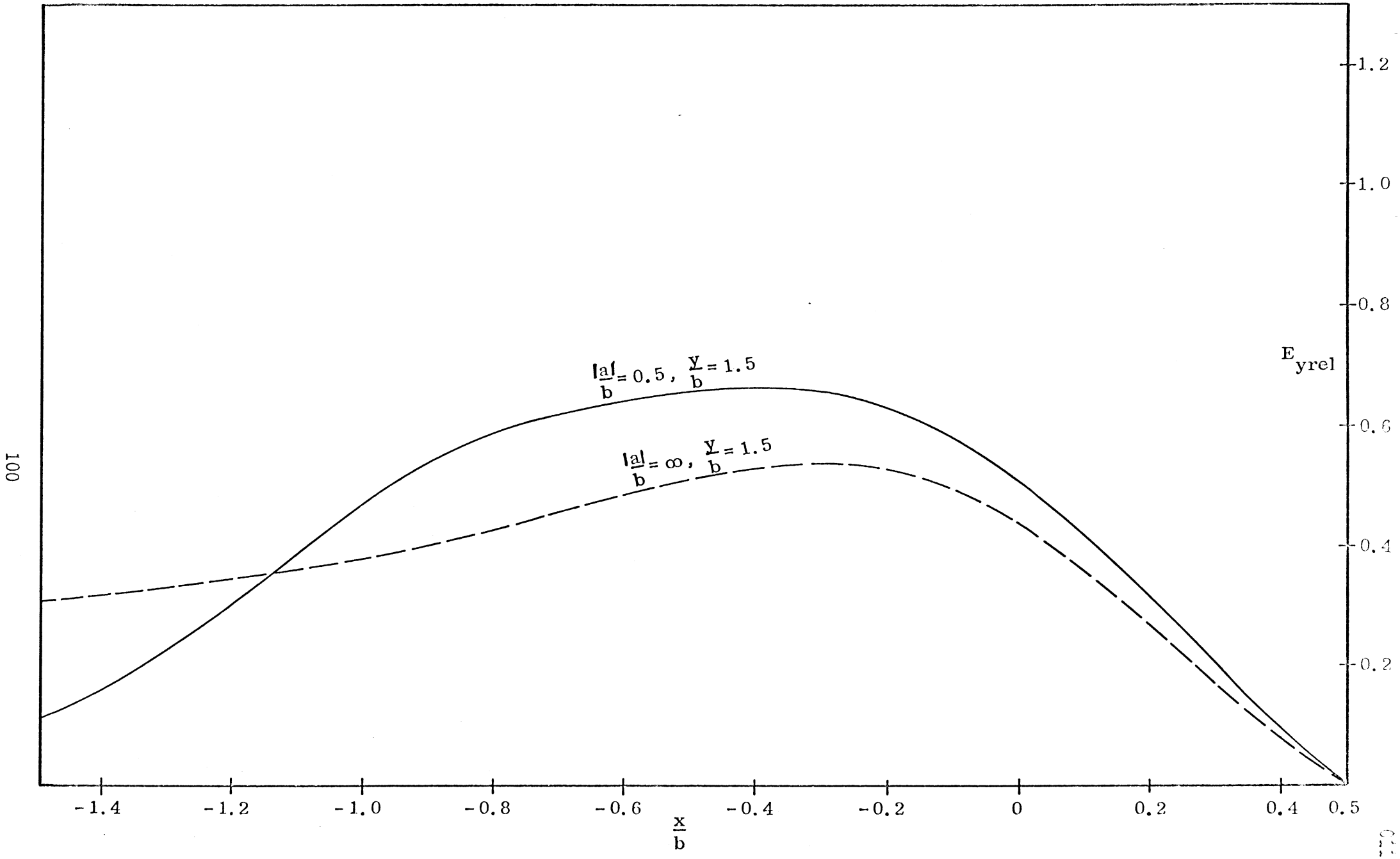

Fig. 3-17-10: Comparison of E_{yrel} on $\frac{y}{b} = 1.5$ line for the case of $\frac{d}{b} = 0.5$ between $\frac{|a|}{b} = 0.5$ and ∞.

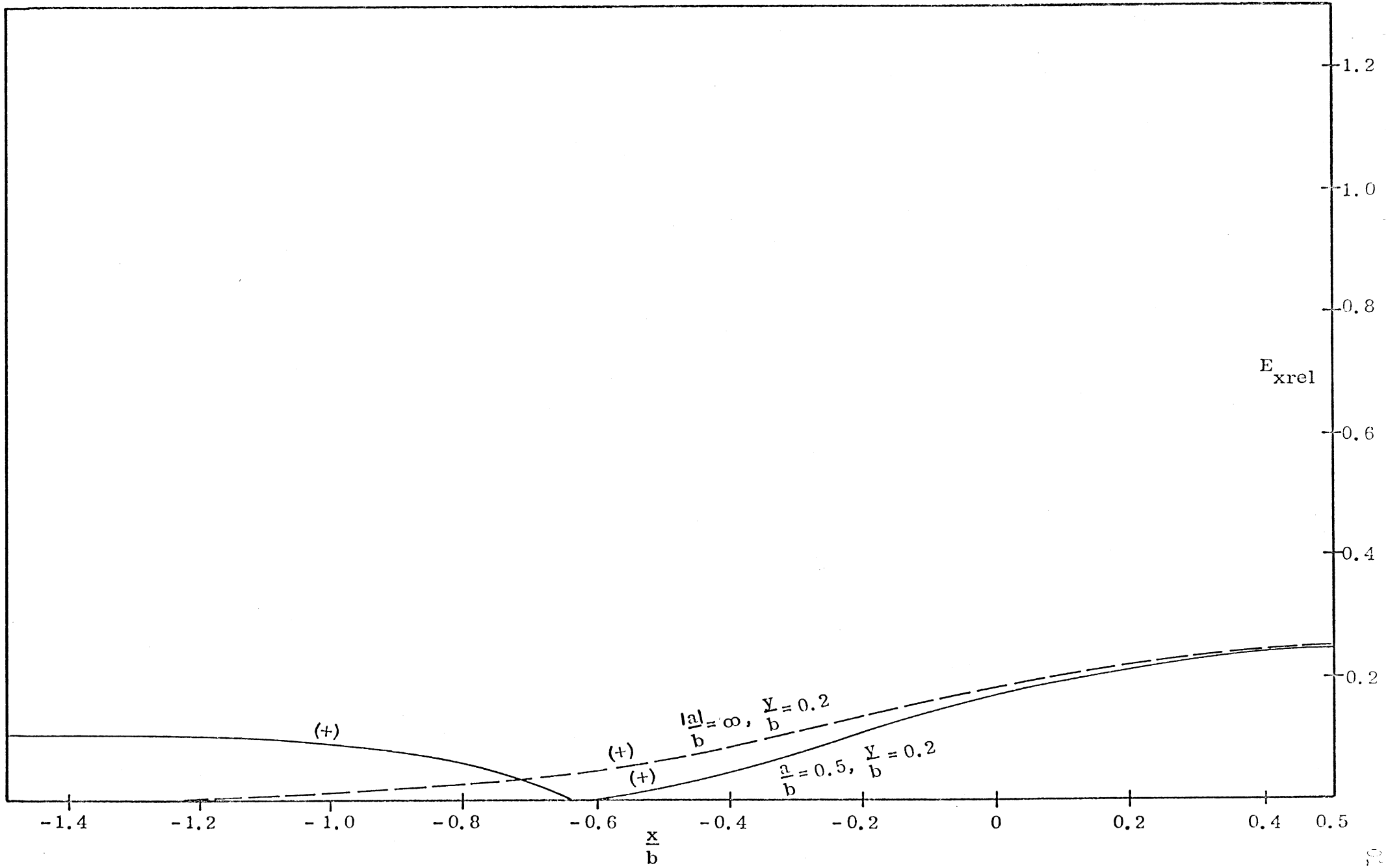

Fig. 3-18-1: Comparison of E_{xrel} on $\frac{y}{b} = 0.2$ line for the case of $\frac{d}{b} = 0.5$ between $\frac{|a|}{b} = 0.5$ and ∞.

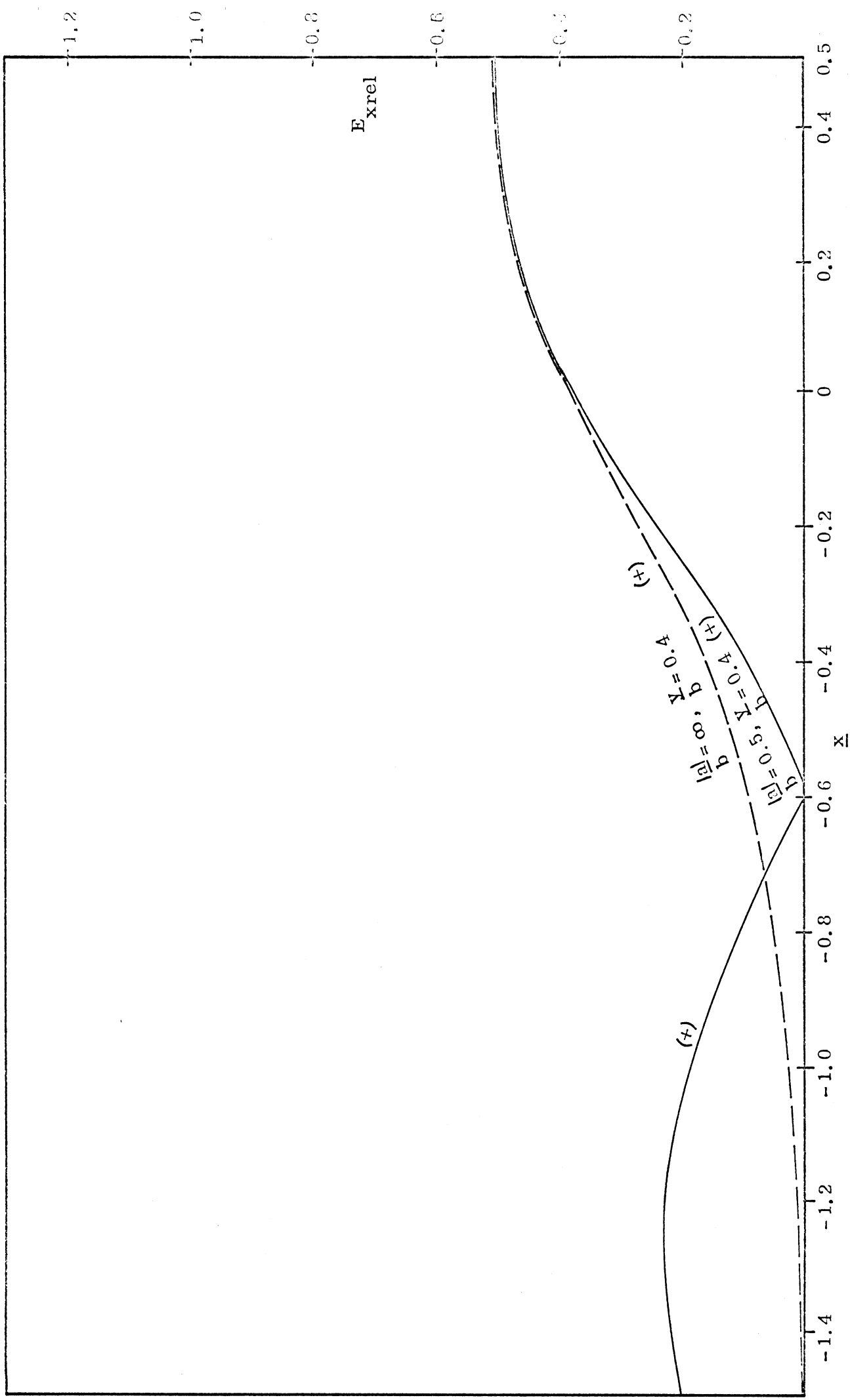

Fig. 3-18-2: Comparison of E_{xrel} on $\frac{Y}{b} = 0.4$ line for the case of $\frac{d}{b} = 0.5$ between $\frac{|a|}{b} = 0.5$ and ∞.

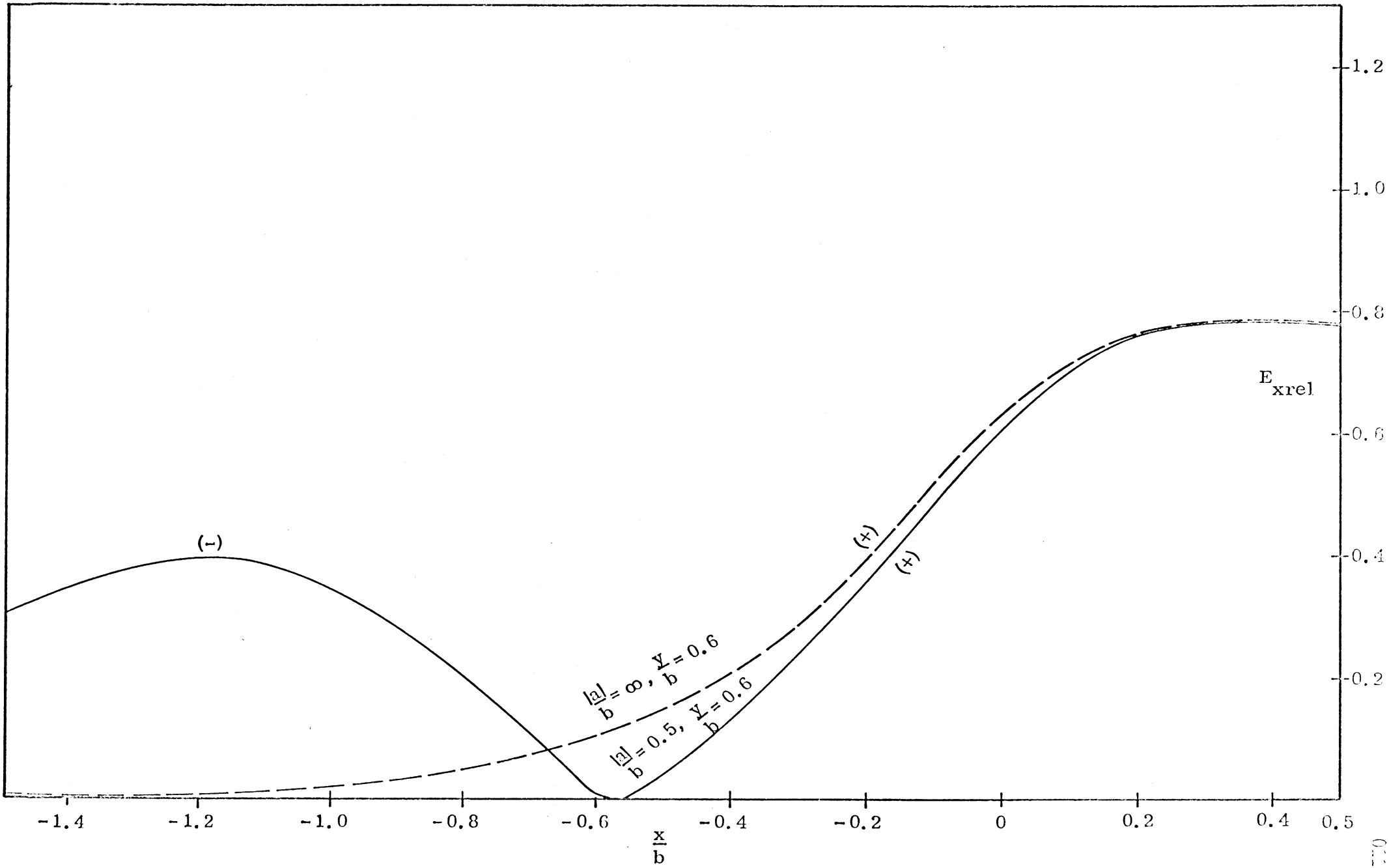

Fig. 3-18-3: Comparison of E_{xrel} on $\frac{y}{b} = 0.6$ line for the case of $\frac{d}{b} = 0.5$ between $\frac{|a|}{b} = 0.5$ and ∞.

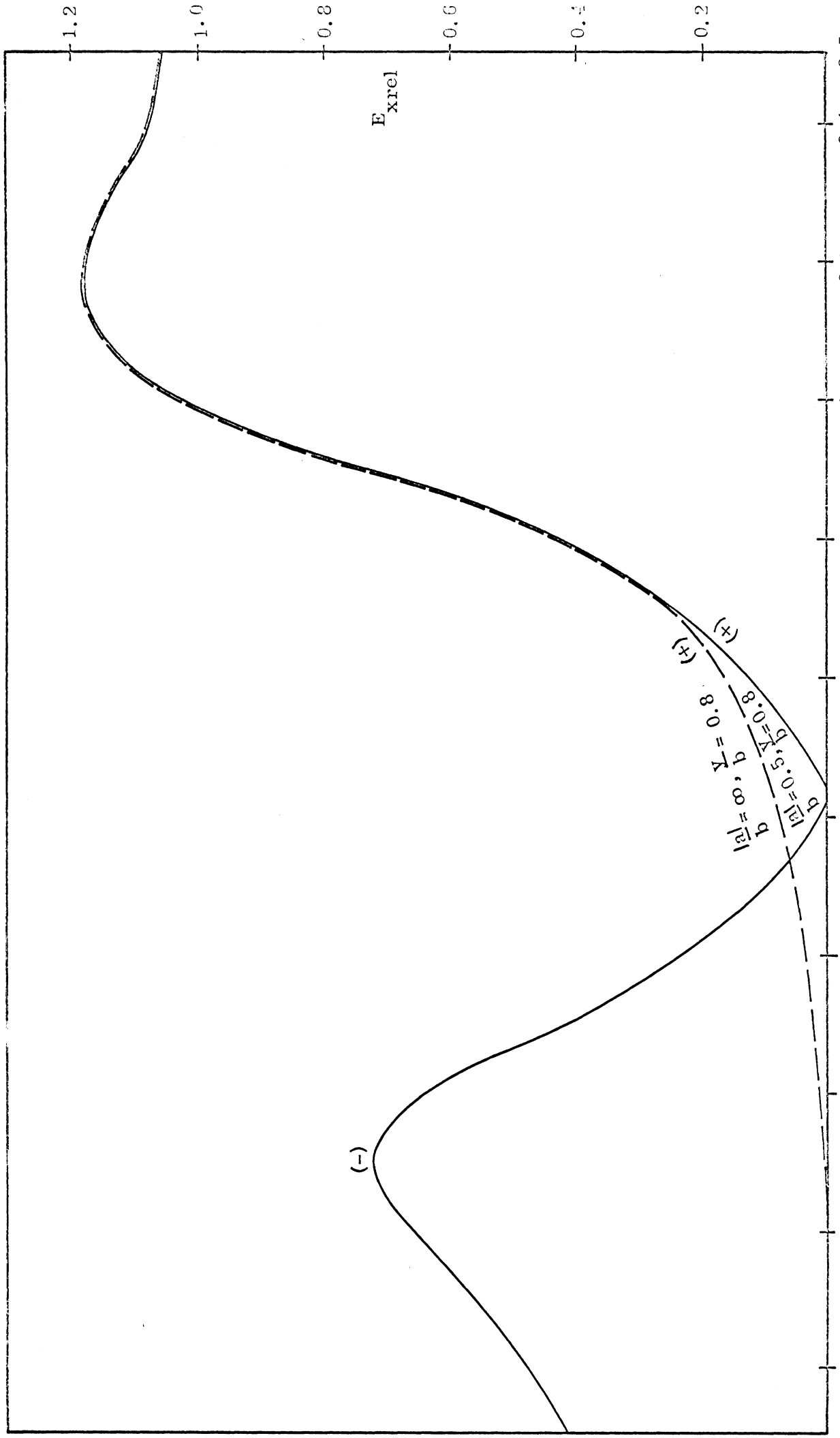

Fig. 3-18-4: Comparison of E_{xrel} on $\frac{Y}{b} = 0.8$ line for the case of $\frac{d}{b} = 0.5$ between $\frac{|a|}{b} = 0.5$ and ∞.

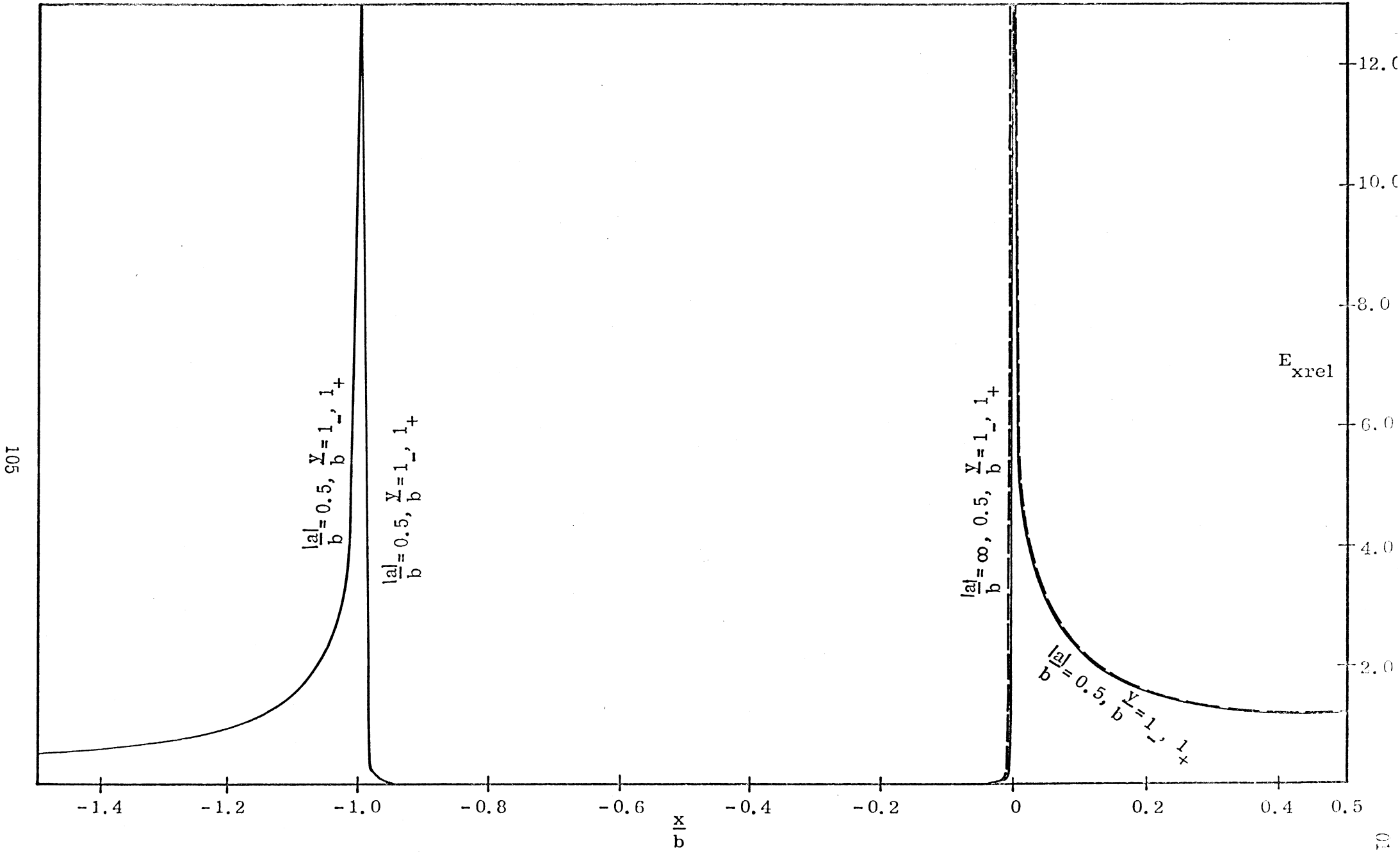

Fig. 3-18-5: Comparison of E_{xrel} on $\frac{Y}{b} = 1_-$ and 1_+ lines for the case of $\frac{d}{b} = 0.5$ between $\frac{|a|}{b} = 0.5$ and ∞,

011323-1-T

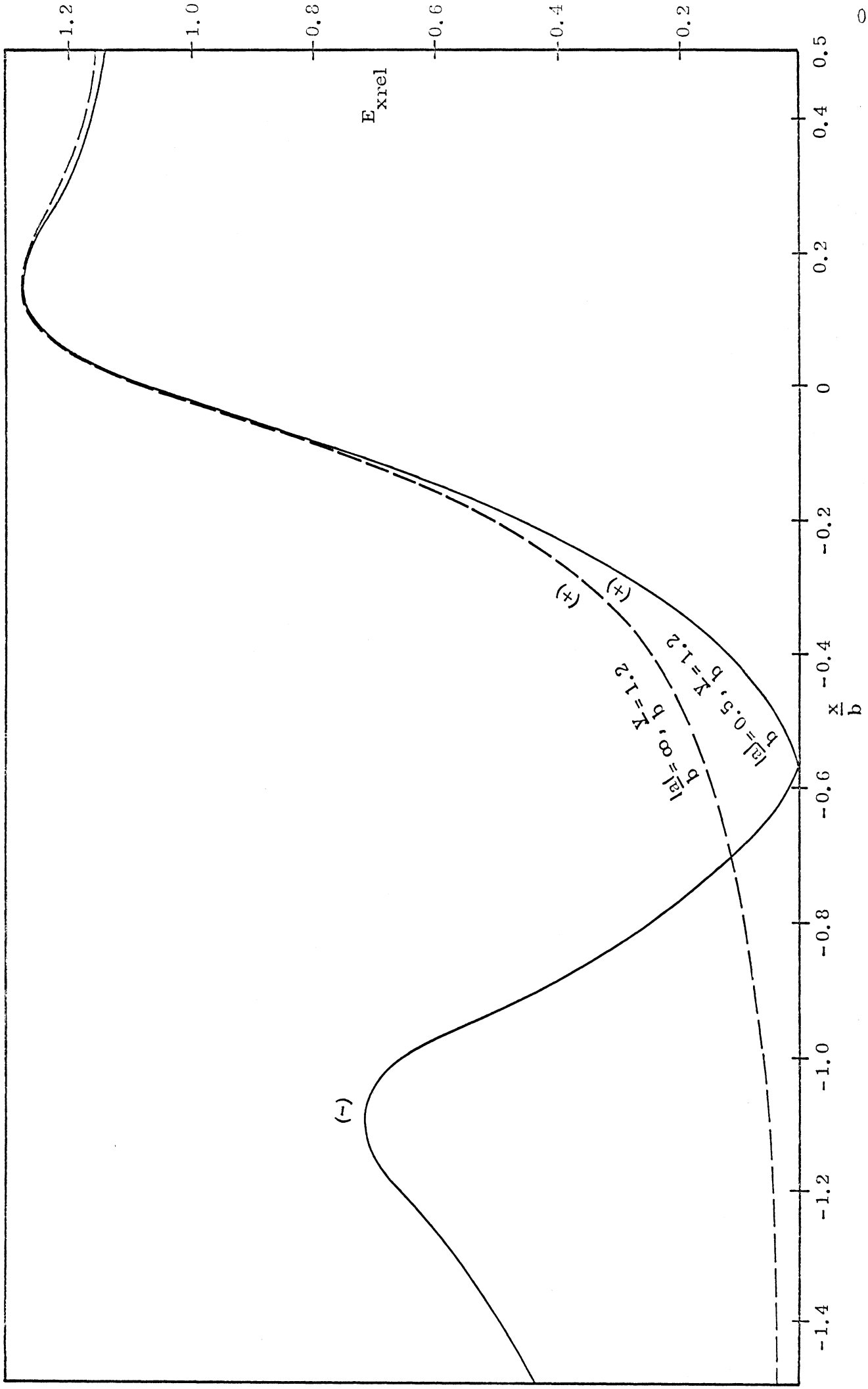

Fig. 3-18-6: Comparison of E_{xrel} on $\frac{y}{b} = 1.2$ line for the case of $\frac{d}{b} = 0.5$ between $\frac{|a|}{b} = 0.5$ and ∞.

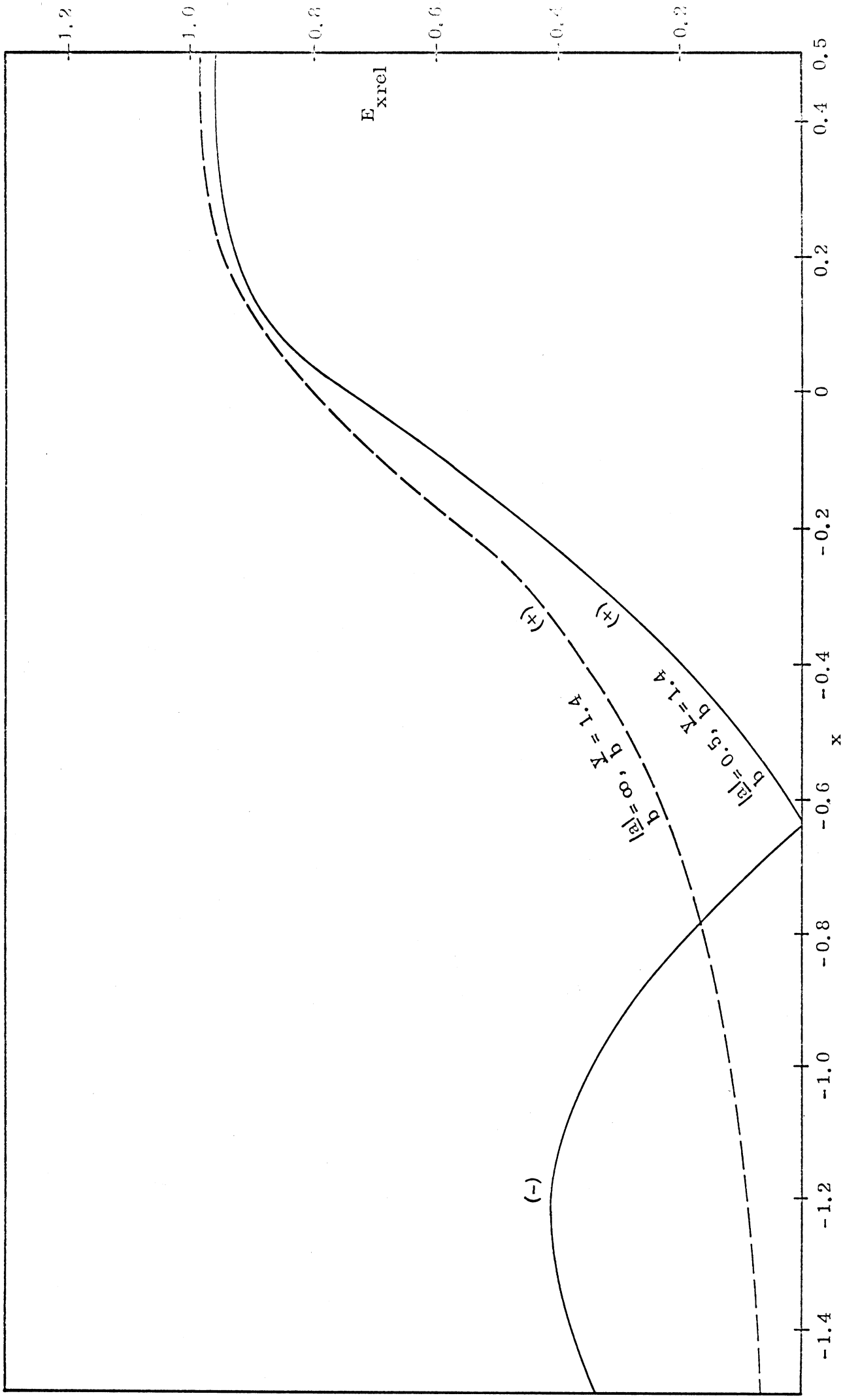

Fig. 3-18-7: Comparison of E_{xrel} on $\frac{Y}{b}$ = 1.4 line for the case of $\frac{d}{b}$ = 0.5 between $\frac{|a|}{b}$ = 0.5 and ∞.

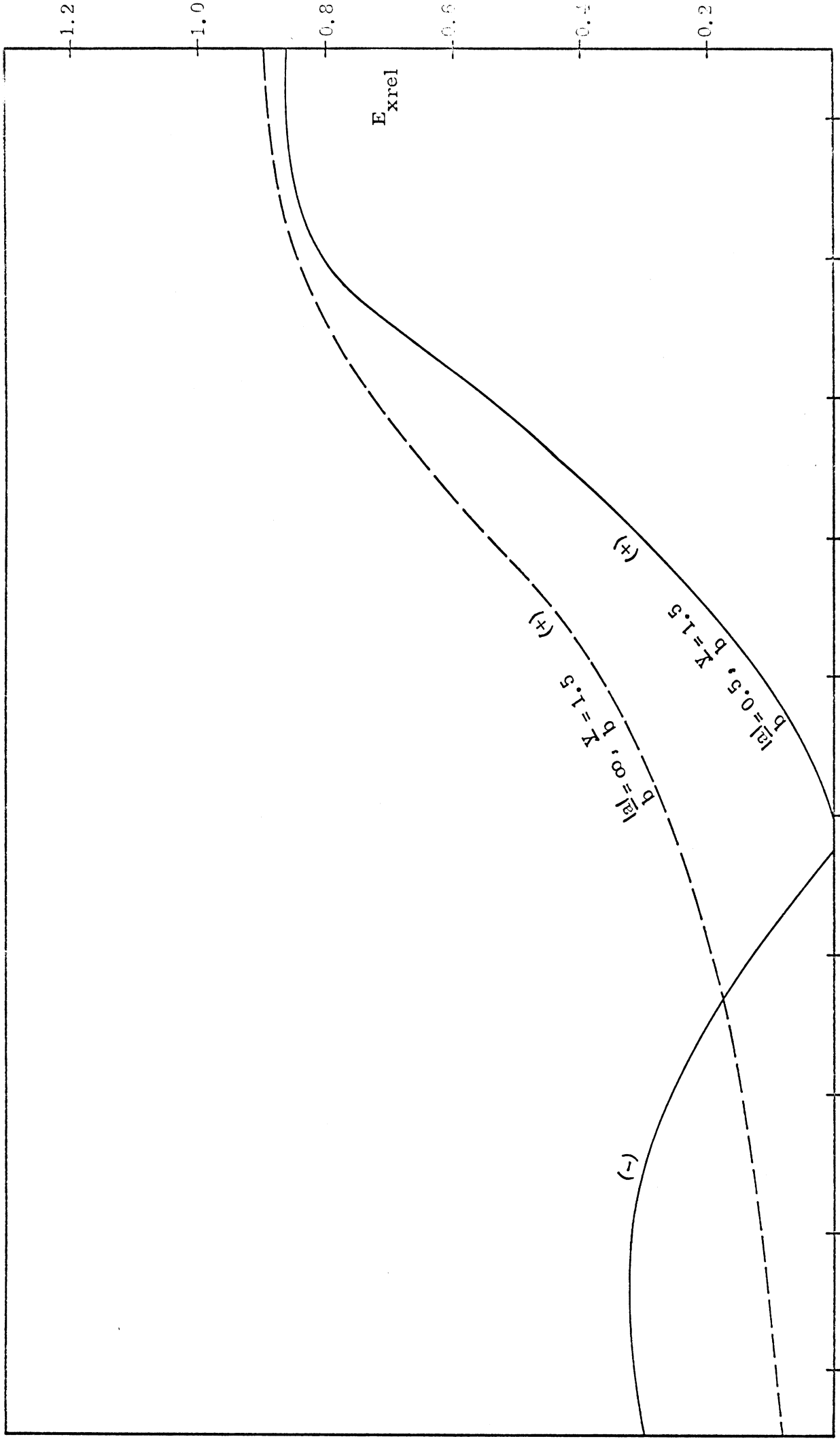

Fig. 3-18-8: Comparison of E_{xrel} on $\frac{Y}{b} = 1.5$ line for the case of $\frac{d}{b} = 0.5$ between $\frac{|a|}{b} = 0.5$ and ∞.

IV

CONCLUSION

From the numerical parametric study of field distribution for imaged parallel-plate transmission line of finite width, the following qualitative observations are made:

(a) The presence of the ground tends to decrease f_g compared to the f_g without the ground. As $\frac{a}{b}$ increases, however, for all ground proximities, the effect of the presence of the ground on f_g increasingly diminishes. In particular, for all $\frac{a}{b}$ it appears that, for $\frac{d}{b} \geq 1$, the decrease of f_g from the value of f_g for $\frac{d}{b} = \infty$ is less than 10 percent.

(b) The ground causes an asymmetry in the charge distribution on the plates; this asymmetry appears to be rather pronounced for $\frac{d}{b} < 0.5$ and increasingly less pronounced as $\frac{d}{b}$ increases.

(c) The division of the charge between the inner and outer surface of the upper plate is effected both by $\frac{a}{b}$ and $\frac{d}{b}$. In general, the ratio (inner-surface charge/outer surface charge) appears to increase with both $\frac{d}{b}$ and $\frac{a}{b}$.

(d) In the region $0 \leq \frac{|x|}{b} \leq \frac{|a|+d}{b}, 0 \leq \frac{y}{b} \leq 1.0$, the deivation of the relative field strength of finite-width case from that of a semi-infinite case tends to be not significant for $\frac{d}{b} > 0.5$.

The conclusions drawn above are qualitative in nature. Based on those, however, it seems to be indicated that some approximate expansion of charge distribution appropriate for various range of the parameters $\frac{a}{b}$ and $\frac{d}{b}$ could be derived based on the solutions of simple problems such as a finite parallel plate without ground and a semi-infinite parallel plate in the presence of a ground. Such an attempt, however, has not been made.

REFERENCES

(1) Baum, Carl E. (June, 1966), Sensor and Simulation Note 21, "Impedance and Field Distribution for Parallel Plate Transmission Line Simulators".

(2) Brown, T. and Granzow, K. (April, 1968), Electromagnetic Pulse Sensor and Simulation Note 52, "A Parameter Study of Two Parallel Plate Transmission Line Simulators of EMP Sensor and Simulation Note 21".

(3) Kammler, D. W., "Calculation of Characteristic Impedance and Coupling Coefficients for Strip Transmission Lines," IEEE Transactions, MTT-16, 1968. pp. 925-937.

(4) Chu, C-M., Cho, S. K., Tai, C-T. (August, 1971), Sensor and Simulation Note 137, "Proximity Effects of Semi-infinite Parallel Plate Transmission Line in the Presence of a Perfectly Conducting Ground".

APPENDIX A: Approximate formulas for the complex potential function and relative electric field intensity

The complex potential function in the z-plane $z = \xi + i\eta$, $V(z) + i\psi(z)$, is related to the charge density function $\sigma(s)$ by the integral equation (Eq. (10)):

$$\frac{2\pi\epsilon_o}{a}\left[V(z)+i\psi(z)\right] = \int_{-1}^{1} ds\,\sigma(s)\,Ln\left[\frac{(z-s+iB)(z+s+D)}{(z-s)(z+s+D+iB)}\right] . \qquad (A\text{-}1)$$

If $\sigma(s)$ for s in $s_j \le s \le s_{j+1}$ for all $j = 1, 2, 3, \ldots, 2M+1$ is approximated by a piece-wise linear equation of the form

$$\sigma(s) = \tau_j + \frac{\tau_{j+1} - \tau_j}{s_{j+1} - s_j}(s - s_j) \quad , \qquad (A\text{-}2)$$

then the Eq. (A-1) becomes

$$\frac{2\pi\epsilon_o}{a}\left[V(z)+i\psi(z)\right]$$

$$= \sum_{j=1}^{2M} \int_{s_j}^{s_{j+1}} ds \left[\frac{(s_{j+1}\tau_j - s_j\tau_{j+1}) + s(\tau_{j+1} - \tau_j)}{s_{j+1} - s_j}\right] \cdot$$

$$Ln\left[\frac{(z-s+iB)(z+s+D)}{(z-s)(z+s+D+iB)}\right] . \qquad (A\text{-}3)$$

In carrying out the integral on the right-hand side of Eq. (A-3), we recognize the

following two types of integrals involved:

$$P(z, s) = \int^{s} ds\ \mathrm{Ln}\left[\frac{(z-s+iB)(z+s+D)}{(z-s)(z+s+D+iB)}\right] \tag{A-4}$$

and

$$Q(z, s) = \int^{s} ds\ s\,\mathrm{Ln}\left[\frac{(z-s+iB)(z+s+D)}{(z-s)(z+s+D+iB)}\right] . \tag{A-5}$$

We know that

$$\int ds\ \mathrm{Ln}\,(a+ib\pm s) = \pm(a+ib\pm s)\,\mathrm{Ln}(a+ib\pm s) - s \tag{A-6}$$

and

$$\int ds\ s\,\mathrm{Ln}(a+ib\pm s) = -\frac{(a+ib)^2 - s^2}{2}\,\mathrm{Ln}(a+s+ib) - \frac{1}{4}(a\pm s+ib)^2 . \tag{A-7}$$

By use of the formulas (A-6) and (A-7), we can write down $P(z, s)$ and $Q(z, s)$. They are

$$\begin{aligned} P(z, s) = {} & (z+s+D)\,\mathrm{Ln}\,(z+s+D) \\ & - (z-s+iB)\,\mathrm{Ln}\,(z-s+iB) \\ & + (z-s)\,\mathrm{Ln}\,(z-s) \\ & - (z+s+D+iB)\,\mathrm{Ln}\,(z+s+D+iB) \end{aligned} \tag{A-8}$$

and $$Q(z, s) = -\frac{(z+D)^2 - s^2}{2}\,\mathrm{Ln}\,(z+s+D)$$

$$- \frac{(z+iB)^2 - s^2}{2} \text{Ln}\,(z-s+iB)$$

$$+ \frac{z^2 - s^2}{2} \text{Ln}\,(z-s)$$

$$+ \frac{(z+D+iB)^2 - s^2}{2} \text{Ln}\,(z+s+D+iB)$$

$$+ i\left(\frac{BD}{2} - Bs\right) . \qquad \text{(A-9)}$$

We can now express Eq. (A-3) in terms of P and Q:

$$\frac{2\pi\epsilon_o}{a}\left[V(z)+i\psi(z)\right]$$

$$= \sum_{j=1}^{2M} \frac{1}{s_{j+1}-s_j} \left\{ (\tau_j s_{j+1} - \tau_{j+1} s_j) \left[P(z, s_{j+1}) - P(z, s_j)\right] \right.$$

$$\left. - (\tau_j - \tau_{j+1}) \left[Q(z, s_{j+1}) - Q(z, s_j)\right] \right\} . \qquad \text{(A-10)}$$

Eq. (A-10) can be rearranged to yield

$$V(z)+i\psi(z) = \frac{a}{2\pi\epsilon_o} \sum_{j=1}^{2M+1} \tau_j R_j(z) , \qquad \text{(A-11)}$$

where

$$R_j(z) = \frac{\left[1 - \delta_{j,2M+1}\right]}{s_{j+1}-s_j} \left\{ s_{j+1} \left[P(z, s_{j+1}) - P(z, s_j)\right] \right.$$

$$- \left[Q(z, s_{j+1}) - Q(z, s_j) \right] \Bigg\}$$

$$+ \frac{\left[1 - \delta_{j,1} \right]}{s_j - s_{j-1}} \left\{ \left[Q(z, s_j) - Q(z, s_{j-1}) \right] \right.$$

$$\left. - s_{j-1} \left[P(z, s_j) - P(z, s_{j-1}) \right] \right\} . \qquad \text{(A-12)}$$

and

$$\delta_{j,r} = \begin{cases} 1 & \text{if } j = r \\ 0 & \text{if } j \neq r \end{cases} . \qquad \text{(A-13)}$$

In Eq. (A-12), if we let z approach to a point on the upper plate, i.e., $z \longrightarrow \xi_k$ (note that $-1 \leq \xi_k \leq 1$ for all $k = 1, 2, 3, \ldots, 2N+1$), then $V(z) = V(\xi_k + iO) \equiv V_o$, which is the potential of the upper plate. The complex potential there assumes the form

$$V_o + i\psi(\xi_k + iO) = \frac{a}{2\pi\epsilon_o} \sum_{j=1}^{2M+1} \tau_j R_j(\xi_k + iO) . \qquad \text{(A-14)}$$

If we denote the real part of $R_j(\xi_k + iO)$ by A_{jk}, then we obtain a system of $2M+1$ linear equations for τ_j:

$$V_o = \frac{a}{2\pi\epsilon_o} \sum_{j=1}^{2M+1} \tau_j A_{j,k} . \qquad \text{(A-15)}$$

To obtain the explicit form of $A_{j,k}$, we first denote real parts of $P(\xi_k + iO, s_j)$ and $Q(\xi_k + iO, s_j)$ by $f_{j,k}$ and $g_{j,k}$, respectively. Then, by Eq. (A-12), we obtain the explicit expression for $A_{j,k}$ in the following form:

$$A_{j,k} = \frac{\left[1-\delta_{j,2M+1}\right]}{s_{j+1}-s_j}\left[s_{j+1}\left(f_{j+1,k}-f_{j,k}\right)-\left(g_{j+1,k}-g_{j,k}\right)\right]$$

$$+\frac{\left[1-\delta_{j,1}\right]}{s_j-s_{j-1}}\left[\left(g_{j,k}-g_{j-1,k}\right)-s_{j-1}\left(f_{j,k}-f_{j-1,k}\right)\right], \qquad \text{(A-16)}$$

where $f_{j,k}$ and $g_{j,k}$ are, by Eqs. (A-8) and (A-9),

$$f_{j,k} = (\xi_k - s_j)\,\mathrm{Ln}\left[\frac{|\xi_k - s_j|}{\sqrt{(\xi_k-s_j)^2+B^2}}\right]$$

$$+(\xi_k+s_j+D)\,\mathrm{Ln}\left[\frac{|\xi_k+s_j+D|}{\sqrt{(\xi_k+s_j+D)^2+B^2}}\right]$$

$$+B\left[\tan^{-1}\left(\frac{B}{\xi_k-s_j}\right)+\tan^{-1}\left(\frac{B}{\xi_k+s_j+D}\right)\right] \qquad \text{(A-17)}$$

and

$$g_{j,k} = \frac{\xi_k^2-s_j^2}{2}\,\mathrm{Ln}\left[\frac{|\xi_k-s_j|}{\sqrt{(\xi_k-s_j)^2+B^2}}\right]$$

$$-\frac{(\xi_k+D)^2-s_j^2}{2}\,\mathrm{Ln}\left[\frac{|\xi_k+s_j+D|}{\sqrt{(\xi_k+s_j+D)^2+B^2}}\right]$$

$$+\frac{B^2}{2}\,\mathrm{Ln}\left[\frac{\sqrt{(\xi_k-s_j)^2+B^2}}{\sqrt{(\xi_k+s_j+D)^2+B^2}}\right]$$

$$+ B\,\xi_k \tan^{-1}\left(\frac{B}{\xi_k - s_j}\right) - B\,(\xi_k + D)\tan^{-1}\left(\frac{B}{\xi_k + s_j + D}\right) \quad . \tag{A-18}$$

In Eqs. (A-17) and (A-18), the principal branch of the arctangent functions must be chosen. Since B is a positive number, it follows, for any A, that

$$0 \leq \tan^{-1}\frac{B}{A} \leq \pi \ .$$

i.e.,

$$0 \leq \tan^{-1}\frac{B}{A} \leq \frac{\pi}{2} \quad \text{for } 0 \leq A \tag{A-19}$$

and

$$\frac{\pi}{2} \leq \tan^{-1}\frac{B}{A} \leq \pi \quad \text{for } A \leq 0 \ . \tag{A-20}$$

In Section 2, the solution of Eq. (A-15) for τ_j is discussed for the case of $V_o = \frac{a}{2\pi\epsilon_o}$. $\{\tau_j\}$ is calculated by a numerical method. Once τ_j is known, then we can obtain the expressions for component electric field intensities by differentiating the complex potential function Eq. (A-11).

i.e.,

$$E_x = -\frac{\partial V}{\partial X} = -\frac{\partial V}{a\partial\xi} \tag{A-21}$$

$$E_y = -\frac{\partial V}{\partial y} = \frac{\partial\psi}{\partial x} = \frac{\partial\psi}{a\partial\xi} \tag{A-22}$$

Therefore, from Eq. (A-11), for $V_o = \frac{a}{2\pi\epsilon_o}$ we have

$$-E_x(z) + iE_y(z) = \frac{1}{2\pi\epsilon_o}\sum_{j=1}^{2M+1}\tau_j R_j'(z) \ . \tag{A-23}$$

The explicit form of $R_j'(z)$ is the same as Eq. (A-12), except that now $P(z, s_j)$ and $Q(z, s_j)$ are replaced by

$$P_j'(z) = P_j'(\xi+i\eta) \equiv \frac{\partial}{\partial \xi} P(z, s_j)$$

$$= \mathrm{Ln}\left[\frac{(z-s_j)(z+s_j+D)}{(z-s_j+iB)(z+s_j+D+iB)}\right] \qquad \text{(A-24)}$$

and

$$Q_j'(z) = Q_j'(\xi+i\eta) \equiv \frac{\partial}{\partial \xi} Q(z, s_j)$$

$$= -(z+D)\,\mathrm{Ln}(z+s_j+D)$$

$$-(z+iB)\,\mathrm{Ln}(z-s_j+iB)$$

$$+(z+D+iB)\,\mathrm{Ln}(z+s_j+D+iB)$$

$$+ z\,\mathrm{Ln}(z-s_j)\ . \qquad \text{(A-25)}$$

For convenience, we normalize the field intensity with respect to the field intensity between the plates of infinite extent, which is $\frac{a}{2\pi\epsilon_o b}$.

Hence, by Eq. (A-23), we obtain the relative field intensity in the following form:

$$-E_{xrel}+iE_{yrel} = \frac{b}{a}\sum_{j=1}^{2M+1} \tau_j R_j'(z)$$

$$= \frac{B}{2}\sum_{j=1}^{2M+1} \tau_j R_j'(z)\ . \qquad \text{(A-26)}$$

Eq. (A-26) is used for numerical computation of the relative field intensities.